EFFECTS OF HYDROLOGIC CONNECTIVITY AND LAND USE ON FLOODPLAIN SEDIMENT ACCUMULATION AT THE SAVANNAH RIVER SITE, SOUTH CAROLINA

THESIS

A thesis submitted in partial fulfillment of the requirements for the degree of Master of Science in the College of Arts and Sciences at the University of Kentucky

By Jeremy Edward Eddy

Lexington, Kentucky

Director: Dr. Kevin M. Yeager, Associate Professor of Earth and Environmental Sciences

Lexington, Kentucky

2017

Copyright © Jeremy Edward Eddy 2017

ABSTRACT OF THESIS

EFFECTS OF HYDROLOGIC CONNECTIVITY AND LAND USE ON FLOODPLAIN SEDIMENT ACCUMULATION AT THE SAVANNAH RIVER SITE, SOUTH CAROLINA

Floodplains, and the sediment accumulating naturally on them, are important to maintain stream water quality and serve as sinks for organic and inorganic carbon. Newer theories contend that land use and hydrologic connectivity (water-mediated transport of matter, energy, and/or organisms within or between elements of the hydrologic cycle) play important roles in determining sediment accumulation on floodplains. This study hypothesizes that changes in hydrologic connectivity have a greater impact on floodplain sediment accumulation than changes in land use. Nine sediment cores from seven sub-basins were collected from the Savannah River Site (SRS), South Carolina, and processed for grain-size, radionuclide dating (⁷Be, ¹³⁷Cs, ²¹⁰Pb), particulate organic carbon (POC), and microscopy. Historical records, including aerial and satellite imagery, were used to identify anthropogenic disturbances in the subbasins, as well as to calculate the percentages of natural vegetation land cover at the SRS in 1951, and 2014. LiDAR and field survey data identified 251 flow impediments, measured elevation, and recorded standard stream characteristics (e.g., bank height) that canaffect hydrologic connectivity. Radionuclide dating was used to calculate sediment mass accumulation rates (MARs) and linear accumulation rates (LARs) for each core. Results indicate that sedimentation rates have increased across all SRS sub-basins over the past 40-50 years, shortly after site restoration and recovery efforts began. Findings show that hydrologic connectivity proxies (i.e., stream characteristics and impediments) have stronger relationships to MARs and LARs than the land use proxy (i.e., vegetation cover), confirming the hypothesis. Asstream channel depth and the number of impediments increase, floodplain sedimentation rates also increase. This knowledge can help future stream restoration efforts by focusing resources to more efficiently attain stated goals, particularly in terms of floodplain sediment retention.

KEYWORDS: Savannah River Site, Hydrologic Connectivity, Radionuclides, Land Use, Particulate Organic Carbon

Jeremy Edward Eddy December 7, 2017	
December 7, 2017	

EFFECTS OF HYDROLOGIC CONNECTIVITY AND LAND USE ON FLOODPLAIN SEDIMENT ACCUMULATION AT THE SAVANNAH RIVER SITE, SOUTH CAROLINA

Jeremy Edward Eddy

Dr. Kevin M. Yeager
Director of Thesis

Dr. Edward W. Woolery
Director of Graduate Studies

December 7, 2017

ACKNOWLEDGEMENTS

I would like to thank my advisor, Dr. Kevin M. Yeager, for his tremendous support during my time in the Department of Earth and Environmental Sciences at the University of Kentucky. His high expectations for a Master's candidate has tested my resolve, increased my knowledge, given me experiences beyond the required curriculum, and has made me a better scientist. I would also like to thank my thesis committee, Dr. Jonathan Phillips and Dr. Christopher Barton, for their support and guidance through this process. Additionally, Dean Fletcher and Dr. Rich Biemiller were instrumental as contacts at the Savannah River Site (SRS), allowing me to use in situ data collected over several years in my work. I would like to thank my fellow Sedimentary and Environmental Radiochemistry Research Laboratory (SER₂L) lab mates and graduate students for their help over the last couple of years: Wei Ji, Stephen Prosser, Cara Peterman, Greg Myers, Sean Swick, Edward Lo, and Kim Schindler. The aid I received at the University of Kentucky—the education, the experiences, and the support—were invaluable to my success, and I couldn't have done it without all of these people. I would also like to thank my family for the moral support that they have given me, not only through this endeavor, but throughout my entire life. Thank you for everything.

TABLE OF CONTENTS

Acknowledgements	iii
List of Tables	vi
List of Figures	vii
Chapter One: Introduction	1
1.1 Biogeomorphology	
1.2 Land Use	1
1.3 Hydrologic Connectivity	
1.4 Present Study	
Chapter Two: Background	7
2.1 Description of Study Area	
2.1.1 Savannah River Site	
2.1.2 MQ1-A-14V	
2.1.3 U10-B-14V	12
2.1.4 TC2A-B-14V and TC2B-B-14V	14
2.1.5 TC5-B-14V	17
2.1.6 MB6-B-14V	19
2.1.7 MBM-A-14V and ODB-1B-14V	21
2.1.8 MCE-A-14V	24
2.2 Previous Research	26
2.2.1 Sedimentation of Floodplains	
2.2.2 Land Use	26
2.2.3 Hydrological Connectivity	27
Chapter Three: Methods	35
3.1 Lithostratigraphy	35
3.1.1 Core Collection	35
3.1.2 Core Processing	35
3.1.3 Particle Size Distribution	37
3.1.4 Particulate Organic Carbon	37
3.2 Radiochemistry	
3.2.1 Alpha Spectrometry	39
3.2.2 Gamma Spectrometry	40
3.3 Remote Sensing	40

Chapter Four: Results41
4.1 Lithostratigraphy41
4.1.1 Stratigraphy42
4.1.2 Lithofacies41
4.1.2.1 MQ1-A-14V42
4.1.2.2 U10-B-14V44
4.1.2.3 TC2A-B-14V46
4.1.2.4 TC2B-B-14V46
4.1.2.5 TC5-B-14V49
4.1.2.6 MB6-B-14V49
4.1.2.7 MBM-A-14V52
4.1.2.8 ODB-1B-14V54
4.1.2.9 MCE-A-14V56
4.2 Radiochemistry58
4.2.1 Gamma Spectrometry58
4.2.2 Alpha Spectrometry63
4.3 Imagery72
Chapter Five: Discussion
Chapter Six: Conclusions87
Appendix89
References
Vita160

LIST OF TABLES

Table 1: Soil erosion rates in select areas worldwide	4
Table 2: Sediment yield in basin studies worldwide	4
Table 3: Characteristics of buffers	31
Table 4: Characteristics of barriers	32
Table 5: Characteristics of blankets	34
Table 6: Average grainsize percentages of all cores	41
Table 7: 137Cs inventory and sedimentation ratio of all nine cores	59
Table 8: Comparison of 137 Cs LAR and SMAR at peak and 1^{st} detection	60
Table 9: ²¹⁰ Pb inventory and sedimentation ratio of all nine cores	66
Table 10: Comparison of ²¹⁰ Pb LAR and SMAR	66
Table 11: Percentage of vegetated areas	72
Table 11: Comparison of R ² values for proxy graphs	80
Table 13: Comparison of p-values for proxy graphs	82
Table 14: Comparison of slope coefficients for proxy graphs	83

LIST OF FIGURES

Figure 1: Regional location of the SRS	6
Figure 2: Aerial imagery of the SRS	9
Figure 3: Location and origin of flow impediments at MQ1-A-14V	11
Figure 4: Location and origin of flow impediments at U10-B-14V	13
Figure 5: Location and origin of flow impediments at TC2A-B-14V	15
Figure 6: Location and origin of flow impediments at TC2B-B-14V	16
Figure 7: Location and origin of flow impediments at TC5-B-14V	18
Figure 8: Location and origin of flow impediments at MB6-B-14V	20
Figure 9: Location and origin of flow impediments at MBM-A-14V	22
Figure 10: Location and origin of flow impediments at ODB-1B-14V	23
Figure 11: Location and origin of flow impediments at MCE-A-14V	25
Figure 12: Examples of buffers	32
Figure 13: Examples of barriers	33
Figure 14: Examples of blankets	34
Figure 15: LiDAR elevation map of the SRS	36
Figure 16: Uranium decay series	39
Figure 17: Lithostratigraphy diagram for MQ1-A-14V	43
Figure 18: Lithostratigraphy diagram for U10-B-14V	45
Figure 19: Lithostratigraphy diagram for TC2A-B-14V	47
Figure 20: Lithostratigraphy diagram for TC2B-B-14V	48
Figure 21: Lithostratigraphy diagram for TC5-B-14V	50
Figure 22: Lithostratigraphy diagram for MB6-B-14V	51
Figure 23: Lithostratigraphy diagram for MBM-A-14V	53
Figure 24: Lithostratigraphy diagram for ODB-1B-14V	55
Figure 25: Lithostratigraphy diagram for MCE-A-14V	57
Figure 26: 137Cs Activity profile for all nine cores	61
Figure 27: Comparison of ¹³⁷ Cs LAR and SMAR for all nine cores	62
Figure 28: ²¹⁰ Pb Activity profile for all nine cores	64

Figure 29: Comparison of ²¹⁰ Pb LAR and SMAR for all nine cores	68
Figure 30: ²¹⁰ Pb-based SMAR and LAR vs Time for all nine cores	69
Figure 31: 1951 and 2013 vegetation imagery for U10-B-14V	73
Figure 32: 1951 and 2013 vegetation imagery for TC5-B-14V	73
Figure 33: 1951 and 2013 vegetation imagery for TC2A-B-14V	74
Figure 34: 1951 and 2013 vegetation imagery for TC2B-B-14V	74
Figure 35: 1951 and 2013 vegetation imagery for ODB-1B-14V	75
Figure 36: 1951 and 2013 vegetation imagery for MQ1-A-14V	75
Figure 37: 1951 and 2013 vegetation imagery for MCE-A-14V	76
Figure 38: 1951 and 2013 vegetation imagery for MBM-A-14V	76
Figure 39: 1951 and 2013 vegetation imagery for MB6-B-15V	77
Figure 40: Box plot of R ² values of all nine proxies	81
Figure 41: Standard deviation plot of elevation vs ¹³⁷ Cs MAR	85
Figure 42: Standard deviation plot of wetted perimeter vs ¹³⁷ Cs MAR	85
Figure 43: Standard deviation plot of max depth vs ¹³⁷ Cs MAR	86
Figure 44: Standard deviation plot of mean depth vs ¹³⁷ Cs MAR	86

CHAPTER ONE: INTRODUCTION

1.1 Biogeomorphology

As early as the late 19th century, natural science researchers proposed links between geology and ecology in regards to landscape evolution (Corenblit et al. 2007). The cycle of erosion proposed by Davis' (1899) "The Geographical Cycle", as well as his notion of landscape evolution, and Cowles' (1899) theory of plant succession, both linked geological processes with biological responses. However, it wasn't until the late 20th century that researchers began to work towards uniting geology and biology—under the name biogeomorphology—to explain landscape evolution (Corenblit et al. 2007; Gregory 1985). Ecological niche construction (Odling-Smee et al. 2003; Griffiths 2005), ecosystem engineers (Jones et al. 1994; 1997; Chapin et al. 1997), and the theory of complexity (Phillips 1999; 2005) are all modern theories that show linkages between these two disciplines. While one-way relationships between geology and plant ecology have been discussed for several decades, only recently have two-way positive feedbacks between each of the two sciences been considered (Corenblit et al. 2007).

1.2 Land Use

Observations of various river systems around the world have provided clear evidence that different types ofland use and related human activities can affect sediment accumulation, erosion, and transportation rates in sub-basins (e.g., Allan et al. 1997; Walling 1999; von Blanckenburg 2005). Some studies have found (Table1) that erosion rates resulting from changes in land use can differ by up to an order of magnitude or more, between, for example natural and cultivated (or agricultural) land uses. Likewise, Abernathy's (1990) study of reservoir sub-basins in Southeast Asia reported annual sediment yields increasing by 2.5- 6% per yearbecause of land use changes from undisturbed vegetation to agricultural. Other studies (Table 2) from around the world have recorded increases in basin sediment yieldsof up to 310 times the previous amount, when land use has changed from undisturbed vegetation to agricultural, or to

urbanized (O'Loughlin et al. 1980; Fredriksen 1970; Painter et al. 1974; Chang et al. 1982; Wolman and Schick 1967). Even within the Piedmont zone, multiple studies have shown that changes in land use have had direct effects on sediment production. Studies by Wolman (1964), Wolman and Schick (1967), and Leopold (1968) showed that sediment yields from urbanized areas ranged from 1,000 to over 100,000 tons mi⁻² y⁻¹. Naturally vegetated areas of the Piedmont show sediment yields between 200 and 500 tons mi⁻² y⁻¹, while farmed lands can be expected to yield around 500 tons mi⁻² y⁻¹. The sediment yield difference of urbanized areas of the Piedmont can vary between 2 and 500 times that of naturally vegetated Piedmont areas.

Land use legacies are also important when considering land use change. Several studies have shown that there are long-term, persistent effects of human land use history, even in areas that have been revegetated for decades (Foster et al. 2003). The National Science Foundation's (NSF) Long Term Ecological Research (LTER) Network has compiled studies usingseveral different approaches. These include paleoecology, dendrochronology, and archaeology (Foster et al. 1998; Swanson et al. 1998), largescale field experiments (Aber et al. 1989; Knapp et al. 1999), and integrative modeling which allow for comparison and testing of diverse studies across disciplines (Parton et al. 1987; Aber and Driscoll 1997). They all confirm that anthropogenic land use changes can influence an area's biogeomorphology for centuries after its existence (Foster et al. 2003). For example, the Mayan civilization declined nearly a millennium ago, and its former landsremained largely unpopulated until the mid-1900s (Turner 1974). However, Turner et al. (2003) and Beach (1998) observed that in these now forested lands, microtopography is still defined by Mayan house mounds, stonewalls, and terraces. The current soil structure here is still tied to erosion, evidenced by a distinct "Maya clay" layer found in many lakes and wetlands, which resulted fromlarge-scale deforestation circa 700-900AD (Foster et al. 2003). While this study only examines the relatively recent effects of land use change (~60 years), it is worth noting that long-term effects can persist for centuries or even millennia.

1.3 Hydrologic Connectivity

Hydrologic connectivity is defined as the water-mediated transfer of matter, energy, and/or organisms within or between elements of the hydrologic cycle (Pringle 2003). This study focuses on the retention of sediment onfloodplains along tributaries of the Savannah River, due to water-mediated transport. Hydrologic connectivity can be influenced many ways, both natural and anthropogenic. Obstacles to flow at thesubbasin-scale can be characterized as buffers, barriers, or blankets (Fryirset al. 2007). Buffers disrupt lateral linkages (i.e., stream-to-floodplain flow); examples of which are natural and anthropogenic levees, intact valley fills, and floodouts (Phillips 1992; Harvey 2001; Brierly and Fryirs 1998; Fryirs and Brierly 1998; 1999). Barriers disrupt upstreamdownstream flow, and can also increase or decrease lateral linkages (Fryirs et al. 2007); study-specific examples include dams, culverts, and large woody debris(LWD) in the form of beaver dams (Tooth et al. 2002; Nicholas et al. 1995). Blankets reduce vertical linkages between surface and sub-surface areas, and include channel bed armoring, riprap, and algal growth (Fryirs et al. 2007; Petts 1988; Church et al. 1988). The presence, addition, and removal of these obstacles can change the sediment transportation and accumulation rates of a river system (Fryirs 2013). For example, the addition of a levee on the stream bank can disconnect the transportation of sediment between the channel and floodplain. Likewise, the addition of a dam can create a stronger connection between stream channel and floodplains by the creation of a retaining pond. The removal of these obstacles can result in the opposite occurring.

Table 1: Soil erosion rates of natural vs. cultivated areas around the world. Adapted from Walling(1999), and Morgan (1986).

Country	Natural Soil Erosion (kg m ⁻² y ⁻¹)	Cultivated Soil Erosion (kg m ⁻² y ⁻¹)
China	<0.20	15.00-20.00
U.S.A.	<0.01-0.02	0.50-17.00
Ivory Coast	<0.01-0.02	0.01-9.00
Nigeria	0.05-0.10	0.01-3.50
India	0.05-0.10	0.03-2.00
Belgium	0.01-0.05	0.30-3.00
U.K.	0.01-0.05	0.01-0.30

Table 2: Basin studies showing the impact of land use change on sediment yield. Adapted from Walling (1999).

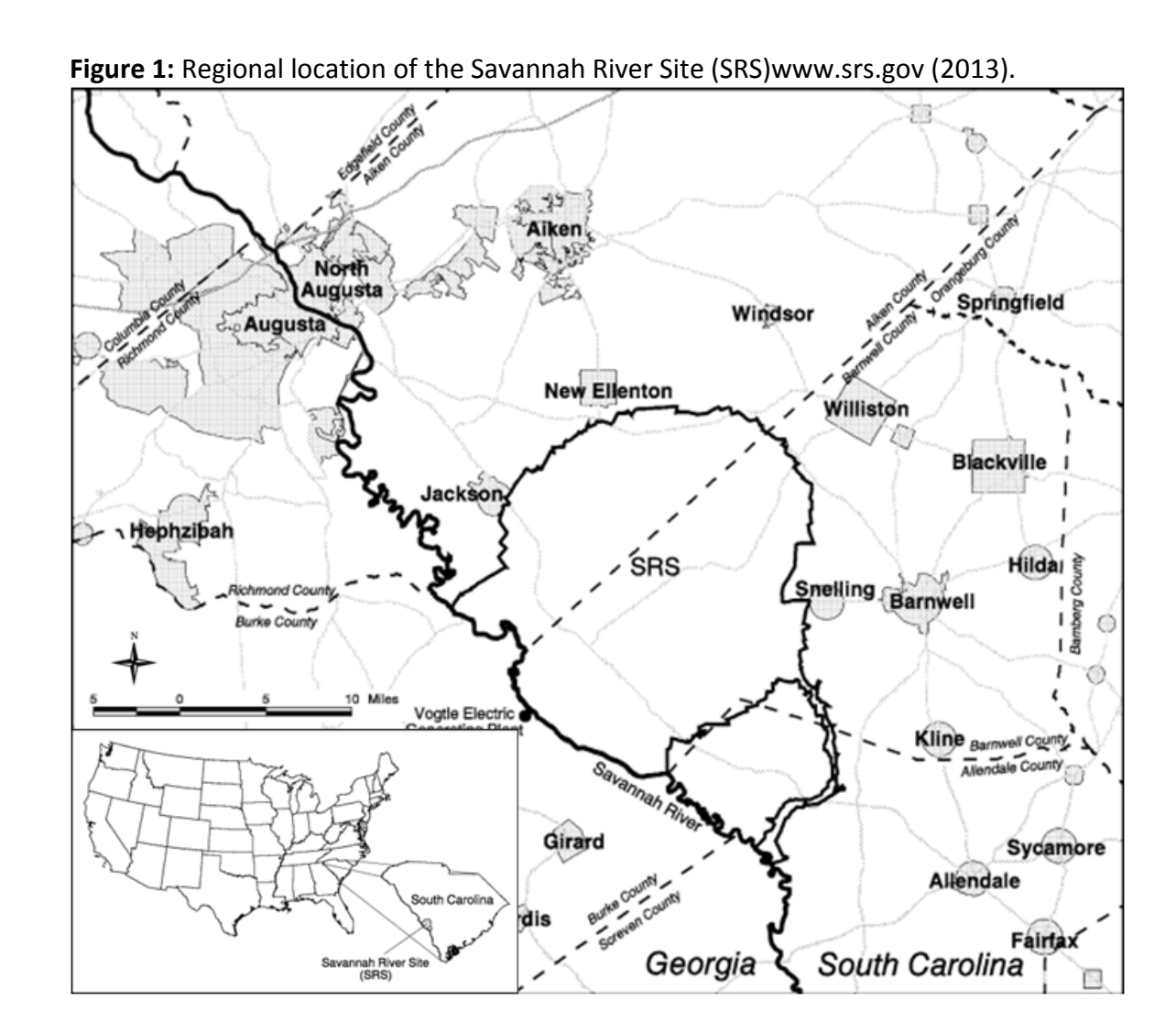
Region	Land Use Change	Factor Increase in Sediment Yield	Reference
Westland, New Zealand	Deforestation	x 8	O'Loughlin et al. (1980)
Oregon, U.S.A.	Deforestation	x 39	Fredriksen (1970)
Northern England	Agricultural	x 100	Painter et al. (1974)
Texas, U.S.A.	Deforestation and Agricultural	x 310	Chang et al. (1982)
Maryland, U.S.A.	Urbanization	x 126-375	Wolman and Schick (1967)

1.4 Present Study

Sediment transport, accumulation, and erosion are large concerns at the SRS. Throughout the SRS's 65-year history, it has housed five nuclear production reactors; two chemical separations facilities; a heavy water extraction plant; a nuclear fuel and target fabrication facility; a tritium extraction facility; waste processing, storage, and disposal facilities; and administration support facilities. Most of these facilities are currently decommissioned, and they are all scheduled to be decommissioned by 2026 (Kilgo 2005). Efforts to revegetate and restore parts of the landscape, as well as to produce, and temporarily store nuclear materials, are on-going and highly scrutinized by the federal and state governments, and by the local community. The presence of ²³⁹Pu and ³He on site is concerning, and knowledge of potential transport pathways and sinks of contaminated sediment is crucial to planning for mitigating and cleaning up a spill. This thesis intends to address the following hypothesis in order to characterize the efficacy of past landscape restoration efforts.

Hypothesis: Changing basin hydrologic connectivity has a greater impact on floodplain sediment accumulation rates at the SRS than changing basin land use from agriculture to forested.

This hypothesis was addressed by utilizing the following objectives: (1) quantify sediment accumulation rates and particulate organic carbon concentrations on several sub-basin floodplains within the SRS, using fallout radionuclides (⁷Be, ¹³⁷Cs, and ²¹⁰Pb) in sediment cores, (2) inventory natural and anthropogenic obstacles to hydrologic connectivity in these sub-basins over the past 100 years, (3) determine land use changes here using aerial photography and LiDAR data, (4) measure the physical characteristics of each of the sub-basins in order to compare and contrast them, and (5) perform statistical regression analyses of variables and responses.



CHAPTER TWO: BACKGROUND

2.1 Study Area Description

2.1.1 Savannah River Site (SRS)

The climate as the SRS is classified as humid subtropical. It has a mean annual temperature of 64°F (18°C) with an average annual precipitation of 48.2in (122.5cm). Monthly precipitation data indicates that precipitation is generally evenly distributed throughout the year, with April, May, October, and November being slightly drier (Kilgo and Blake, 2005). The topography at the SRS is gently rolling to flat, with elevation ranging from 130m to 20m above mean sea level. The geologic stratigraphy of the SRS includes formations from the Lumbee, Black Mingo, Orangeburg, and Barnwell groups, deposited in the late Cretaceous and Tertiary periods. These are sedimentary rocks, mostly comprised of sands and some clays, which give the area its iconic name, "The Sand Hills" (Kilgo and Blake, 2005).

The 800 km² of the SRS are owned and maintained by the U.S. Department of Energy (DOE) and have been since 1951 (White 2004). Extensive records exist for this area, both before and after DOE stewardship, creating a unique scenario in which to correlate observed changes in land use and topography with the sedimentary record over the last several decades. The history of the SRS can be categorized into three main time periods: pre-European settlement, European settlement until the 1950s, and 1951 to the present day.

Before Native American and then European settlement, the landscape of the SRS was primarily pine savannas, mixed with wetlands. While Native American impacts on the landscape were minimal—compared to Europeans—agricultural practices and hunting did affect the natural setting. In fact, extensive use of fire in both hunting and land clearing was most likely the main source of geomorphic change in the area prior to European settlement (White 2004). Despite periods of sustained seasonal habitation, native populations in the area declined in the 1400-1500s, allowing the area to naturally

restore itself by the time European settlers arrived (White 2004). In the early 1600s, colonists observed and recorded a topography mainly influenced by natural disturbances and, to a lesser extent, the relic influences of Native Americans.

Colonial settlement in the area began in the 1760s, although cattle grazing was reported as early as 1730 (Brown 1894). The widespread savanna grasses allowed cattle grazing to become the predominant land use, along with subsistence farming. The growing population of cattle likely had negative impacts on native grazers, soil erosion, and water quality along streams near farms and ranches (White 2004). Increased numbers of grain and saw mills directly impacted the streams and rivers of the SRS (Brooks and Crass 1991). The increase in saw mills, timber, and fuel-wood harvesting decimated the forests in the northern headwaters of the Savannah River, while the lowland, swampy forests adjacent to the river itself remained largely untouched (Ruffin 1992; White 2004). Transporting log-rafts by the release of water from dams, and flooding the streams was the primary way to move lumber towards the coast (White 2004), and was likely one of the main erosional and depositional mechanisms along SRS streams for decades between 1760 and 1830 (Kilgo 2005).

After the Civil War (1865), the recovery of the southern economy depended largely on cotton production (Aiken 1998; White 2004). A post-war increase in farming led to another extensive forest clearing, and an estimated two-thirds of the wetlands in the SRS were drained (White 2004). By 1925, the areal extent of remaining woodlands surrounded by cultivated land had decreased from 66% to 33% (White 2004), and by 1938, 70% of SRS wetlands were impacted by logging operations (Mackey and Irwin 1994). Mechanized farming practices were introduced to the area in the 1930s, and dramatically increased soil erosion here (White 2004).

When the U.S. Atomic Energy Commission (DOE's predecessor) took ownership of the newly formed SRS in 1951, the U.S. ForestService (USFS) was granted authority to restore most of the area to natural woodlands and wetlands (Savannah River Operations Office, 1959). According to the U.S. Army Corps of Engineers' (USACE) 1951 inventory,

about 48,724 ha were classified as forestland, including 25,643 ha of pine, 10,296 ha of hardwood, 11,021 ha of swamp, and 1,764 ha of plantation, as well as 32,265 ha of agricultural land. The main USFS directive was to reforest the abandoned farm land. By 1960, 24,000 ha of trees had been planted (White 2004). Figure 2 shows that by 2013, almost all of the SRS had been reforested, except areas still maintained for the production of radioactive materials, and the storage of nuclear waste. This is a dramatic contrast with the surrounding areas, which experiencedwidespread agricultural and urbanized land use (Fig. 2).

Ecological restoration efforts at the SRS occurred regularly during the 1950s and 1960s, including planting of longleaf pine, prescribed burning efforts, removal and draining of impoundment ponds, and the reintroduction of animal species, such as the eastern wild turkey and red-cockaded woodpecker. These efforts have continued to the present, and now include preserving established wetlands, Carolina bays (ephemeral bays that range in size from <0.1 to 124ha and retain water for most of the year), and savannas, as well as reintroducing hardwoods, such as white oaks (Kilgo 2005). Its 800 km² area has been imaged using aerial photography as far back as 1938, and LiDAR in 2009. Extensive ecological studies have been conducted at the SRS, resulting in many diverse peer-reviewed publications over the last several decades.

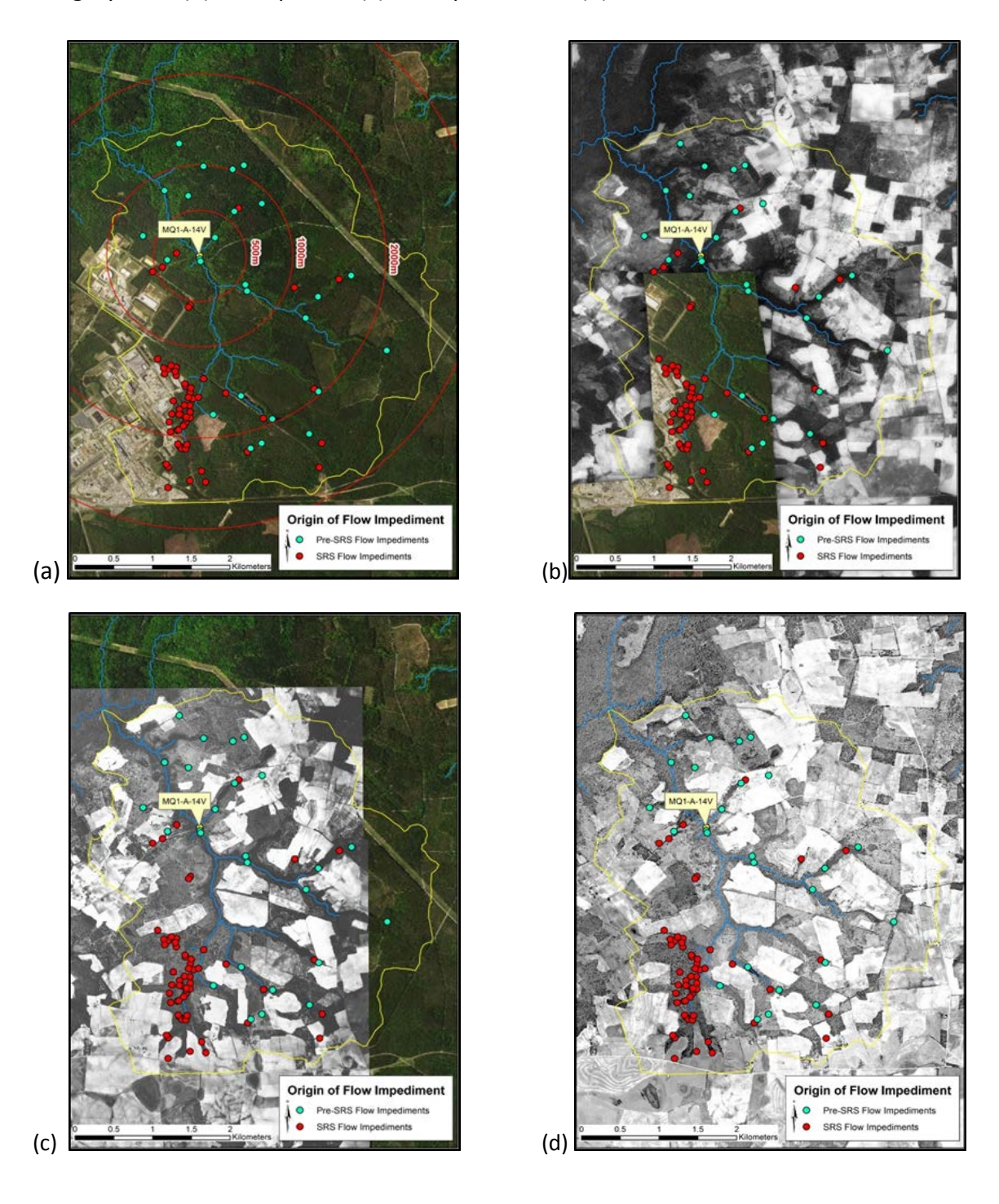
Figure 2: Imagery showing the reforestation of the SRS (Google Maps 2013).



2.1.2 Station MQ1-A-14V

Stream characteristics of all sub-basins can be found in Appendix E (modified from Fletcher et al. 2012). The McQueen Branch (Fig. 3) of the Upper Three Runs stream has a drainage area of 11.59km², and a drainage perimeter of 16.22 km. The main stream length is 5.20 km, with a cumulative stream length of 10.40 km. Annual base flow discharge was calculated using measurements from the United States Geological Survey's (USGS) National Water Information System (NWIS) over several years in the 1990s and 2000s and was 2.17 m³ s⁻¹. The SRS has identified 84 flow impediments in the McQueen Branch sub-basin; 26 of these were identified on aerial imagery before 1951 (year of SRS acquisition), and 58 were created after 1951. Most pre-SRS impediments are related to both currently active and abandoned road crossings. The five impediments not related to road crossings include three levees and two general obstructions. These two obstructions, found ~0.5 km upstream of core MQ1-A-14V, are most likely remnants of a historical stream crossing that was partially breached before 1943, as the crossing does not appear on the 1943 imagery. Most of the impediments of SRS-origin are directly related to the industrialized area in the western part of the sub-basin. These include active road and railroad crossings, levees, culverts, outfall and waste runoff pipes, a fire lane, and rip rap used to prevent bank erosion. The majority of the impediments, including those due to industrialization, are upstream of the location where core MQ1-A-14V was taken. The closest flow impediments to the location of core MQ1-A-14V are ~100 m upstream, and include an abandoned, breached levee, and an active road crossing with culverts. Both of these impediments are pre-SRS in origin, and exhibit evidence of beaver impaction (Fletcher et al. 2012).

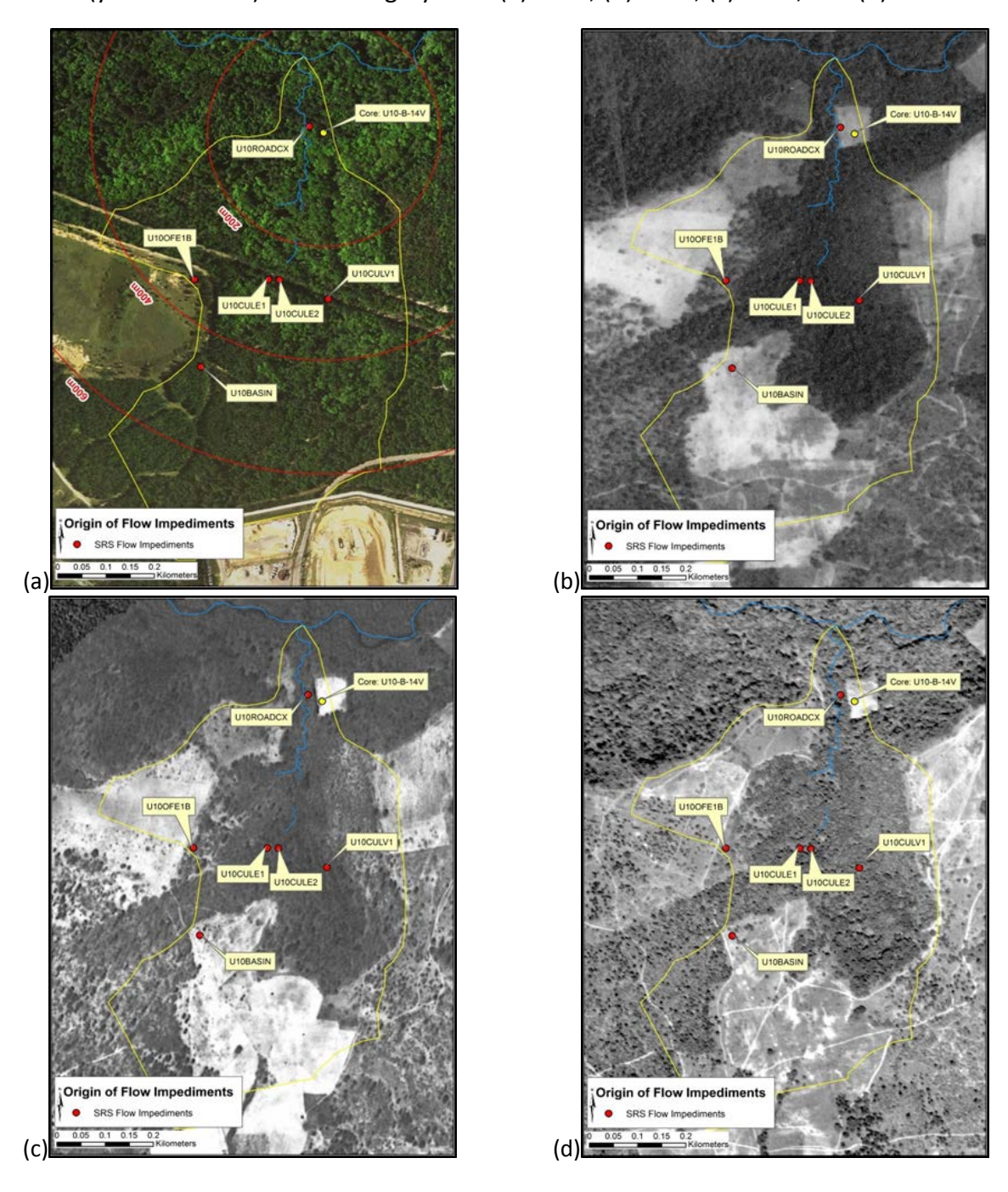
Figure 3:Locations of pre- and post-SRS flow impediments within the MQ1-A-14V subbasin (yellow outline). Colored aerial imagery from (a) 2013; black and white aerial imagery from (b) 1938-partial, (c) 1942-partial, and (d) 1951.



2.1.3 Station U10-B-14V

The Upper Three Runs basin (U-10) (Fig. 4) has a drainage area of 0.277 km², and a drainage perimeter of 2.546 km, which makes it the smallest sub-basin in this study. The drainage area of U-10 was significantly decreased by construction of an adjacent burial ground and borrow pit in the mid-1980s. The main stream length is 0.473 km, with a cumulative stream length of 0.528 km. Base flow discharge was 0.0045 m³s⁻¹. The SRS has identified six flow impediments in the U-10 sub-basin. All six are of SRS origin, and five of them are located upstream of the location where core U10-B-14V was taken. Three of these are culverts from an inactive railroad crossing, although only the middle culvert was observed to significantly impede water flow due to sediment and root build-up. The other two upstream impediments are related to the adjacent borrow pit, and include an emergency overflow standpipe, and an active service road. The overflow standpipe does not appear to be a source of flow, as the entire borrow pit (> 90,000 m²) would need to be flooded for the overflow pipe to function. The closest impediment to the location of core U10-B-14V is an active road crossing ~35 m away. It was built between 1982 and 1986, with no observed beaver activity or upstream obstructions (Fletcher et al. 2012).

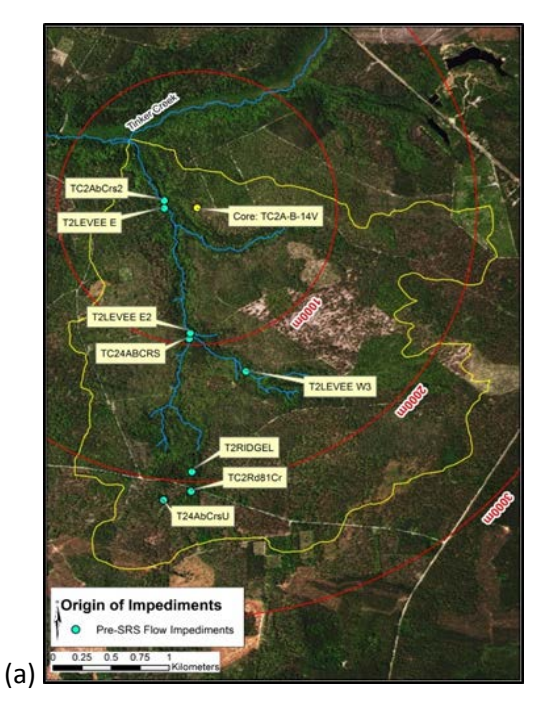
Figure 4:Locations of pre- and post-SRS flow impediments within the U10-B-14V subbasin (yellow outline). Aerial imagery from (a) 2013, (b) 1938, (c) 1942, and (d) 1951.

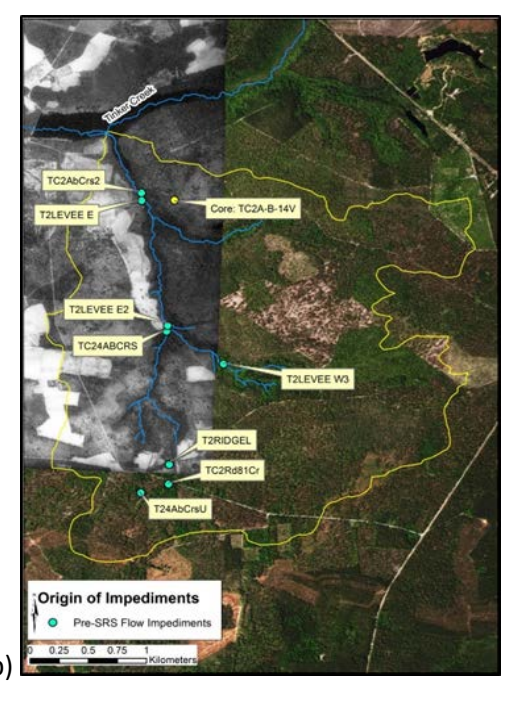


2.1.4 TC2A-B-14V and TC2B-B-14V

The Tinker Creek basin, designated TC-2 (Figs. 5 and 6), has a drainage area of 6.65 km² and a drainage perimeter of 13.84 km. The main stream length is 2.92 km with a cumulative stream length of 6.79 km. Base flow discharge was 0.086 m³s⁻¹. The SRS has identified eight flow impediments in the TC-2 sub-basin. All of these are pre-SRS in origin, and no SRS outfalls are located in the TC-2 sub-basin. They are all created by levees and road crossings, but no active roads currently cross the perennial stream. All of the levees and crossings now have narrow breaches allowing water flow, and there is no evidence of any recent beaver activity impeding flow. An active road crossing and abandoned dam are located ~600 m downstream of the confluence of the TC-2 tributary with Tinker Creek (not shown in Figs. 5 and 6). The dam was breached after 1951, and has since been impacted by beavers. Previous to the breach, the dam impounded Kennedy Pond. However, the areas from which both cores TC2A-B-14V and TC2B-B-14V were taken were not flooded in either the 1942 or 1951 photos (Fletcher et al. 2012).

Figure 5:Locations of pre- and post-SRS flow impediments within the TC2A-B-14V subbasin (yellow outline). Colored aerial imagery from (a) 2013; black and white aerial imagery from (b) 1942-partial, and (c) 1951.





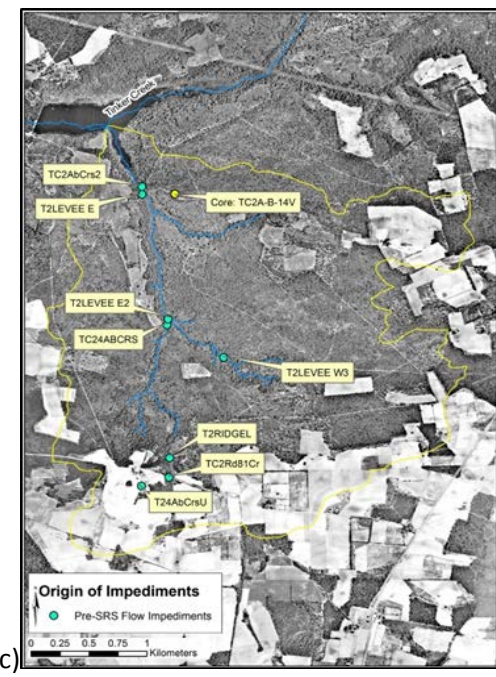
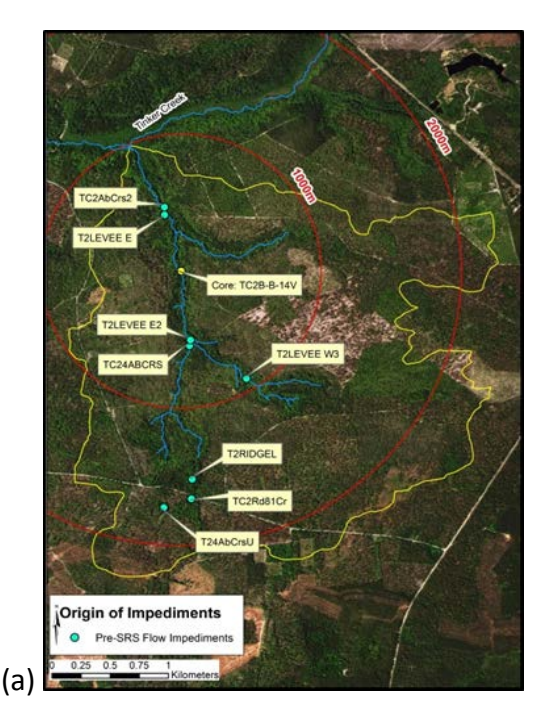
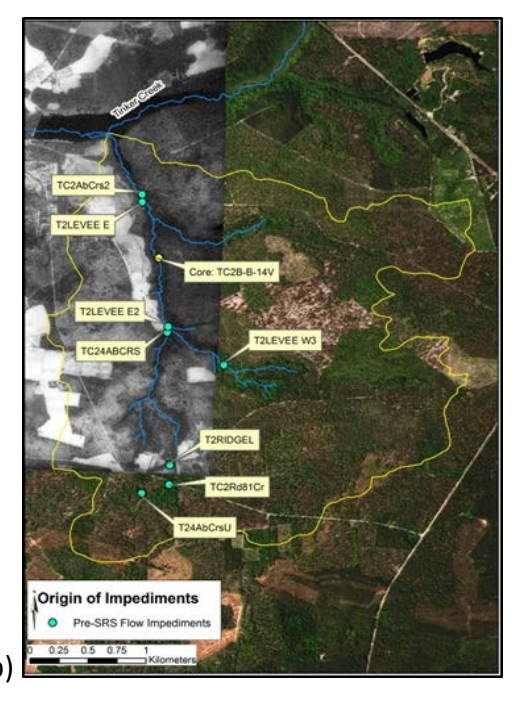
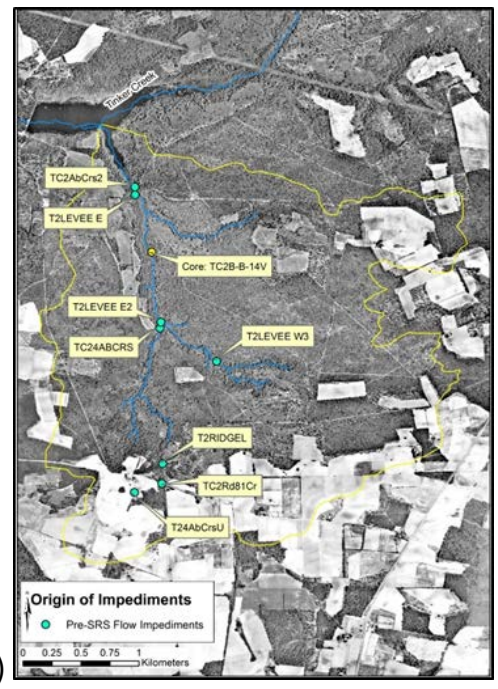


Figure 6:Locations of pre- and post-SRS flow impediments within the TC2B-B-14V subbasin (yellow outline). Colored aerial imagery from (a) 2013; black and white aerial imagery from (b) 1942-partial, and (c) 1951.



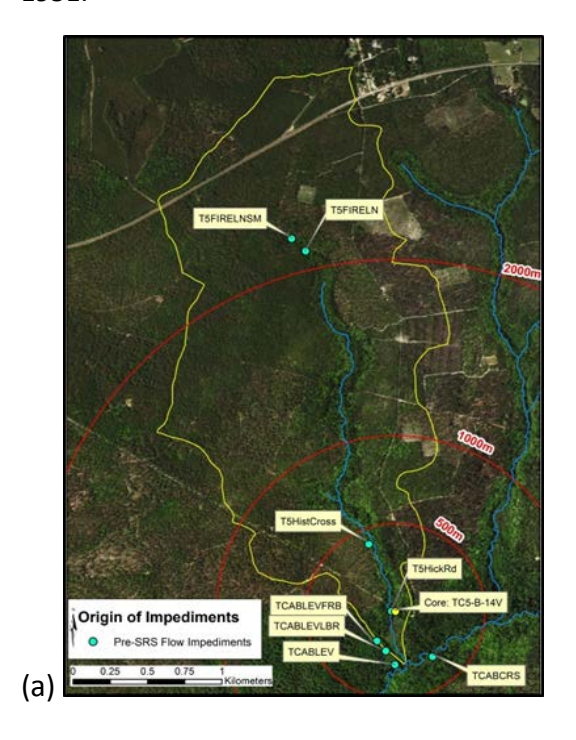


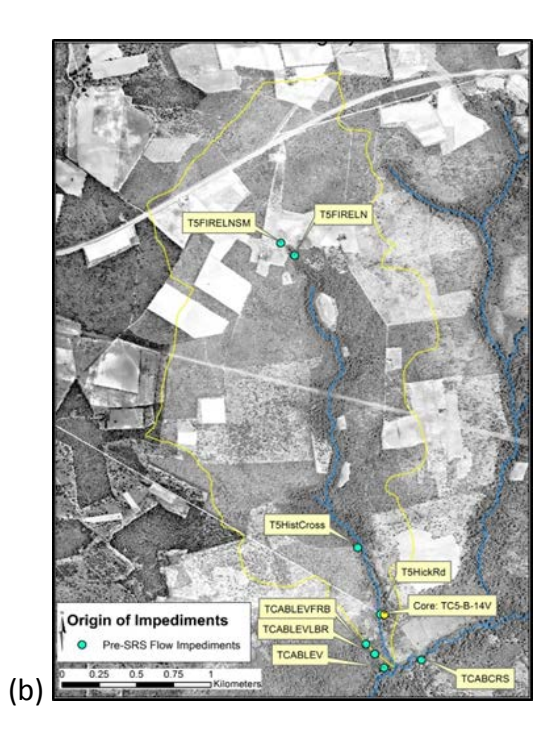


2.1.5 TC5-B-14V

The Tinker Creek sub-basin, designated TC-5 (Fig. 7), has a drainage area of 3.38 km² and a drainage perimeter of 9.49 km. The main stream length is 2.68 km with a cumulative stream length of 2.81 km. Base flow discharge was 0.044 m³s⁻¹. The SRS has identified eight flow impediments in the TC-5 sub-basin. All of these are pre-SRS in origin, and no SRS outfalls are located in the TC-5 sub-basin. The two obstructions farthest upstream are an abandoned road that has been converted to a fire lane. It remains intact, but does not inhibit flow; surface runoff is minimal. An abandoned road crossing is located ~450 m upstream from core TC5-B-14V, running perpendicular across the stream channel. The levee narrows the floodplain, but is not considered a major impediment to flow. Hickson Mill Road is an active crossing built sometime between 1943 and 1951, and is located ~20 m from the core location. There is one culvert that allows water flow, and no beaver activity was evident. There is a steep gradient of boulder-sized rubble on the downstream side of the culvert, which impedes flow during low water levels. An abandoned dam with three obvious breaches is located < 100 m downstream from the confluence of the TC-5 tributary with Tinker Creek. It was not intact in the 1938 or 1951 imagery, but would have created a large pond before it was breached. Given the proximity of this dam to the location of core TC5-B-14V, and the time frame of this study (~100 y), there may be some evidence of the pond in the core (Fletcher et al. 2012).

Figure 7:Locations of pre- and post-SRS flow impediments within the TC5-B-14V sub-basin (yellow outline). Colored aerial imagery from (a) 2013; black and white aerial imagery from (b) 1951.

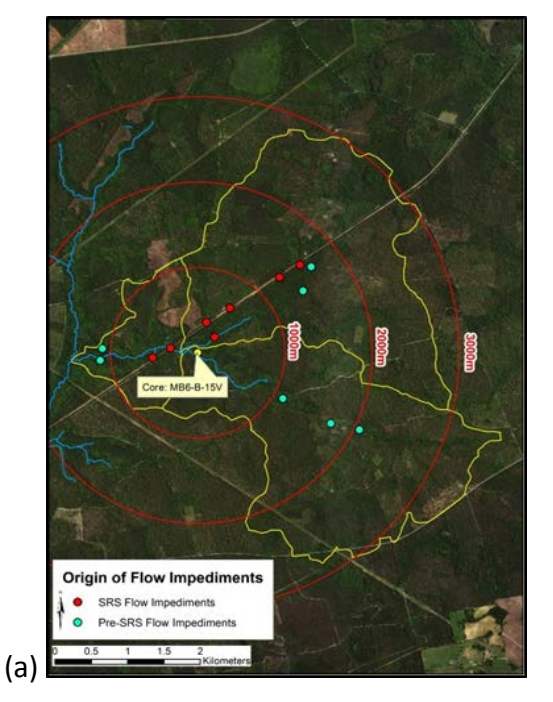


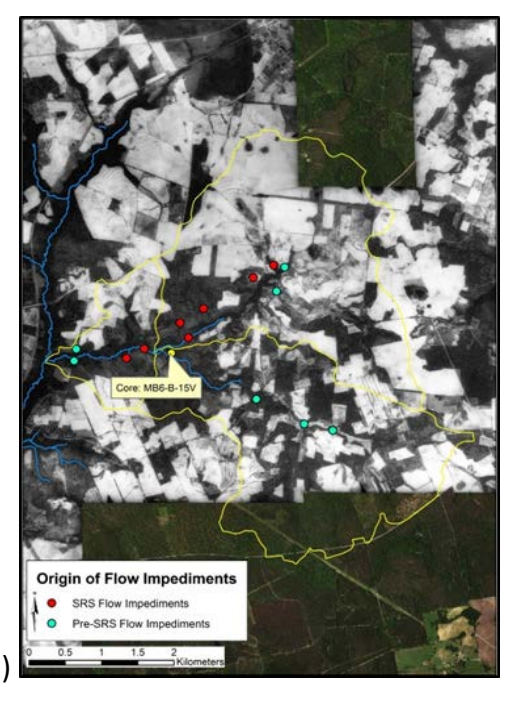


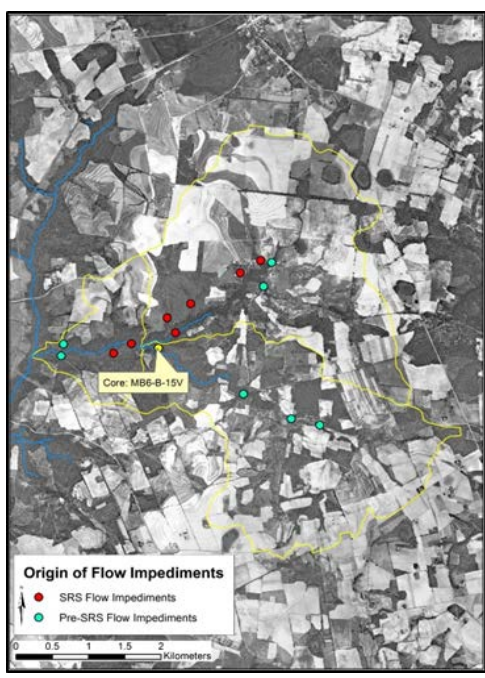
2.1.6 MB6-B-15V

The Meyers Branch sub-basin, designated MB-6 (Fig. 8) has a drainage area of 12.70 km² and a drainage perimeter of 18.50 km. The main stream length is 2.92 km, with a cumulative stream length of 4.14 km. Base flow discharge was 0.033 m³s⁻¹. The SRS has identified14 flow impediments in the MB-6 sub-basin. Seven of these are of pre-SRS in origin, and the other seven are post-SRS. Six of the seven post-SRS impediments are culverts related to an active railroad levee that bisects the MB-6 sub-basin. This levee was constructed between 1951 and 1955, in response to regulations pertaining to the proximity of the previous railroad to the nuclear reactor. Building this levee was a large construction effort, which greatly disturbed the surrounding area. At its closest point, the railroad is located ~275 m from the location of core MB6-B-15V, but the closest upstream culvert is ~430 m away. The other post-SRS impediment is a small dam structure of unknown origin, located ~320 m upstream from core MB6-B-15V, on the northern tributary. It appears to be a natural structure, either a root dam or beaver impaction. Water was observed flowing under the dam in 2005; however, in 2009, a 50 cm tall beaver dam had been constructed to reinforce the impediment, flooding the stream channel. The three southern, pre-SRS flow impediments are from an active secondary road crossing, which is present on both the 1938 and 1951 aerial photos. The western-most impediment of these three is the only one with a culvert. The two northern, pre-SRS flow impediments are from an active road, and levee, that are visible on the 1938 and 1951 aerial photos. Despite surface runoff eroding the roads, it has been observed that most runoff is blocked by the levee. Coupled with its location far upstream in the ephemeral stream valley, it is determined that there is no impact to the stream under current forested conditions. This may not have been the case under past agricultural practices. The only two pre-SRS flow impediments downstream from the core location result from a ~1 m tall earthen levee composed of sand and gravel. The levee was breached in the middle, but has been dammed by beavers in the recent past. It had formed a large beaver pond between 1996 and 2006 before being removed (Fletcher et al. 2012).

Figure 8:Locations of pre- and post-SRS flow impediments within the MB6-B-15V sub-basin (yellow outline). Colored aerial imagery from (a) 2013; black and white aerial imagery from (b) 1942-partial, and (c) 1951.







2.1.7 MBM-A-14V and ODB-1B-14V

The entire Meyers Branch sub-basin, which includes the cores MBM-A-14V (Fig. 9), ODB-1B-14V (Fig. 10), and the previously described MB6-B-15V, has a drainage area of 49.69km², and a drainage perimeter of 37.98km. The main stream length is 11.22km, with a cumulative stream length of 34.61km. Base flow discharge was 0.210 m³ s⁻¹.The SRS has identified 75 flow impediments in the Meyers Branch sub-basin. Fifty two of these are pre-SRS in origin, and the other 23 are post-SRS. Besides the impediments described in the MB-6 sub-basin, most of the other post-SRS impediments in this basin are directly related to the northern, industrialized area, located ~6,200m from MBM-A-14V, and ~4,100m from ODB-1B-14V. They include several culverts from active road crossings and wastewater management outfalls. Most of the pre-SRS impediments are directly related to both active and abandoned road crossings. There are two small, abandoned dams located ~2,200m from ODB-1B-14V, and ~4,300m from MBM-A-14V. Neither dam appears on the 1938 aerial photos, but both dams show impounded ponds on the 1951 photos; the upper pond is larger. Currently, these dams have not been breached, and both impound small ponds. These dams have been observed obstructing flow during non-drought years. A third dam is located~1,300m upstream from MBM-A-14V, just above the confluence between the main branch and a small tributary. This is a 3m tall, historical dam visible on both the 1938 and 1951 aerial imagery. The 1951 photos show exposed soil on the dam, possibly indicating renovation attempts. It currently has a narrow breach in the middle allowing water flow (Fletcher et al. 2012).

Figure 9:Locations of pre- and post-SRS flow impediments within the MBM-A-14V subbasin (yellow outline). Colored aerial imagery from (a) 2013; black and white aerial imagery from (b) 1942-partial, and (c) 1951.

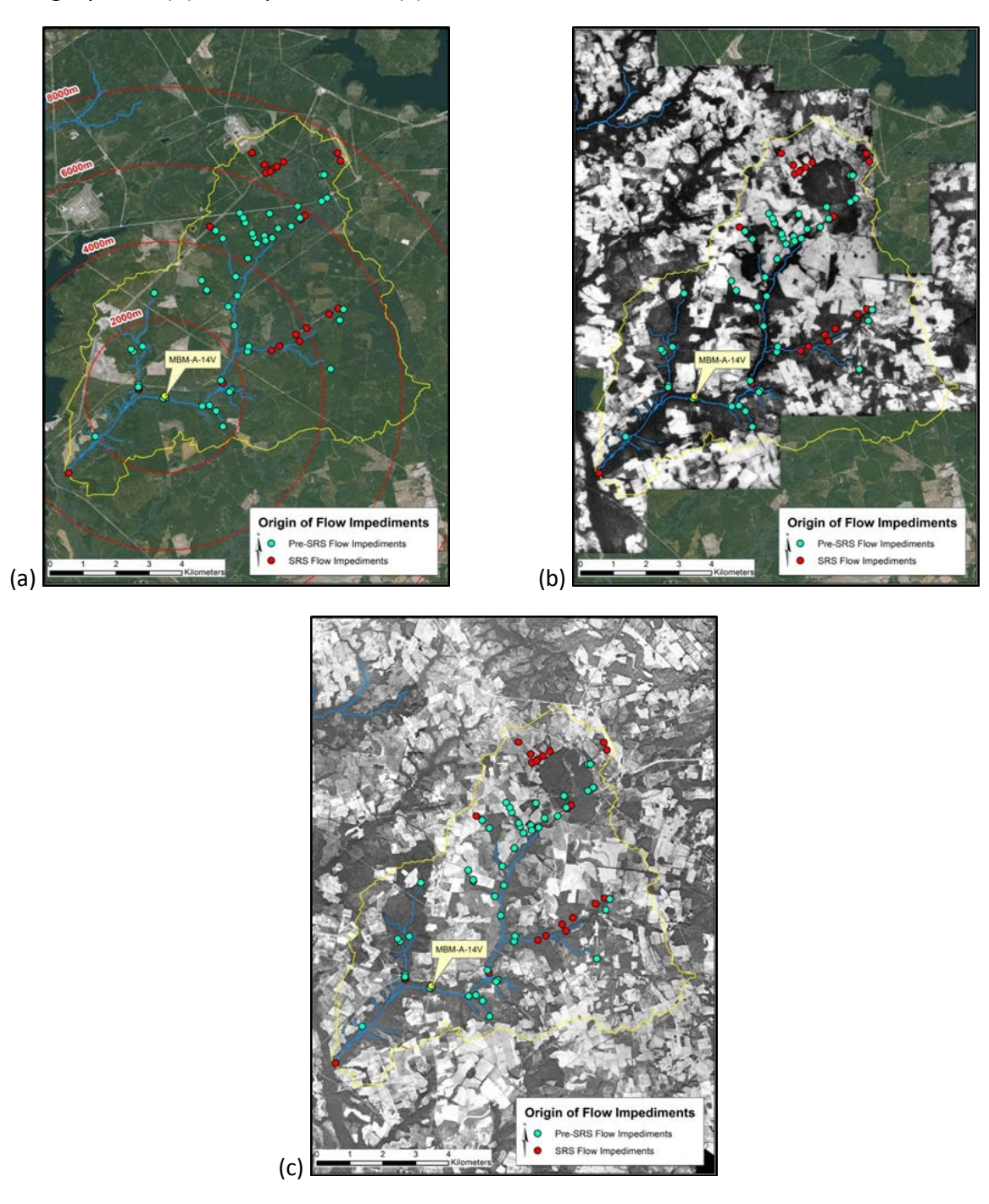
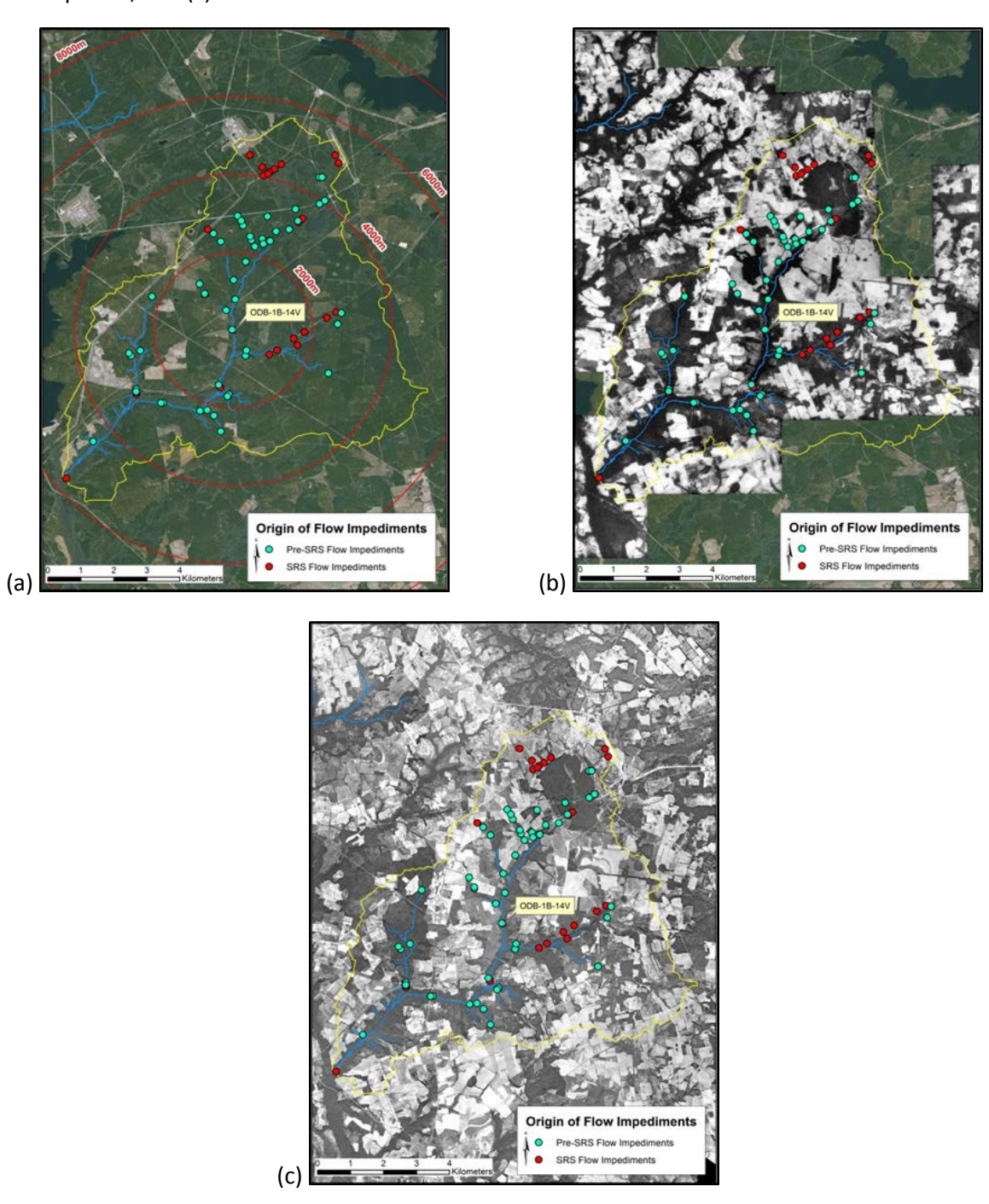


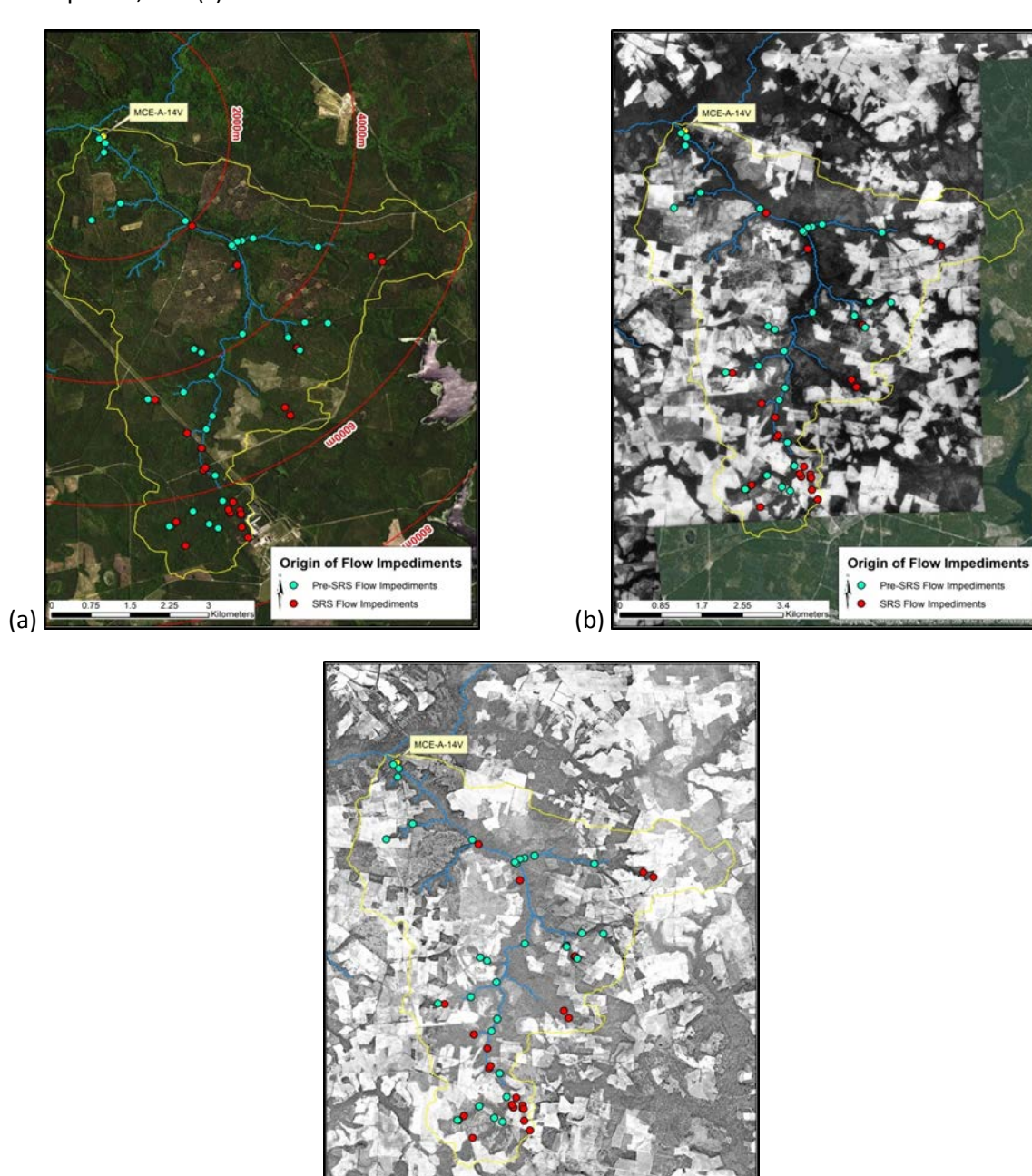
Figure 10:Locations of pre- and post-SRS flow impediments within the ODB-1B-14V sub-basin (yellow outline). Colored aerial imagery from (a) 2013; black and white aerial imagery from (b) 1942-partial, and (c) 1951.



2.1.8 MCE-A-14V

The Mill Creek basin, designated MCE (Fig. 11), has a drainage area of 23.44km² and a drainage perimeter of 28.03km. The main stream length is 9.36km, with accumulative stream length of 20.39km. Base flow discharge was 0.284 m³ s⁻¹. The SRS has identified 56 flow impediments in the MCE sub-basin. Of these, 32 are of pre-SRS origin, and the other 24 are post-SRS. The majority (25) of the pre-SRS flow impediments are related to active and abandoned road crossings, with the remaining seven being dams. The closest impediment to core MCE-A-14V is located ~100m upstream from the core. The dam appears to have been breached before 1938, since no impoundment is seen on either the 1938 or 1951 imagery. Currently, there is a narrow breach in the center and erosional breaks on the east side. Severe beaver activity has been noted in the recent past along the floodplain upstream of the dam. Another dam is located ~2,300m upstream of MCE-A-14V, on the main branch of Mill Creek. As with the previous dam, an impoundment is not visible on either the 1938 or 1951 imagery, implying that it was breached before 1938. There are currently several breaches across the abandoned dam, but beaver activity has been noted in the past, and several old beaver dams are still present upstream. A third dam is located ~2,500m upstream of MCE-A-14V, along a tributary of Mill Creek. Like the previous dams, no impoundment is visible on any imagery, and a narrow breach allows water flow. Unlike the previous dams, no beaver activity in the area was observed. The other four dams are located > 4km upstream from the core location. All but one of the post-SRS flow impediments are directly related to active road crossings and culverts for wastewater/overflow management. The post-SRS dam is located ~5,800m upstream from core MCE-A-14V, and is a partially breached, abandoned beaver dam. It includes rooted trees growing on the ridge and alters the hydrology around it. Water is impounded above the dam, although water flows over the dam in multiple areas (Fletcher et al. 2012).

Figure 11:Locations of pre- and post-SRS flow impediments within the MCE-A-14V sub-basin (yellow outline). Colored aerial imagery from (a) 2013; black and white aerial imagery from (b) 1942-partial, and (c) 1951.



Pre-SRS Flow Impediments

2.2 Previous Research

2.2.1 Floodplain Sedimentation

Floodplains are important areas, which affect the water quality of streams, provide unique wildlife habitats, and help attenuate flooding (Conner and Day 1982; Burgess et al. 2013; Varga et al. 2013). They also provide sites for nutrient uptake during flooding, serve as sinks for organic and inorganic carbon, and facilitate dissolved and particulate fractionation of nitrogen and phosphorus (Tockner et al. 2002; Noe and Hupp 2005). Floodplains can also be important as nursery habitats for fisheries (Welcomme 1979; Burgess et al. 2013), and they support regional biodiversity as an ecotone between aquatic and terrestrial environments (Kuiper et al. 2014; Clarke 2014).

Craft and Casey (2000) calculated sediment deposition rates for several depressional wetlands and floodplains along rivers in southwestern Georgia. They averaged 100-year rates of sediment deposition on floodplains at $0.1036 \, \mathrm{g \ cm^{-2} \ y^{-1}}$. They also observed that these were much higher than 30-year rates (0.0118 g cm⁻² y⁻¹), concluding that this is attributed to the greater number of farms and livestock grazing at the turn of the century. Noe and Hupp (2005)have calculated sediment accumulation rates along Piedmont riversat between 0.02 and 0.50 g cm⁻² y⁻¹.

2.2.2 Land Use

Floodplain characteristics are linked to the effects of land use and hydrologic connectivity (Noe and Hupp 2005; Varga et al. 2013). Land use has been found to affect the rates of erosion, transportation, and deposition of sediments along stream channels and floodplains (e.g., Hupp 1992; Ross et al. 2004; Restrepo et al. 2015). Urbanized and agricultural land uses often result in the disconnection friver channels from floodplains by channelization, and/or by the construction of levees and dams (e.g., Sparks 1995), often decreasing sediment accumulation rates on floodplains (Poff et al. 1997; Wohl 2015). For example, a study by Ross et al. (2004) found that sedimentation rates in the Piedmont zone increased from 0.19 – 3.2 mm y⁻¹ in channelized floodplains farther

from urbanized areas, to 3.0 – 7.2 mm y⁻¹ in floodplains near urbanized areas. Land use change has become a significant, global issue. In the U.S., 121,000km² of land was converted to urban uses between 1982 and 1997 (Natural Resources Conservation Service 1999; Agarwal et al. 2002). Ramankutty and Foley (1999) estimated that nearly 1.2 million km² of forest and woodland, and 5.6 million km² of grasslands have been converted to other uses in the past 300 years, globally. Theseland use changes can greatly increase sediment transport rates, both by wind and water.

2.2.3 Hydrologic Connectivity

Noe and Hupp (2005)concluded that hydrologic connectivity between channels and floodplains, and land use, have large effects on floodplain sedimentation. For example, urbanized sub-basins have higher rates of sediment deposition downstream than forested sub-basins, and reduced hydrologic connectivity between channels and floodplains limits sediment accumulation(Hupp 1992; Kleiss 1996; Ross et al. 2004). Understanding the relative importance of the factors determining the production, transportation, and storage of sediment within fluvial systems will allow researchers to more accurately predict the probable future paths of geomorphic change. Fluvial geomorphologists can use this information to determine where future sediment erosion and accumulation zones are most likely to be. This research could also lead to a greater understanding of river recovery potential, landscape sensitivity, and how local biota are affected by and respond to restoration efforts (Fryirs et al. 2007).

Recently, researchers have acknowledged the need to look beyond traditional Hortonian infiltration processes, and the variable source area (VSA) model, when describing generated runoff (McDonnell 2003; Ambroise 2004). Hydrologic connectivity is one possible successor to these models (Bracken and Croke 2007). Hydrologic connectivity is defined as the water-mediated transport of matter, energy, and/or organisms within or between elements of the hydrologic cycle (Freeman et al. 2007). This term can be further sub-divided into three broad categories: (1) landscape connectivity, which describes the physical coupling (or decoupling) of landforms within a

sub-basin, (2) hydrological connectivity, which expresses the passage of water from one part of the landscape to another, and (3) sediment connectivity, which describes the transfer of sediments through the sub-basin (Bracken and Croke 2007). For the purposes of this thesis—and in many published papers—the term "hydrologic connectivity" will be used to refer to <u>all</u> of these situations.

Table 3 from Bracken et al. (2013)'s review, shows the locations of 21 study sites from published research dealing with hydrologic connectivity. Researchers have concentrated on small, temperate, forested sub-basins with steep slopes and relatively deep soils, much like the SRS. Bracken et al. (2013) categorized the research of hydrologic connectivity into five different approaches by studying: (1) soil-moisture connectivity and water-table connectivity, (2) flow-process connectivity, (3) terrain connectivity, (4) models of hydrological connectivity, and (5) indices of hydrological connectivity.

Terrain connectivity examines topographic controls on run-off and flood production, such as levees, dams, and culverts, as well as the effects of land use. Noe and Hupp (2005) used carbon, nitrogen, and phosphorus accumulation rates to compare subbasins with different land uses (urban, forested, and agricultural). They also used these accumulation rates to compare areas of the same land use that had varied hydrologic connectivity. Their results were that "...watershed land use has a large effect on sediment and nutrient retention in floodplains, and that limiting the hydrologic connectivity between river channels and floodplains minimizes material retention by floodplains." (Noe and Hupp 2005). They concluded that streams with urbanized headwaters had greater downstream, floodplain sediment accumulation rates than comparable streams with vegetated headwaters. They also concluded that the greater the hydrologic connectivity between channels and floodplains, the greater the floodplain sediment accumulation rates. However, they did not study whetherheadwater area land use or hydrological connectivity has a greater effect on floodplain sediment accumulation rates.

A stream channel can be connected, or disconnected, to the landscape in three ways:(1) longitudinal connectivity describes how well a channel can transport water, energy, and sediment in an upstream-to-downstream, or tributary-to-trunk, direction;(2)lateral connectivity describes a stream's ability to transport water, energy, and sediment in a slope-to-channel or channel-to-floodplain direction (channel-to-floodplain connectivity is controlled by flooding frequency and magnitude of overbank events);and (3)vertical connectivity describes surface-to-subsurface interactions between water and sediments within the floodplain (Fryirs et al. 2007). While these linkages are not independent (e.g., a change in lateral connectivity can have an effect on longitudinal and/or vertical connectivity), this thesis will focus on lateral connectivity between channels and floodplains.

Fryirs et al. (2007) categorized forms of landscape (dis)connectivity into buffers, barriers, and blankets. Buffers are landforms that act to prevent sediment from entering a system. They can affect longitudinal and/or lateral connectivity within a subbasin. Table 3 shows the characteristics of common buffers (Fig. 12). Barriers, however, are defined as landforms that can disrupt the transportation of sediment within the system (Fig. 13). They can also affect longitudinal connectivity (e.g., woody debris) and lateral connectivity (e.g., levees) (Table 4). Finally, blankets (Fig. 14) are landforms that interrupt vertical connectivity by constraining sediment. Table 5 shows characteristics of common blankets, such as channel bed armoring (Fryirs et al. 2007). While all three landform types act to disconnect areas of a sub-basin, the focus of this thesis is on barriers (e.g., levees, dams, culverts, etc.).

Anthropogenic disturbances can have varied effects in different landscapes. For example, some river channels have been substantially altered by human-built dams and reservoirs, disconnecting the transport of sediment longitudinally downstream, but increasing lateral continuity by flooding the area upstream of the dam (Fryirs et al. 2007). Human structures (e.g., dams, levees, culverts) can exercise considerable control of sediment transport for all but the finest suspended sediments (e.g., Brune 1953;

Williams and Wolman 1984; Graf 1999). Human impacts can also alter effective time scales of disturbance recovery via changes in land use. For example, in the Weraamaiasub-basin in New Zealand, deforestation in the 1800 and 1900s made direct slope-to-channel erosion the major source of sediment. However, after reforestation in the 1980s, the dominant sediment source shifted to shallow landslides, resulting in episodic disturbances, which recover after a few years (Fryirs et al. 2007). By determining the relative importance of hydrologic connectivity versus land use, researchers might better predict the probable future paths of geomorphic change, particularly in terms of where future sediment erosion and accumulation zones are most likely to be. By knowing how the landscape will adapt to changes in soil erosion and sediment accumulation zones, the effect on ecological systems can be predicted. This information can also provide a basis to examine river recovery potential, landscape sensitivity, and the effects on local biota through water flow, organic matter processing, and nutrient cycling (Fryirs et al. 2007). With this knowledge, scientists can better design and implement restoration efforts.

Table 3: Characteristics of buffers, adapted from Fryirs et al. (2007).

Form of Buffer	Spatial Scale (m²)	Sedimentary Character	Shape	Postulated Effective Time Scale (y)	Breaching Capacity
Intact valley fills/floodouts	10 ² -10 ³	Fines	Elongate to lobed	10 ³ -10 ⁴	Extreme event; infrequently reworked/breached
Floodplain pockets	10 ¹ -10 ³	Mixed	Elongate and stepped	10 ³ -10 ⁴	Overbank flow stage; infrequently reworked/breached
Continuous floodplains	10 ¹ -10 ³	Mixed	Elongate and stepped	10 ³ -10 ⁴	Extreme event; infrequently reworked/breached
Alluvial fans	10 ² -10 ³	Mixed	Conical	10 ² -10 ⁴	Extreme event; infrequently reworked/breached
Piedmont zones	10 ³	Mixed	Planar	10 ³ -10 ⁴	Extreme event; infrequently reworked/breached
Terraces	10 ² -10 ³	Sands and gravels	Elongate and stepped	10 ³ -10 ⁴	Extreme event; infrequently reworked/breached
Trapped tributary fills	10 ² -10 ³	Fines	Irregular	10 ² -10 ⁴	Overbank flow stage; infrequently reworked/breached

Figure 12: Examples of buffers impeding sediment transport into channels, including (a) swamps, (b) alluvial fans and piedmonts, (c) trapped tributary fills, and (d) alluvial plains, from Fryirs et al. (2007).

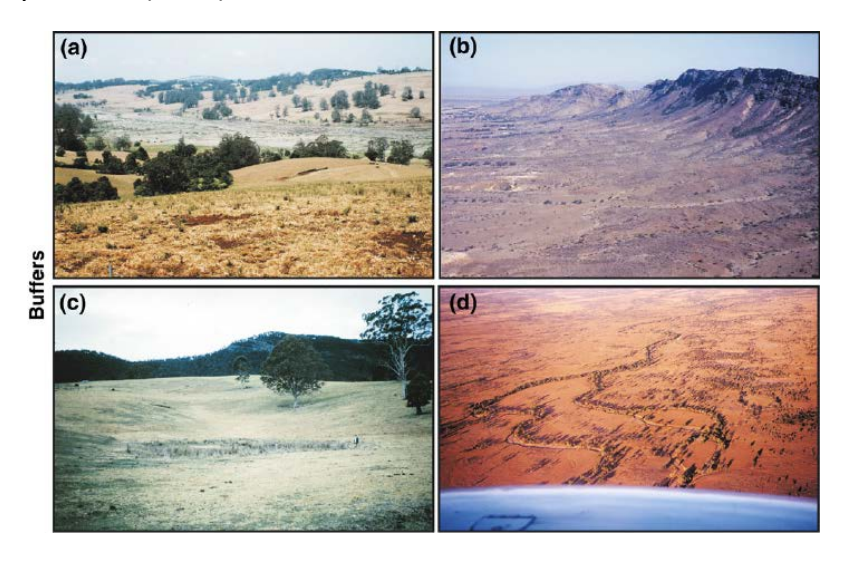


Table 4: Characteristics of barriers, adapted from Fryirs et al. (2007).

Form of Barrier	Spatial Scale (m²)	Sedimentary Character	Shape	Postulated Effective Time Scale (y)	Breaching Capacity
Bedrock steps	10 ⁰ -10 ¹	Bedrock	Stepped, irregular	10 ³ -10 ⁴	Extreme event; infrequently reworked/breached
Valley constriction	10 ² -10 ³	Bedrock	Irregular	10 ³ -10 ⁴	Overbank flow stage; infrequently reworked/breached
Sediment slugs	10 ² -10 ³	Sand or gravel	Elongate and lobed	10 ¹ -10 ³	Channel flows with ability to entrain materials of varying sizes
Channel capacity (width/depth)	10 ¹ -10 ²	Mixed	Symmetrical, asymmetrical, irregular	10 ¹ -10 ³	Channel flows with ability to entrain materials of varying sizes
Woody debris	10 ¹ -10 ²	N/A	Irregular	10 ¹ -10 ⁴	Channel flows with ability to entrain materials of varying sizes
Dams	10 ²	N/A	N/A	Permanent unless removed	Extreme event; infrequently reworked/breached

Figure 13: Examples of barriers impeding sediment transport along the channel, including (a) valley constrictions, (b) dams, (c) large woody debris, and (d) sediment slugs, from Fryirs et al. (2007).

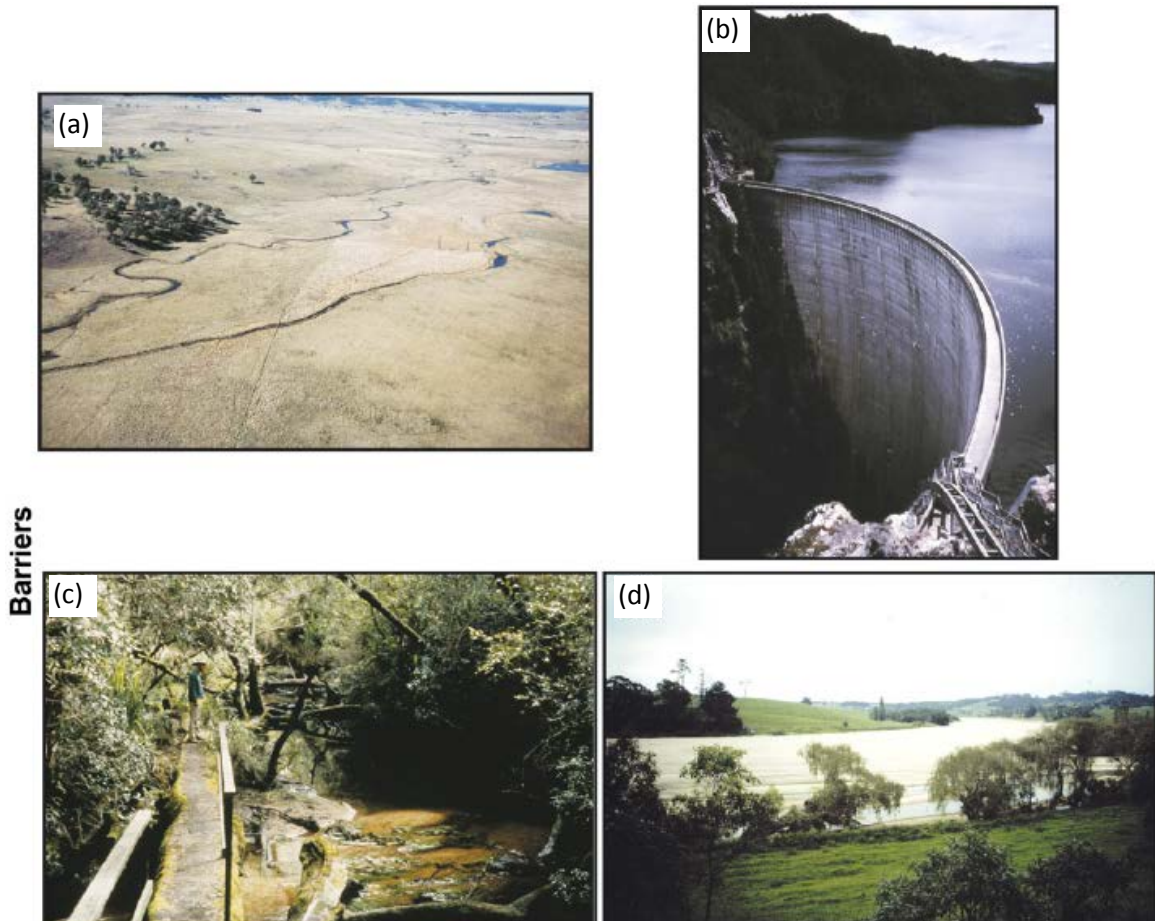
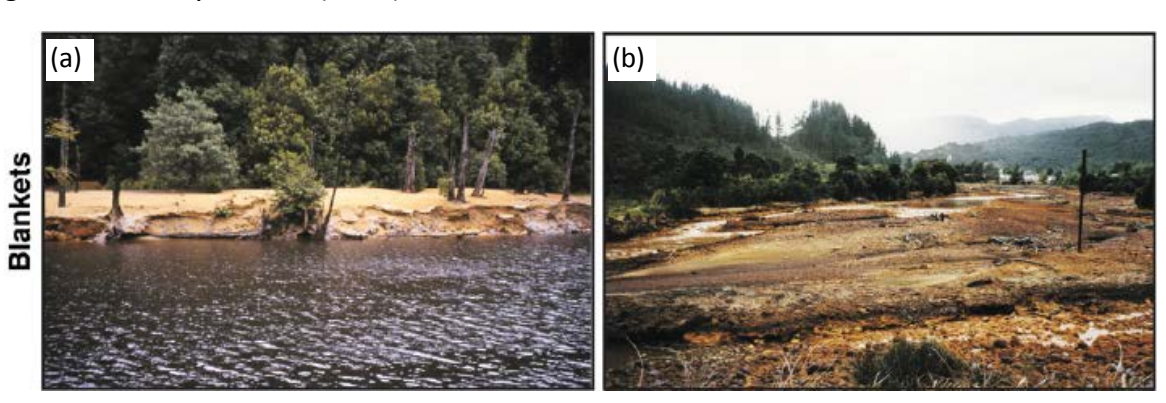


Table 5: Characteristics of blankets, adapted from Fryirs et al. (2007).

Form of Blanket	Spatial Scale (m²)	Sedimentary Character	Shape	Postulated Effective Time Scale (y)	Breaching Capacity
Floodplain sediment sheets	10 ¹ -10 ³	Mixed	Planar sheets	10 ¹ -10 ³	Overbank flow events; recurrently reworked/breached
Fine-grained materials in interstices of gravels	10 ⁻¹ - 10 ¹	Fines	Planar, draped	10 ⁰ -10 ²	Channel flows up to bankfull; recurrently reworked/breached
Channel bed armoring	10 ¹ -10 ²	Mixed but mostly gravels and cobbles	Various	10 ⁰ -10 ²	Channel flows with ability to entrain, armor; recurrently reworked/breached

Figure 14: Examples of blankets impeding vertical transport of sediments, including (a) floodplain sediment sheets, and (b) fine-grained materials within the interstices of gravels, from Fryirs et al. (2007).



CHAPTER THREE: METHODS

Nine sediment cores were taken from different floodplains at the SRS (Fig.15). Floodplain sediment accumulation rates were determined for each of these sites, and compared against land use and hydrologic connectivity data. Acceptable sites were determined by using LiDAR imagery, records kept by the DOE and the USFS, and field observations.

3.1 Lithostratigraphy

3.1.1 Core Collection

Cores were collected using a vibracore system. Once an acceptable location was identified, two cores from the floodplain were taken, approximately 2-5 meters from each other. Both cores were taken on the floodplain, approximately 5-10 meters from the stream channel. Aluminum core sleeves, 20ft.in length, were driven into the ground using a motor and vibrating head connected to the core sleeves by an umbilicus. Coring stopped when met with refusal, the excess tubing was cut off, the top sealed, and the core was recovered using a winch. The bottom of each core was then sealed, and each core was labeled and brought back to the laboratory for processing.

3.1.2 Core Processing

Cores are identified using a simple naming convention, e.g. TC2-A-14V. This name conveys the sub-basin the core was collected from (e.g., Tinker Creek-2), which of the two coresit was (A, B), the year it was collected (e.g., 2014), and what type of core it is (e.g.,V for vibracore). Each core sleevewas scored using a table saw, and splitlengthwise, and the sediment inside was carefully split using a wire and spatula. Care was taken to prevent sediment mixing during this process. The sediment was then photographed and described using a Munsell color chart and standard techniques. When the cores were not in use, they were wrapped in moist paper towels and plastic to prevent desiccation.

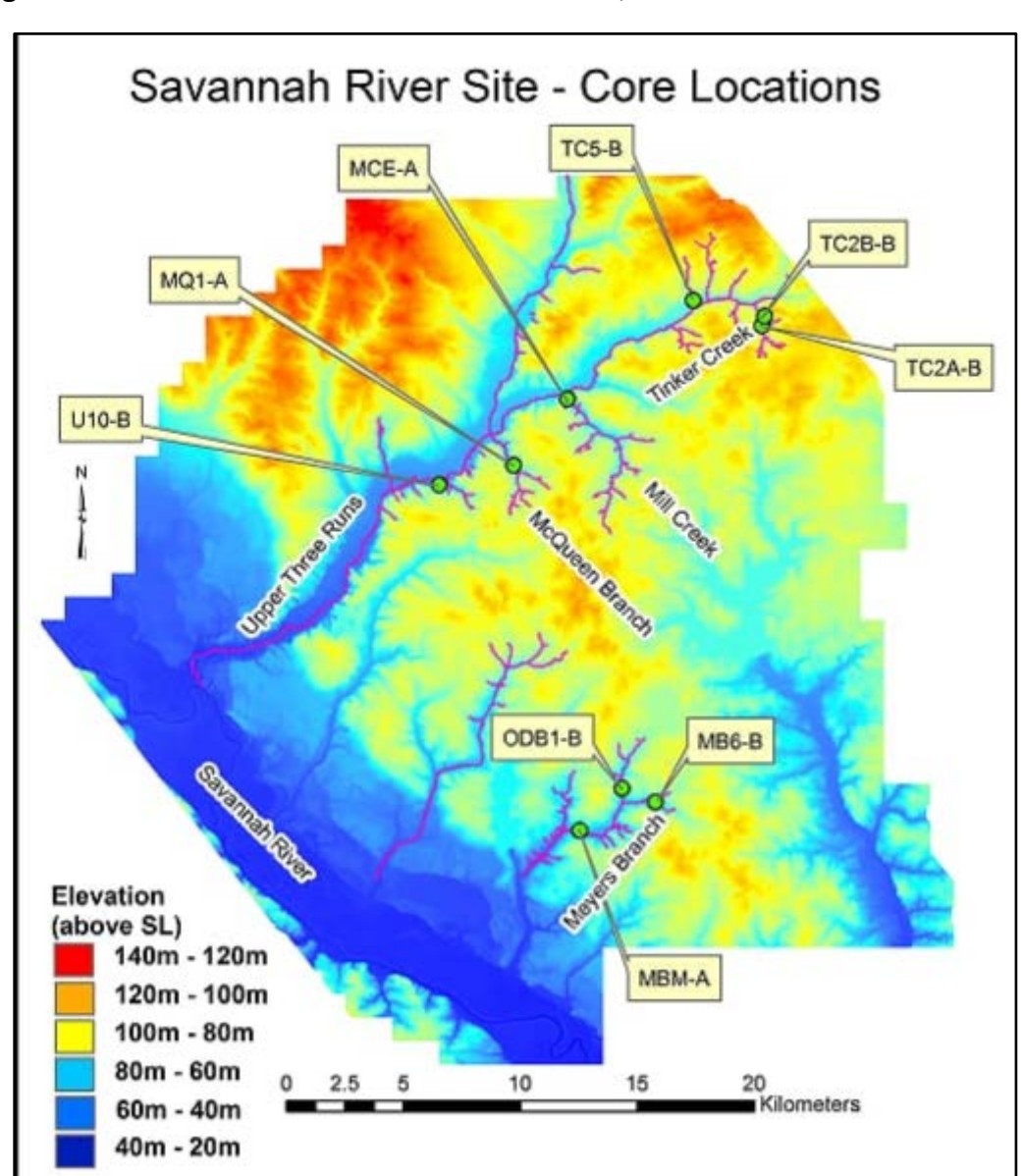


Figure 15:LiDAR-derived elevation data from 2009, and core locations from the SRS.

The cores were then sectioned at 1cm intervals from the surface to a depth of 50cm; after 50cm, the cores were sectioned at 2cm intervals to the end of core. A wet sample of each interval was archived by filling a 1ml amber glass bottle with wet sediment, and was refrigerated. Samples from each interval were then weighed wet, dried for at least two days at 70°C in a convection oven, and then weighed dry in order to calculate % water content.

3.1.3 Particle Size Distributions

Sampleswere weighed (2-2.5 g), placed in 250 mL glass beakers, and disaggregated using sodium hexametaphosphate for 24 hours. Sodium hexametaphosphate acts as a dispersant in wet grain size separation procedures (Plouffe et al. 2001). Any macroorganic matter (> 500 μ m) present was wet sieved, dried in an oven at 70°C, and weighed. After disaggregation, samples were treated with 30% hydrogen peroxide to destroy micro-organic matter (< 500 μ m), which can act as sediment binding agents (Hillier 2001; Yeager et al. 2005). Each sample was rinsed into a 50 mL centrifuge tube, and spun at 2,000-3,000 revolutions per minute in a centrifuge. The samples wererinsed and decanted several times with deionized water to remove hydrogen peroxide. Samples werethen dried in an oven at 70°C. The dried samples were weighed and analyzed using a Malvern Mastersizer S2000 to achieve grain size measurements between 0.02 and 2000 μ m. The Mastersizerprovided percentages of the sand (2 mm-63 μ m), silt (63-4 μ m), and clay (<4 μ m) fractions (Wentworth, 1922) for each sample. The results weredigitally recorded, and the remaining sediment was archived.

3.1.4 Particulate Organic Carbon

Particulate organic carbon (POC) was measured in each core between the surface and 30 cm depth. Approximately 300 mg of sample was placed into a small glass beaker, and 10 ml of 10% HCl was added. These samples were left to react for one hour and placed in a convection oven for another hour at 70°C. After removal from the oven, the samples were rinsed and filtered using 0.4 μm filter paper. The filters were then placed back into the convection oven at 70°C until dry (~two days). The dry samples were then transferred into sample vials. Each sample was packaged into individual tin capsules for analysis using a Costech ECS 4010 CHNS-O Elemental Analyzer.

3.2 Radiochemistry

Three fallout radionuclides were used in this study. Beryllium-7 (7 Be) was used to determine short-term (≤ 1 y) rates of particle mixing (Sharma et al. 1987; Krishnaswami et al. 1980), while sediment mass accumulation rates (MARs) were calculated using two other fallout radionuclides: Lead-210 (210 Pb) and Cesium-137 (137 Cs). Because core shortening can be a limitation withvibracoring, MARs (g cm $^{-2}$ y $^{-1}$) were calculated *in lieu* of linear sediment accumulation rates (cm y $^{-1}$), which were derived later using mean sediment bulk density data over MAR-modeled intervals. All samples were homogenized using a Retsch RM200 mortar mill to a size less than 500 µm, prior to wet chemistry and radiochemical analysis.

⁷Be is the shortest-lived of the three radionuclides, with $t_{1/2}$ = 53.3d. Sediment mixing depths can be identified by examining ⁷Be activity profiles (e.g., Rice 1986; Walling et al. 2013; Xu et al. 2015). Thesedata can also be used to support ²¹⁰Pb and ¹³⁷Cs activity concentration profiles at near-surface locations (Baskaran 2011).

 210 Pb is a daughter isotope in the 238 U decay series (Fig. 16). 226 Ra and 210 Pb strongly adsorb onto fine-grained sediments, such as silts and clays, due to their relatively low solubility in Earth surface environments (e.g., Santschi et al. 1980; Huntley et al. 1995; Noller 2000; Baskaran 2011). 222 Rn, an inert gas, escapes from Earth's surface into the atmosphere, after which it decays into 210 Pb within a matter of days ($t_{1/2}$ = 3.8 d), and adsorbs onto sediments as a solid (Yeager et al. 2004; 2005). With a $t_{1/2}$ = 20.2 y, 210 Pb is the preferred dating method over decadal time scales.

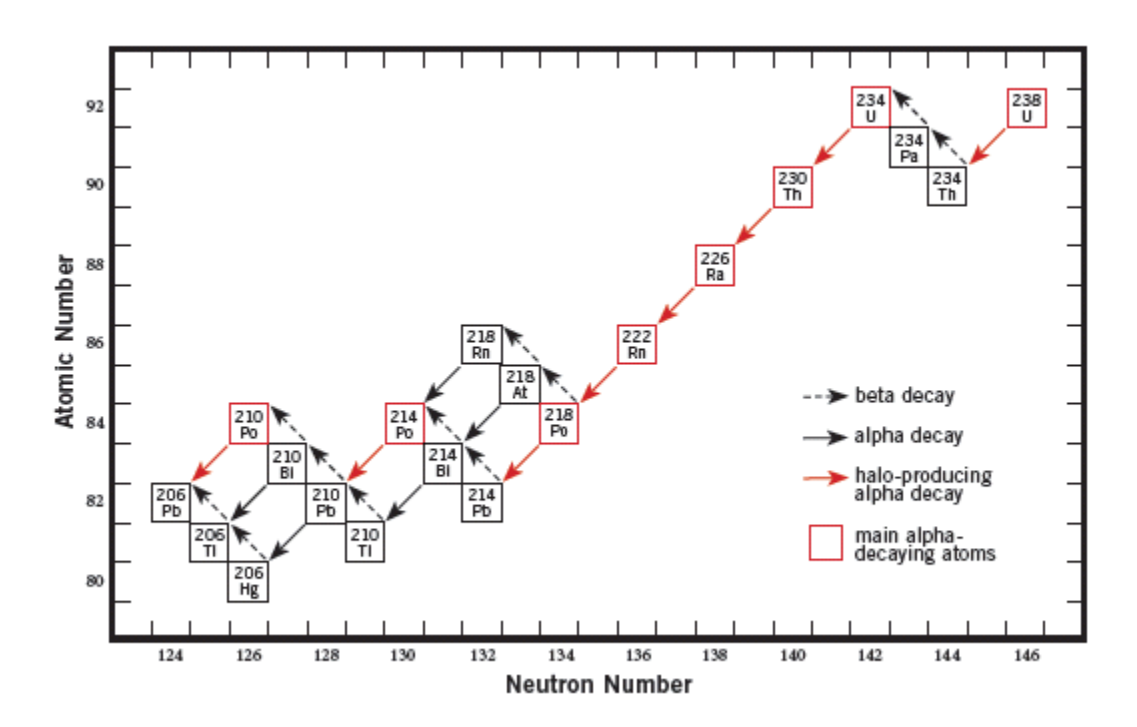
 137 Cs is an anthropogenic fallout radionuclide derived primarily from above-ground nuclear weapon detonations. Like 210 Pb, it can be used to determine sediment MARs. Traces of 137 Cs appear in sediment deposited in 1952-1953 and reached a maximum concentration in 1963—the year before the Partial Nuclear Test Ban Treaty went into effect. Using these data, the activity concentration of 137 Cs in each sample was plotted against depth until the peak in 1963 is discovered. The MARs were calculated using the equation:

$$S = \frac{(D_{pk})}{t}$$

Where S = MAR (g cm⁻² yr⁻¹), D_{pk} = cumulative mass depth (g cm⁻²) at which maximum ¹³⁷Cs is observed, and t = time since 1963 (y) (Yeager et al. 2007). With $t_{1/2}$ = 30.2 y, ¹³⁷Cs is also a preferred dating method over decadal time scales.

3.2.1 Alpha Spectrometry

Figure 16: Uranium-238 decay series (courtesy of University of Wisconsin-Madison).



Each sample was weighed to 1.00-1.01 g and placed in a TeflonTM beaker. Exactly $500 \,\mu\text{L}$ of ^{209}Po tracer was added to allow for an accurate measurement of ^{210}Po (^{210}Pb and ^{210}Po were assumed to be in secular equilibrium). Samples were then processed with multiple treatments of hydrochloric (HCl⁻), nitric (HNO₃), and hydrofluoric (HF⁻) acids until the sediment was completely dissolved. Samples were brought up in dilute ($1.5 \, \text{N}$) HCl, and ascorbic acid was then added to bind free Fe⁺³ ions (Yeager et al. 2012). A one cm² silver disc was added to each sample to provide a substrate for polonium deposition (Santschi et al. 1980; 1999; Yeager et al. 2004; 2007; 2012). Samples were then analyzed using a Canberra 7200 Integrated Alpha Spectrometer.

3.2.2 Gamma Spectrometry

Each sample wasmixed with silica gel (if needed) to obtain a volume to mass ratio of 1 mL: 1 g, and sealed in a test tube with epoxy. Isotopic equilibrium was attained for all isotopes of interest after 21 days. Samples were then analyzed using Canberra High Purity Germanium (HPGe) well detectors and multi-channel analyzers (DSA-1000) to resolve ¹³⁷Cs and ⁷Be activities.

3.3 Remote Sensing

LiDAR and aerial imagery were provided by the SRSand the University of Kentucky's Forestry Department. Aerial imagery was taken in 1938, 1942, and 1951, andLiDAR imagery was taken in 2009.

CHAPTER FOUR: RESULTS

4.1 Lithostratigraphy

4.1.1 Stratigraphy

The top 50 cm of all vibra-cores were processed for grain size (Appendix B). The sand/silt/clay percentages were plotted versus depth to show changes or trends in the grain sizes of accumulated sediment. They were also plotted on the Universal Soil Classification System (USCS) used by the U.S. Department of Agriculture (USDA) to show dominant grain size classifications. The sand, silt, and clay percentages were averaged for each of the nine cores, and these results were averaged for a site-wide percentage. All cores were predominantly composed of sand-sized sediment (Table 6), with the maximum average value of 89.8% at TC2A-B-14V, and a site-wide average of 76.4%. Silt-sized sediment were the second most abundant, with a site-wide average of 18.9%. Clay-sized sediment made up the least amount, with a site-wide average of 4.7%, and a minimum averaged value of < 1%, also at TC2A-B-14V. The first 50 cm of each core are believed to encompass the past 100 years, and to coincide with the fallout radionuclide data. Core image mosaics were also constructed over the same interval to show visual physical characteristics.

Table 6: Average grainsize percentages for all nine cores (0-30 cm).

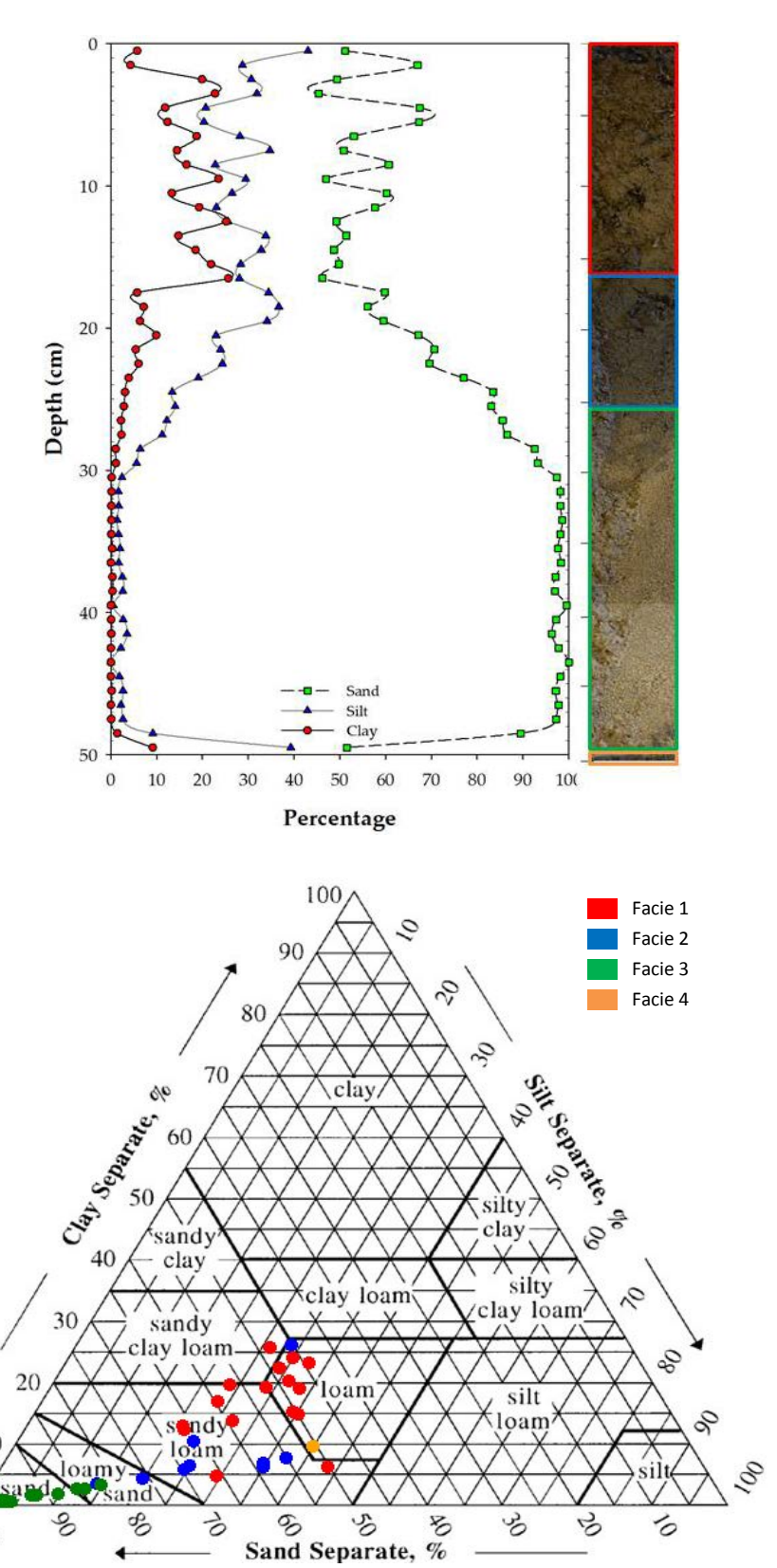
Core	Sand (%)	Silt (%)	Clay (%)
MBM-A	74.8	20.3	4.9
MQ1-A	76.2	16.6	7.2
U10-B	85.7	9.6	4.6
ODB-1B	75.6	15.2	9.2
MCE-A	80.9	16.0	3.1
TC2A-B	89.8	9.3	0.8
MB6-B	67.9	25.7	6.5
TC2B-B	81.2	16.8	2.0
TC5-B	56.3	39.7	4.0
Site-wide	te-wide 76.4		4.7

4.1.2 Lithofacies

4.1.2.1 MQ1-A-14V

This core was taken along the main stream channel of the McQueen Branch sub-basin. It consists of four distinct facies (Fig.17). The top 16cm includes the first facies, a mixture of sediment and organic matter, with a Munsell color designation of 2.5Y 4/3. The sediment is mostly(54.8%) sand-sized on average, with 28.8% silt-sized, and 16.4% clay-sized particles. The macro-organic matter consists of fibrous plant roots up to 3mm in diameter and leaf litter, and the color suggests some micro-organic matter. The second facies occurs between 16-25cm, with a Munsell color designation of 2.5Y 3/2. This layer contains an average of 65.5%sand-, 26.3% silt-, and 8.2% clay-sized particles. There is little macro-organic matter visible, but the color suggests that some microorganic matter is present. The third facies occurs between 25-49cm, with a Munsell color designation of 2.5Y 6/3. This layer contains an average of 95.5% sand-, 3.9% silt-, and 0.6% clay-sized particles. There is no macro-organic matter visible, and the light color suggests little micro-organic matter is present. The fourth facies occurs after an abrupt contact between 49-50cm, with a color of 2.5Y 2.5/1. It has an average of 51.6% sand-, 39.3% silt-, and less than 9.1% clay-sized particles. There is some vascular root matter visible, and the dark color suggests densely packed micro-organic matter in this layer. The microscopy data indicate that the dominant mineral present in MQ1-A-14V is quartz (see Appendix F).

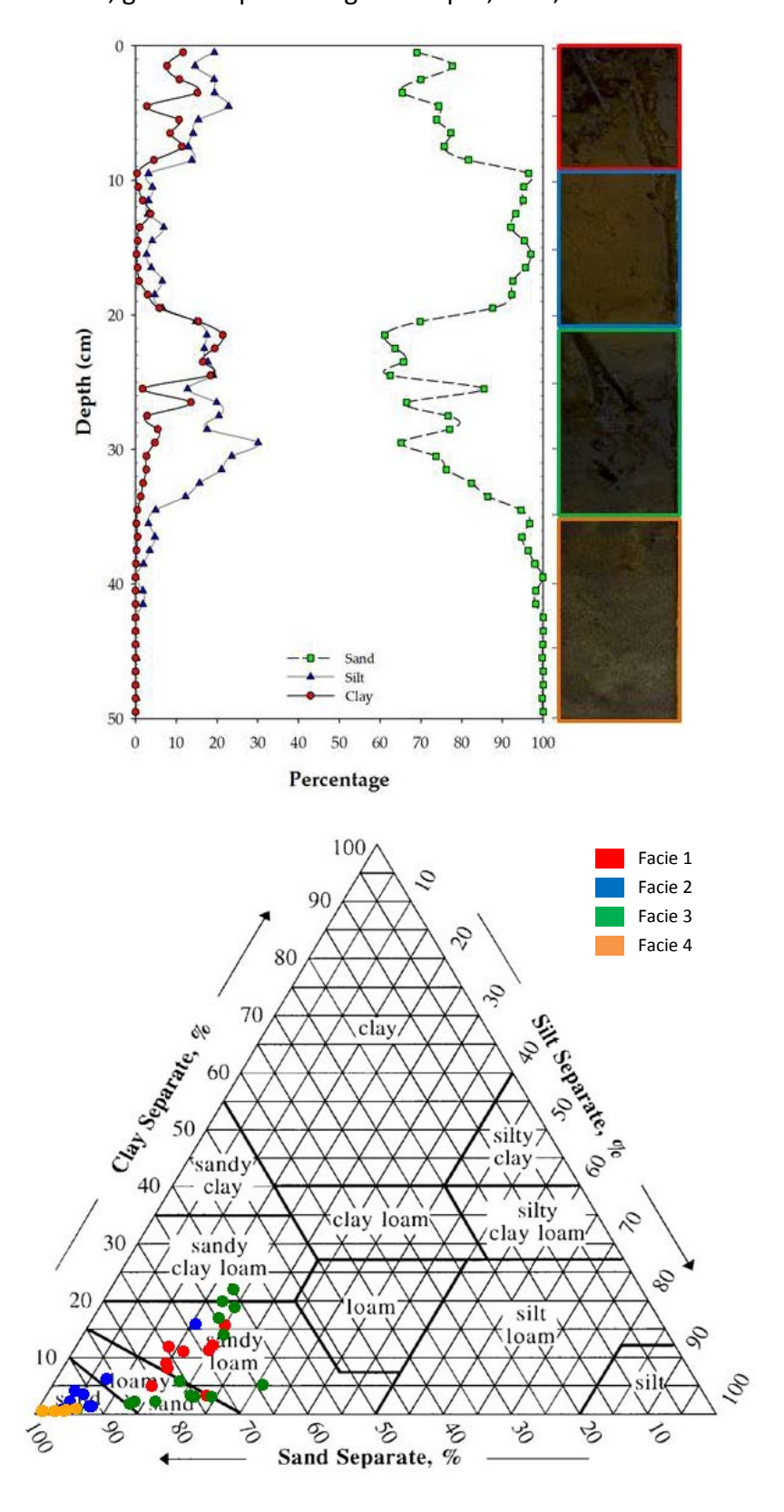
Figure 17: MQ1-A-14V; grain size percentage vs. depth, core mosaic, and soil textural class.



4.1.2.2 U10-B-14V

This core was taken near the mouth of the Upper Three Runs (U10) sub-basin. It consists of four distinct facies (Fig.18). The top 9cm is a mixture of sediment and organic matter, with a Munsell color designation of 2.5Y 4/3. The sediment consists of an average of 73.9% sand-, 16.9% silt-, and 9.2% clay-sized particles. The macro-organic matter consists of fibrous and vascular plant roots and leaf litter, and the color suggests the presence of some micro-organic matter. The second facies occurs between 9-21cm, with a Munsell color designation of 10YR 5/4, and contains an average of 91.9% sand-, 5.3% silt-, and 2.8% clay-sized particles. There is no macro-organic matter visible, but the color suggests that some micro-organic matter is present. The third facies occurs between 21-35cm, with a Munsell color designation of 10YR 2/1. This layer contains an average of 74.1% sand-, 17.8% silt-, and 8.1% clay-sized particles. There are vascular rootspresent with sub-millimeter diameters, and the darker color suggests densely packed micro-organic matter is abundant. The fourth facies occurs between 35-50cm, with a predominateMunsell color of 2.5Y 4/2, with two small spots of 10YR 6/3. It has an average of 98.8% sand-, 1.2% silt-, and < 0.1% clay-sized particles. There is no macroorganic matter visible, and the mottled color suggests a variable amount of microorganic matter in this layer. The microscopy data indicate that the dominant mineral present in U10-B-14V is quartz (See Appendix F).

Figure 18: U10-B-14V; grain size percentage vs. depth, core, and soil textural class.



4.1.2.3 TC2A-B-14V

This core was taken from the southern tributary of the Tinker Creek (TC2) sub-basin. It consists of only one distinct facies (Fig.19). The entire 50cm interval is a mixture of sediment and organic matter, with a Munsell color designation of 10YR 2/1. The sediment consists of an average of 89.8% sand-, 9.3% silt-, and 0.9% clay-sized particles. Macro-organic matter consists of vascular plant roots no larger than 1mm in diameter, and the dark color suggests denselypacked micro-organic matter. There is an obvious coarsening of sediment in the top 20cm, as shown in Figure 38. The microscopy data indicate that the dominant mineral present in TC2A-B-14V is quartz (see Appendix F).

4.1.2.4 TC2B-B-14V

This core was taken from the northern tributary of the Tinker Creek (TC2) sub-basin. It consists of three facies (Fig.20) with a few subtle changes in color and texture. The top 12cm is a mixture of sediment and organic matter, with a Munsell color designation of 2.5YR 2.5/1. The sediment consists of an average of 52.3% sand-, 41.8% silt-, and 5.9% clay-sized particles. The macro-organic matter consists of fibrous and vascular plant roots and leaf litter, and the dark color suggests densely packed micro-organic matter. The second facies occurs between 12-20cm, with a Munsell color designation of 5YR 2.5/1. This layer contains an average of 75.8% sand-, 21.7% silt-, and 2.5% clay-sized particles. There is no macro-organic matter visible, but the dark color suggests that micro-organic matter is present. The grainsize data indicates a gradual coarsening of sediment over this interval. The third facies occurs between 20-50cm, with a Munsell color designation of 5YR 3/1. This layer contains an average of 94.2% sand-, 5.4% silt-, and 0.4% clay-sized particles. There are fibrous roots, and the darker color suggests that micro-organic matter is present. The microscopy data indicate that the dominant mineral present in TC2B-B-14V is quartz (see Appendix F).

Figure 19: TC2A-B-14V; grainsize percentage vs. depth, core mosaic, and soil textural class. (Surface interval of 0-3 cm did not contain sediment, only leaf litter.)

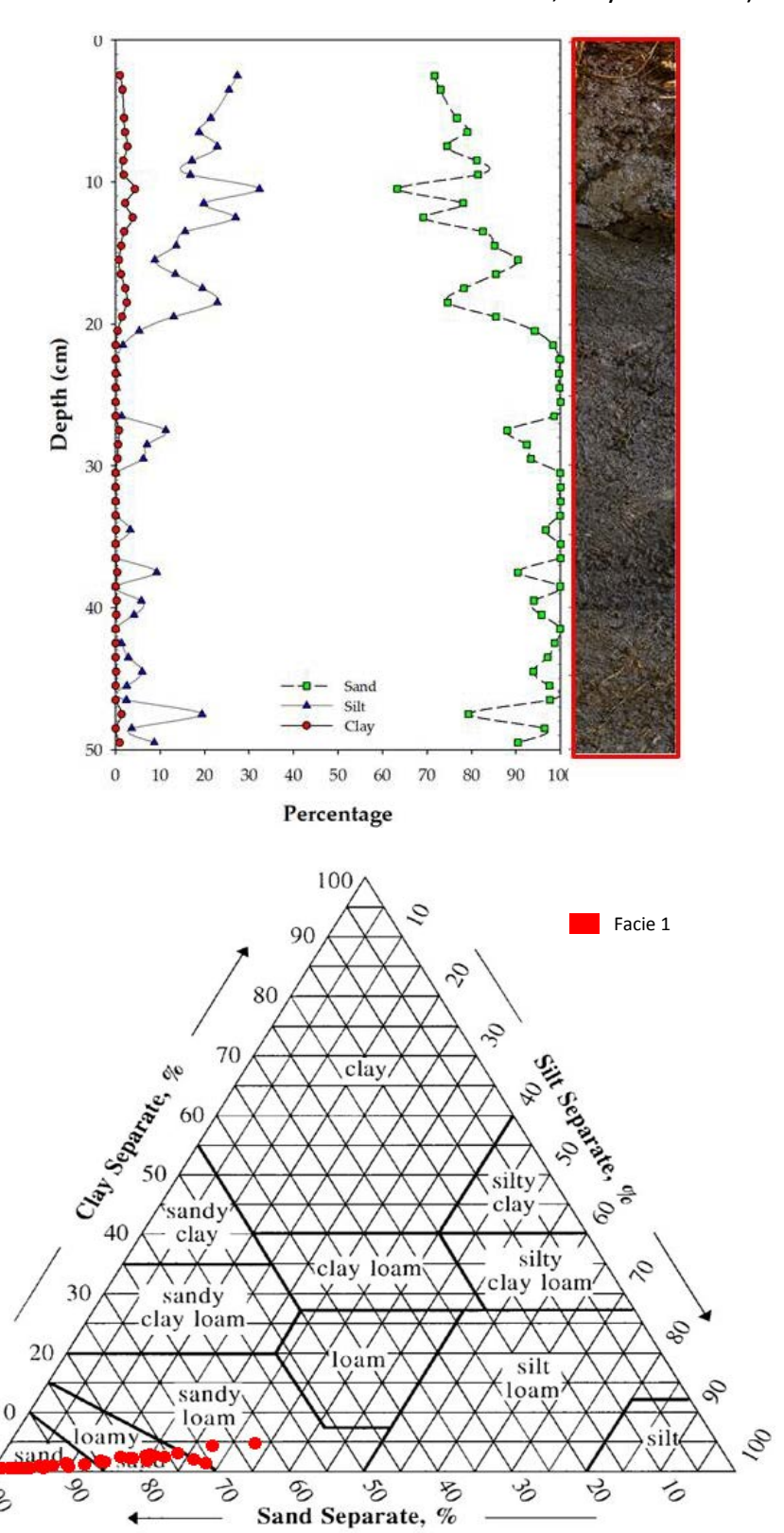
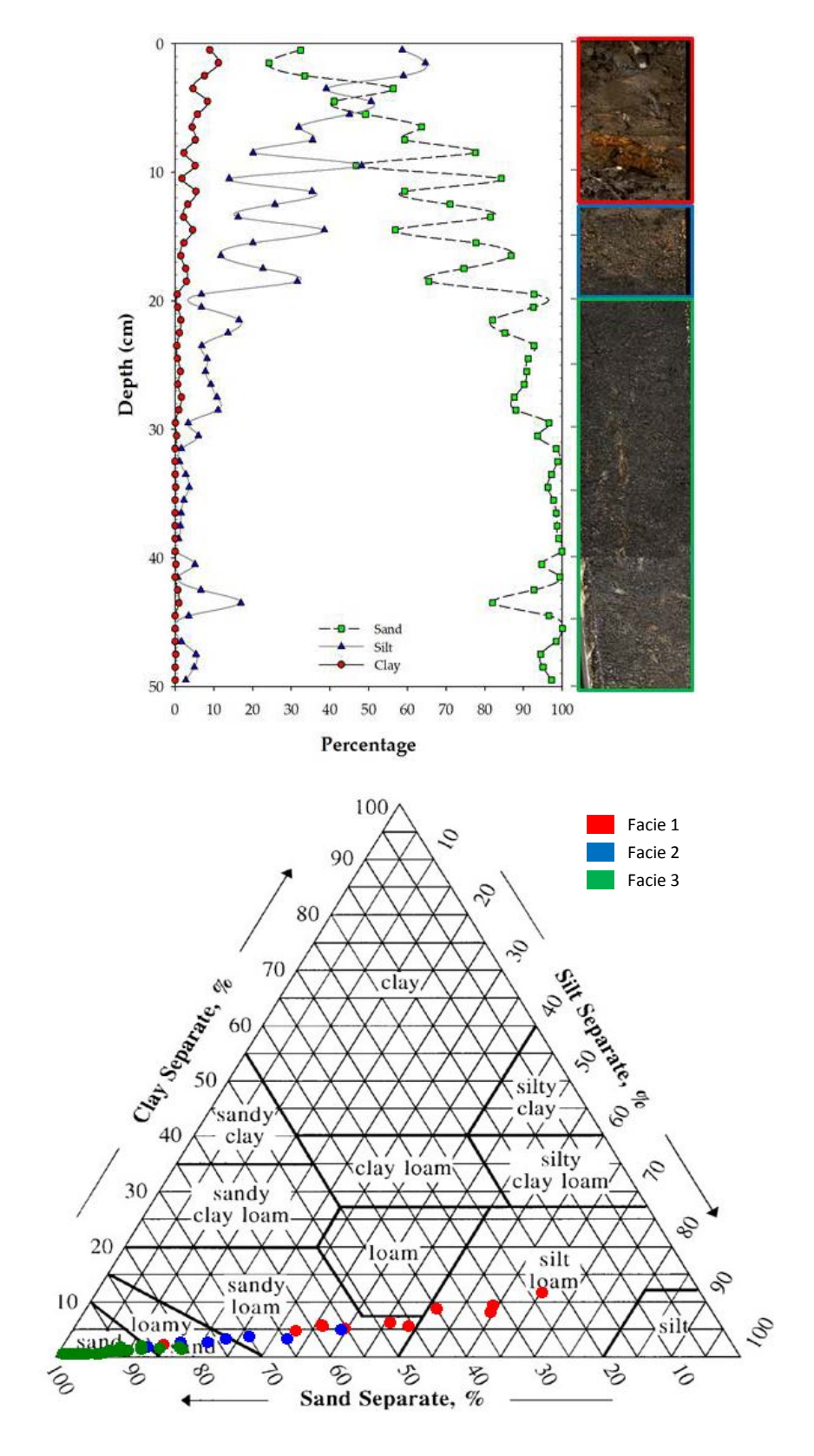


Figure 20: TC2B-B-14V; grainsize percentage vs. depth, core mosaic, and soil textural class.



4.1.2.5 TC5-B-14V

This core was taken near the mouth of the Tinker Creek (TC5) sub-basin. It consists of two facies (Fig.21) with little variability. The top facies (0-16cm) is a mixture of sediment and organic matter, with a Munsell color designation of 10YR 2/1. The sediment consists of an average of 27.3% sand-, 65.6% silt-, and 7.1% clay-sized particles. The macro-organic matter consists of fibrous and vascular plant roots up to 1cm in diameter, with very little leaf litter. The second facies occurs between 16-50cm, with a Munsell color designation of 10YR 2/1. This layer contains an average of 70.0% sand-, 27.5% silt-, and 2.5% clay-sized particles. There are sub-millimeter diametervascular plant roots mixed throughout this layer. While the color and presence of micro-organic matter matches with the top facies, the lack of fibrous roots and the coarsening of sediments allows for the designation of two facies. The microscopy data indicate that the dominant mineral present in TC5-B-14V is quartz (see Appendix F).

4.1.2.6 MB6-B-14V

This core was taken from the eastern tributary of the Meyers Branch sub-basin. It consists of two distinct facies (Fig.22). The top 23cm is a mixture of sediment and micro-organic matter, and has a Munsell color designation of 10YR 2/2. There are fibrous and vascular plant roots whose thicknesses range from 1-10 mm. The sediment consists of an average of 60.2% sand-, 31.1% silt-, and 8.7% clay-sized particles. The second facies occurs between 23-50cm, with a Munsell color designation of 10YR 2/1. This layer contains an average of 74.4% sand-, 21.0% silt-, and 4.6% clay-sized particles. Vascular and fibrous root systems are still present in this facies. The microscopy data indicate that the dominant mineral present in MB6-B-15V is quartz (see Appendix F).

Figure 21: TC5-B-14V; grainsize percentage vs. depth, core mosaic, and soil textural class.

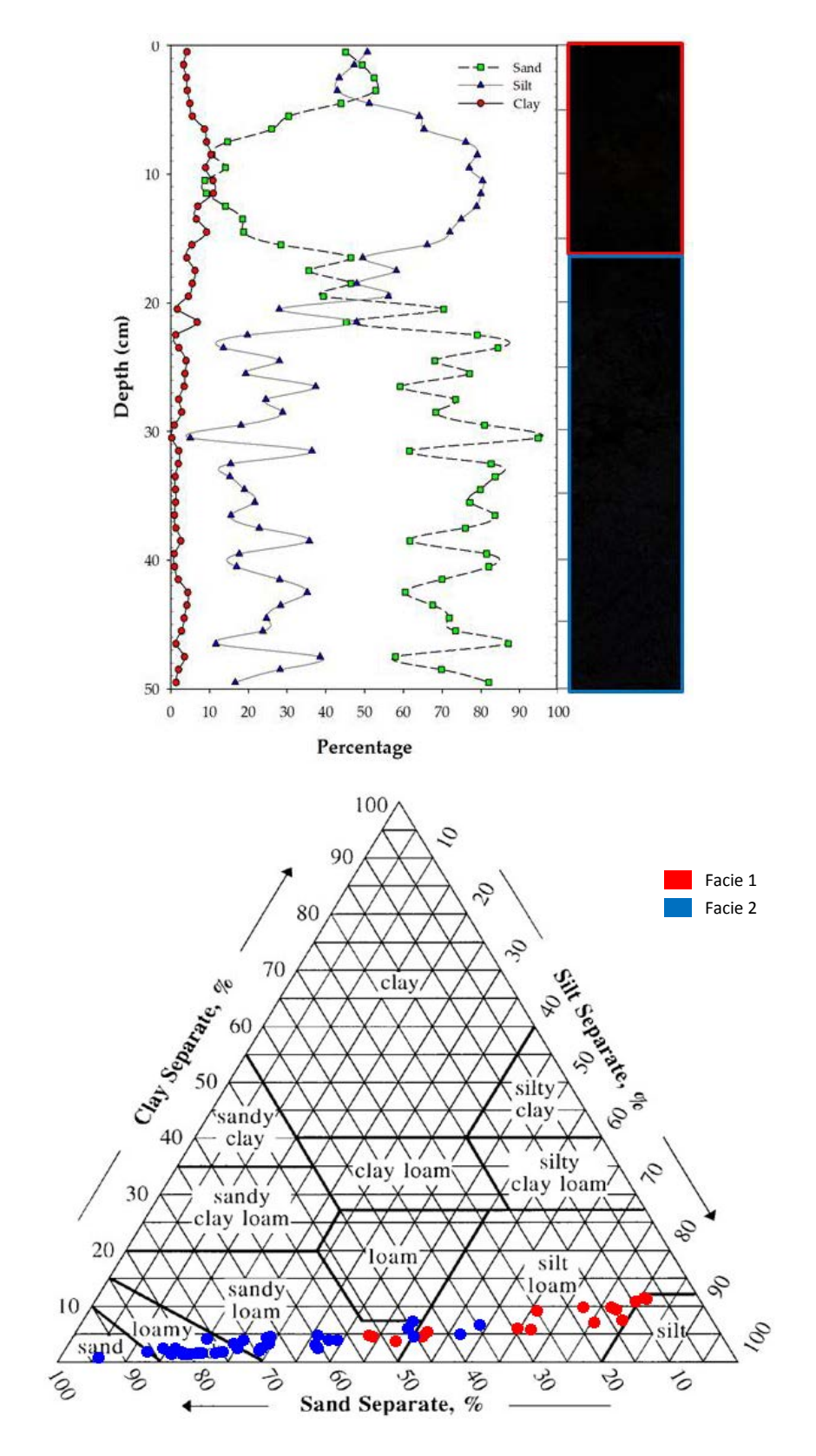
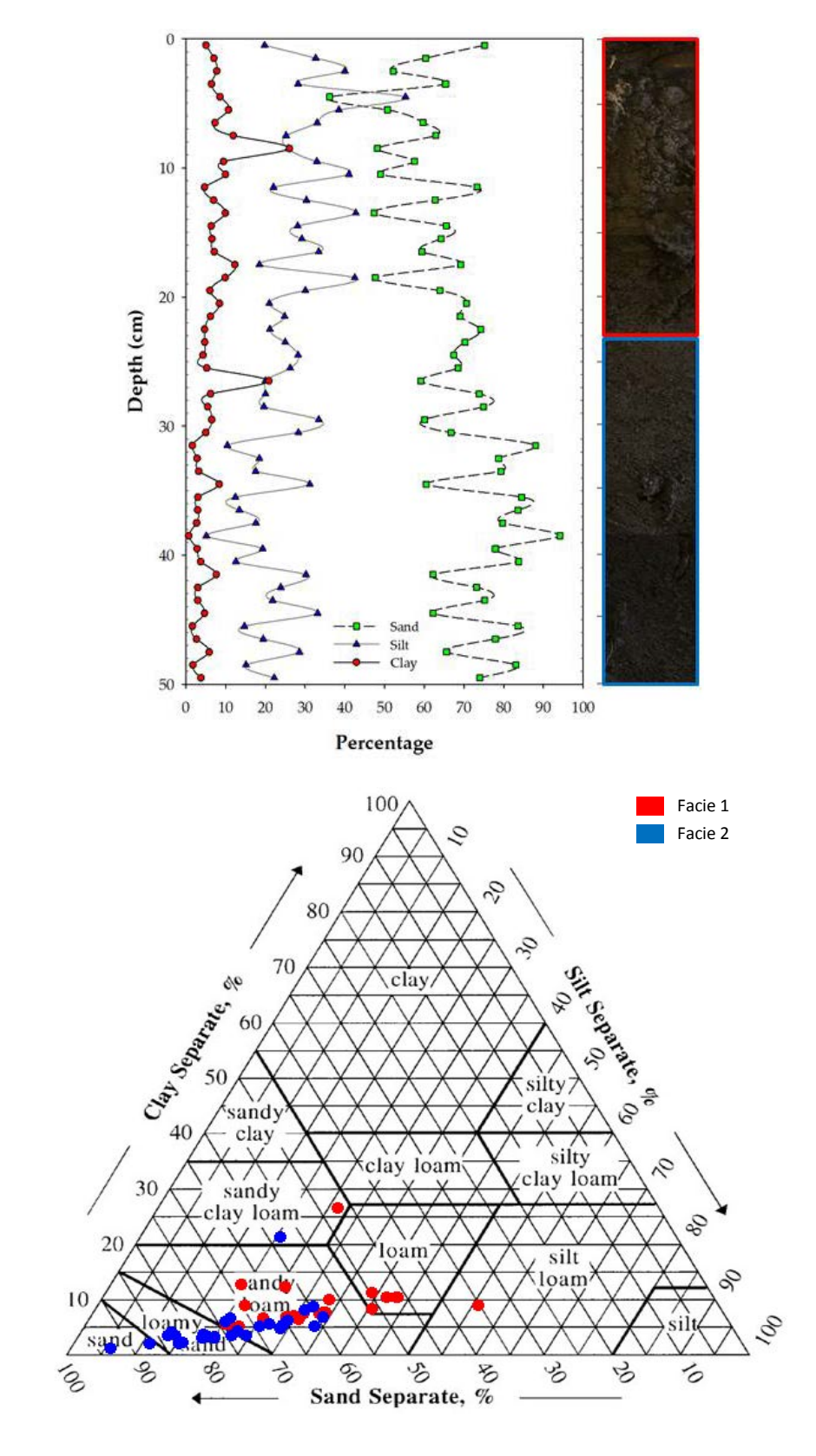


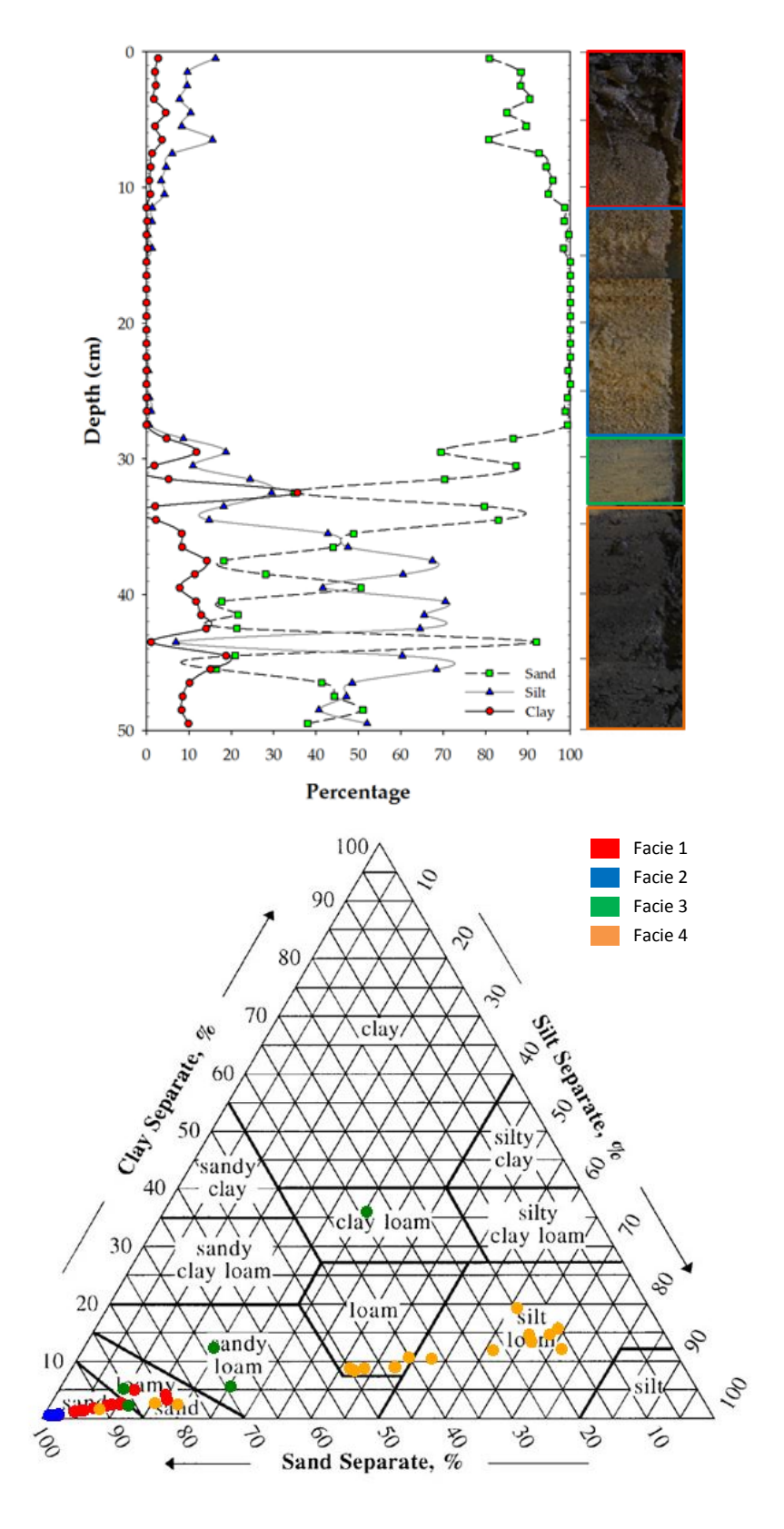
Figure 22: MB6-B-14V; grain size percentage vs. depth, core mosaic, and soil textural class.



4.1.2.7 MBM-A-14V

This core was taken from the main stream channel of the Meyers Branch sub-basin. It consists of four distinct facies (Fig.23). The top 12cm is a mixture of sediment and organic matter, with a Munsell color designation of 10YR 2/1. The sediment consists of an average of 90.0% sand-, 8.1% silt-, and 1.9% clay-sized particles. The macro-organic matter consists of fibrous and vascular plant roots up to 3mm in diameter and leaf litter, and the color suggests some micro-organic matter. The second facies occurs between 12-28cm, with a Munsell color designation of 2.5Y 5/4. This layer contains an average of 99.6% sand-, 0.4% silt-, and < 0.1% clay-sized particles. There is no macro-organic matter visible, but the light color suggests some micro-organic matter is present. The third facies occurs between 28-33cm, with an interbedded Munsell color of 2.5Y 5/4 and 7.5YR 4/1. This layer contains an average of 74.7% sand-, 15.5% silt-, and 9.8% claysized particles. No macro-organic matter is apparent in this interval, and the interbedded texture suggests a transition from little to densely packed micro-organic matter. The fourth facies occurs between 33-50cm, with a color of 2.5Y 2.5/1. It has an average of 42.2% sand-, 48.1% silt-, and 9.7% clay-sized particles. There is no macroorganic matter visible, but the dark color suggests an abundance of micro-organic matter in this layer. The microscopy data indicate that the dominant mineral present in MBM-A-14V is quartz (see Appendix F).

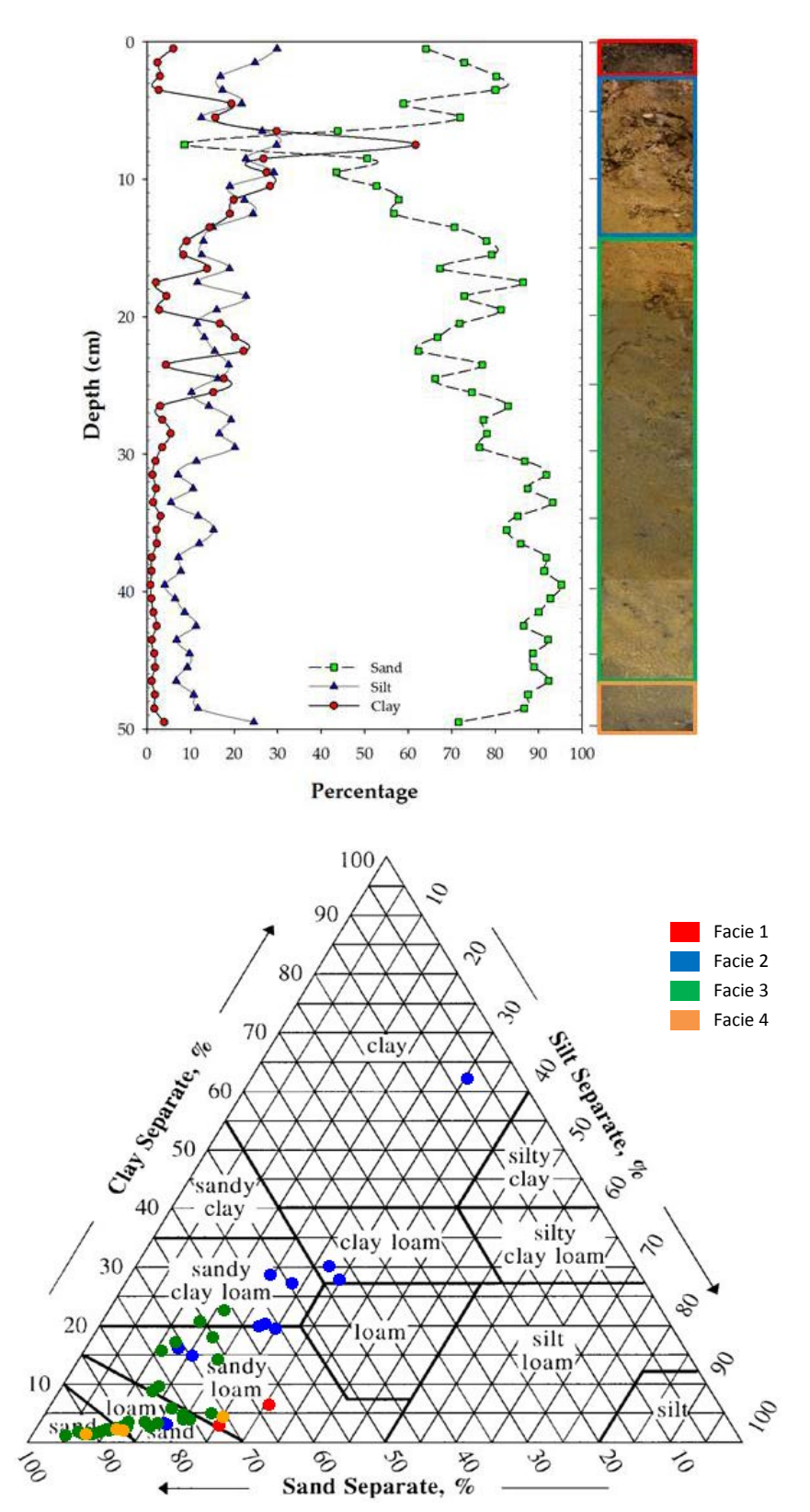
Figure 23: MBM-A-14V; grain size percentage vs. depth, core mosaic, and soil textural class.



4.1.2.8 ODB-1B-14V

This core was taken from the northern tributary of the Meyers Branch sub-basin. It consists of four distinct facies (Fig.24). The top 2.5cm is a mixture of sediment and organic matter, with a Munsell color designation of 10YR 3/1. The sediment consists of an average of 72.4% sand-, 23.8% silt-, and 3.8% clay-sized particles. The macro-organic matter consists of fibrous and vascular plant roots and leaf litter, and the dark color suggests abundant micro-organic matter. The second facies occurs between 2.5-14cm, with a Munsell color designation of 2.5YR 3/4. This layer contains an average of 54.1% sand-, 21.8% silt-, and 24.1% clay-sized particles. There are vascular plant roots visible in this layer. While the grainsize data show a decrease in sediment particle size between 7-14cm, there is a marked, anomalous decrease in sand-size particles at 8cm that is not obvious in the core mosaic. The third facies occurs between 14-46cm, with a Munsell color designation of 7.5YR 3/1. This layer contains an average of 82.2% sand-, 12.3% silt-, and 5.5% clay-sized particles. There are a few vascular roots with submillimeter diameters in this facies, but the lighter color suggests less micro-organic matter is present. Grainsize data shows a gradational coarsening of sediment down core, confirmed by the core mosaic. The fourth facies occurs between 46-50cm, and is a transitional layer, with a mottled color texture of 7.5YR 3/1 and 5YR 2.5/1. It has an average of 84.5% sand-, 13.4% silt-, and 2.1% clay-sized particles. There are a few vascular roots visible, and the mottled color suggests a variable amount of microorganic matter in this layer. The microscopy data indicate that the dominant mineral present in ODB-1B-14V is quartz (see Appendix F).

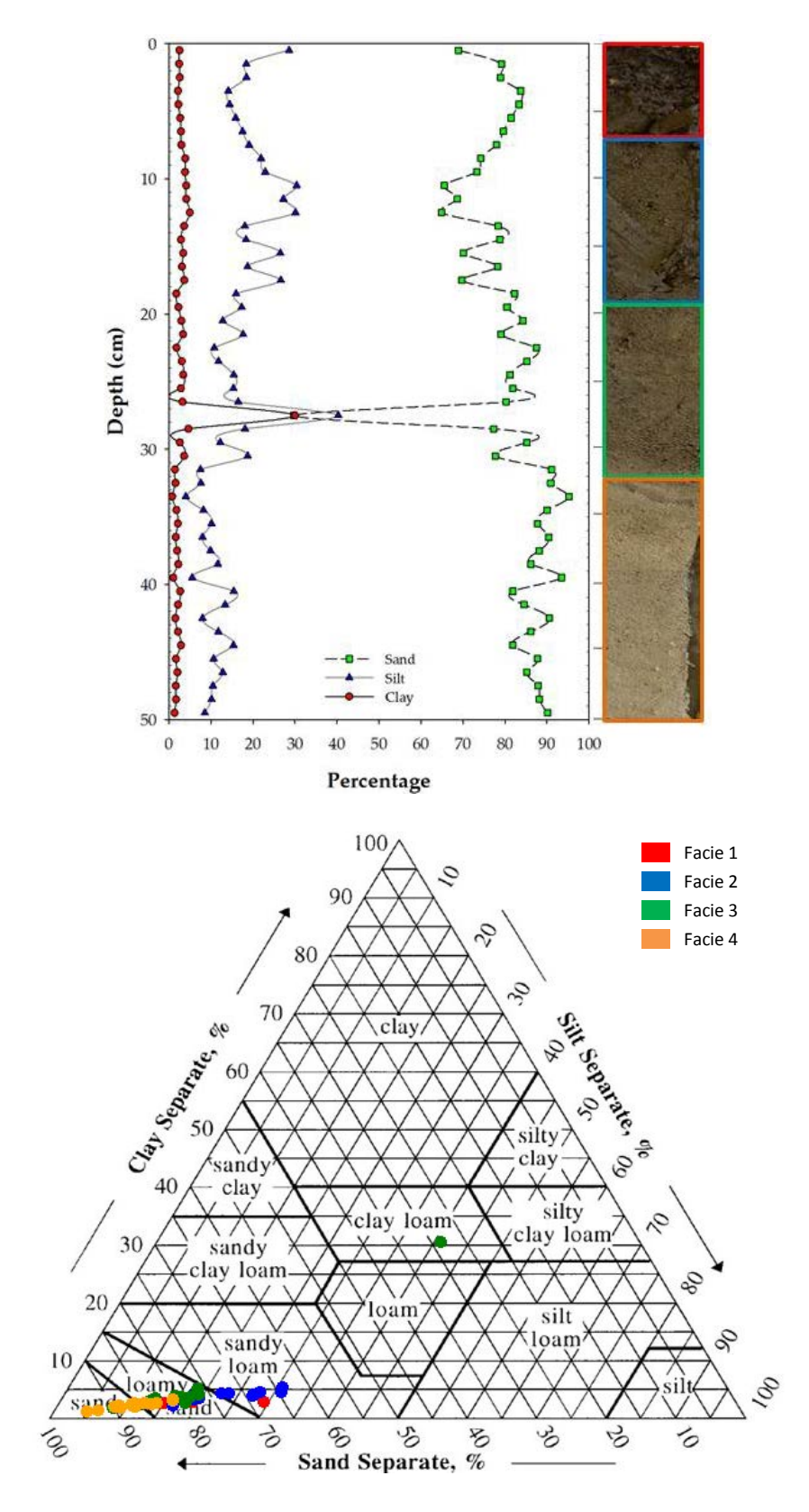
Figure 24: ODB-1B-14V; grainsize percentage vs. depth, core mosaic, and soil textural class.



4.1.2.9 MCE-A-14V

This core was taken near the mouth of the Mill Creek sub-basin. It consists of four distinct facies (Fig.25). The top 7cm is a mixture of sediment and organic matter, with a Munsell color designation of 7.5YR 2.5/1. The sediment consists of an average of 79.3% sand-, 18.2% silt-, and 2.5% clay-sized particles. The macro-organic matter consists of fibrous and vascular plant roots and leaf litter, and the dark color suggests the presence of micro-organic matter. At 7cm, the layer is bisected by a 1cm-diameter fibrous root. The second facies occurs between 7-19cm, with a Munsell color designation of 5YR 2.5/1. This layer contains an average of 73.5% sand-, 23.0% silt-, and 3.5% clay-sized particles. The dark color suggests the presence of micro-organic matter, and there are fewer root structures visible. The roots visible in this interval are only from vascular plants. The third facies occurs between 19-32cm, with a Munsell color designation of 7.5YR 3/2. This layer contains an average of 78.5% sand-, 16.5% silt-, and 5.0% claysized particles. There is no macro-organic matter visible, and the color suggests some micro-organic matter is present. The fourth facies occurs between 32-50cm, with a Munsellcolor designation of 7.5YR 5/1. It has an average of 88.1% sand-, 10.1% silt-, and 1.8% clay-sized particles. There is no macro-organic matter visible, and the light color suggests little micro-organic matter in this layer. The microscopy data indicate that the dominant mineral present in MCE-A-14V is quartz (see Appendix F).

Figure 25: MCE-A-14V; grainsize percentage vs. depth, core mosaic, and soil textural class.



4.2 Radiochemistry

4.2.1 Gamma Spectrometry

 137 Cs activity profiles were produced for all cores (Fig. 26). The 137 Cs and 7 Be activity inventories for all cores are listed in Appendix C. Only three cores exhibited 7 Be activities above detection limits: U10-B-14V, TC2A-B-14V, and TC2B-B-14V. U10-B-14V and TC2A-B-14V had measurable 7 Be in the 0-1cm interval; TC2B-B-14V had 7 Be from 0-2cm. Since 7 Be has such a short half-life ($t_{1/2} = 53.3$ days), it is usually only found within the top few cm unless there has been recent sediment mixing (Mabit et al. 2008; Hancock et al. 2013). Therefore, there does not appear to be any appreciable and recent sediment mixing in the top layers of any cores. Total 137 Cs inventories for all cores are listed in Table 7, including the expected inventory from atmospheric deposition alone (270.10 mBq cm $^{-2}$, Burger et al. 2001).

The sedimentation ratio is calculated by dividing the measured 137 Cs inventory in each core by the expected 137 Cs inventory in the area due to fallout alone to determine if the core was in a net erosional or a net depositional setting. The 137 Cs inventories from eight of the nine cores have sedimentation ratios < 1, indicating that these sub-basins have been net-erosional systems in the past $^{\sim}50$ years. Table 8 shows the calculated sediment mass accumulation and linear accumulation rates using both the first detection (1952) and peak detection (1963) years. The activities based on first detection have been identified on each core and labeled 1951; the activities based on peak inventories were best approximated on each core and labeled 1963.

Figure 27 shows that cores MQ1-A-14V, U10-B-14V, and ODB-1B-14V had the highest ¹³⁷Cs-based accumulation rates, while MBM-A-14V and MB6-B-15V had moderate accumulation rates. Cores TC2-A-14V, TC2B-B-14V, MCE-A-14V, and TC5-B-14V had the lowest accumulation rates. Figure 27also shows that calculated MARs were higher than LARs in five of the nine cores: MQ1-A-14V, MBM-A-14V, ODB-1B-14V, MCE-A-14V, and MB6-B-15V. The LARs were higher than the MARs in only three of the nine cores, all of them from the Tinker Creek sub-basin area: TC2A-B-14V,TC2B-B-14V, and TC5-B-14V.

U10-B-14V is the only core with equal MAR and LAR. Comparing MARs and LARs indicates differences in sediment sourcing between the sub-basins. For example, MARs that are higher than LARs in a core indicate sediments with relatively high mass (e.g., quartz), while LARs that are higher than MARs indicate sediments with lower mass and more volume (e.g., organic content).

Table 7: 137 Cs inventories and calculated sedimentation ratios for all cores.

Core	¹³⁷ Cs Inventory (mBq cm ⁻²)	Sedimentation Ratio
Atmospheric	270.10	
MQ1-A-14V	294.77	1.09
U10-B-14V*	110.16	0.41
MBM-A-14V	140.68	0.52
ODB-1B-14V	214.28	0.79
TC2A-B-14V	116.64	0.43
MCE-A-14V	92.50	0.34
TC2B-B-14V	101.12	0.37
TC5-B-14V	46.82	0.17
MB6-B-15V	214.52	0.79

Table 8: Comparison of ¹³⁷Cs-based LARs and MARs, based onboth the 1951 and 1963 peaks.*Denotes that the rate is based on the removal of an anomalous period of extreme accumulation related to nearby construction effort in 1985.

Core	¹³⁷ Cs LAR (1963) (cm y ⁻¹)	¹³⁷ Cs LAR (1951) (cm y ⁻¹)	137Cs MAR (1963) (g cm ⁻² y ⁻¹)	¹³⁷ Cs MAR (1951) (g cm ⁻² y ⁻¹)
MQ1-A-14V	0.304 ± 0.02	0.411 ± 0.016	0.372 ± 0.074	0.519 ± 0.126
U10-B-14V*	0.029 ± 0.02	0.465 ± 0.113	0.038 ± 0.008	0.465 ± 0.113
MBM-A-14V	0.127 ± 0.02	0.250 ± 0.016	0.153 ± 0.031	0.365 ± 0.089
ODB-1B-14V	0.167 ± 0.02	0.379 ± 0.016	0.163 ± 0.033	0.492 ± 0.12
TC2A-B-14V	0.186 ± 0.02	0.347 ± 0.016	0.063 ± 0.013	0.232 ± 0.056
MCE-A-14V	0.049 ± 0.02	0.234 ± 0.016	0.024 ± 0.005	0.240 ± 0.058
TC2B-B-14V	0.029 ± 0.02	0.250 ± 0.016	0.013 ± 0.003	0.127 ± 0.031
TC5-B-14V	0.049 ± 0.02	0.250 ± 0.016	0.014 ± 0.003	0.088 ± 0.021
MB6-B-15V	0.167 ± 0.02	0.315 ± 0.016	0.163 ± 0.033	0.390 ± 0.095

Figure 26: ¹³⁷Cs activity vs.depth profiles for all cores.

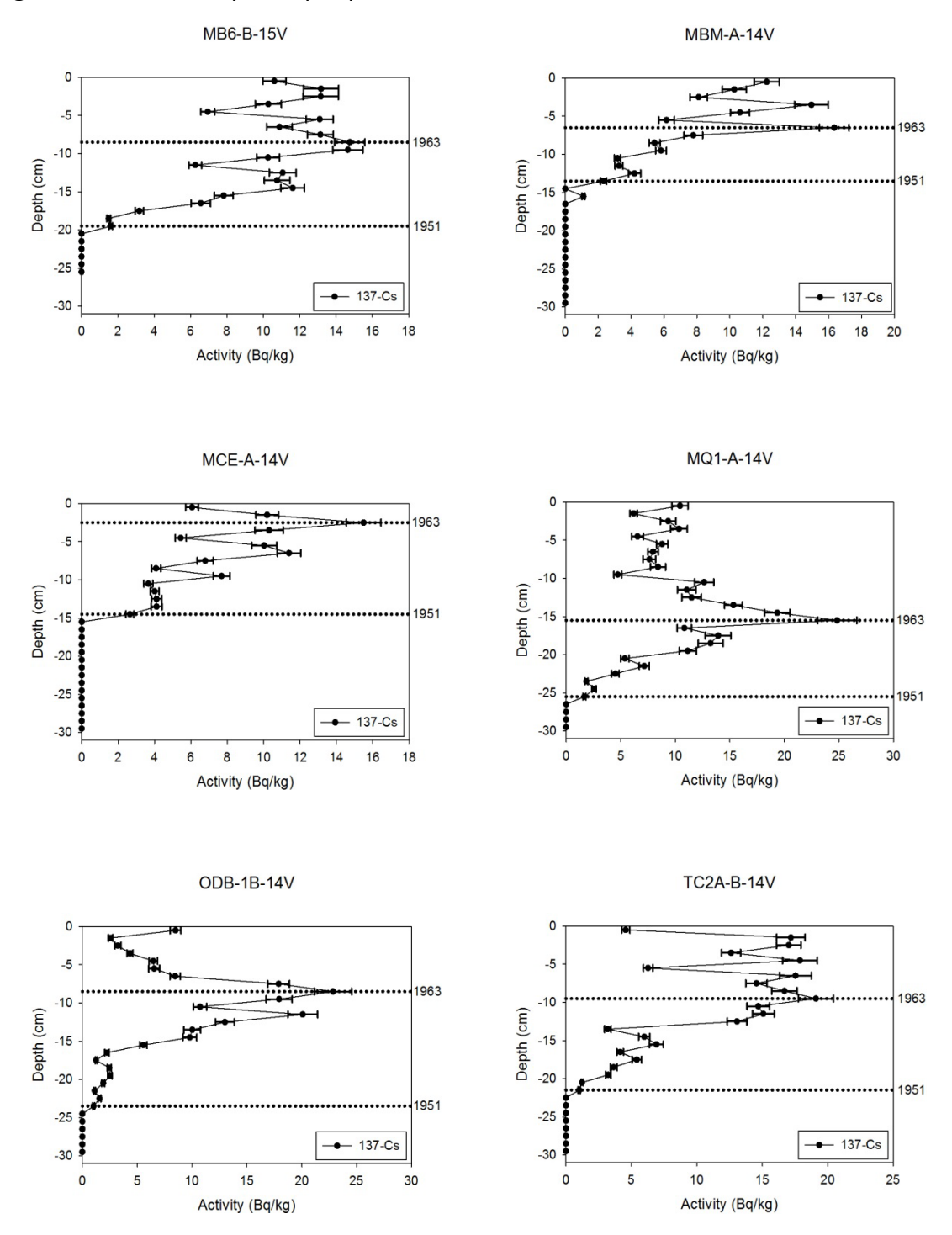


Figure 26:(continued)

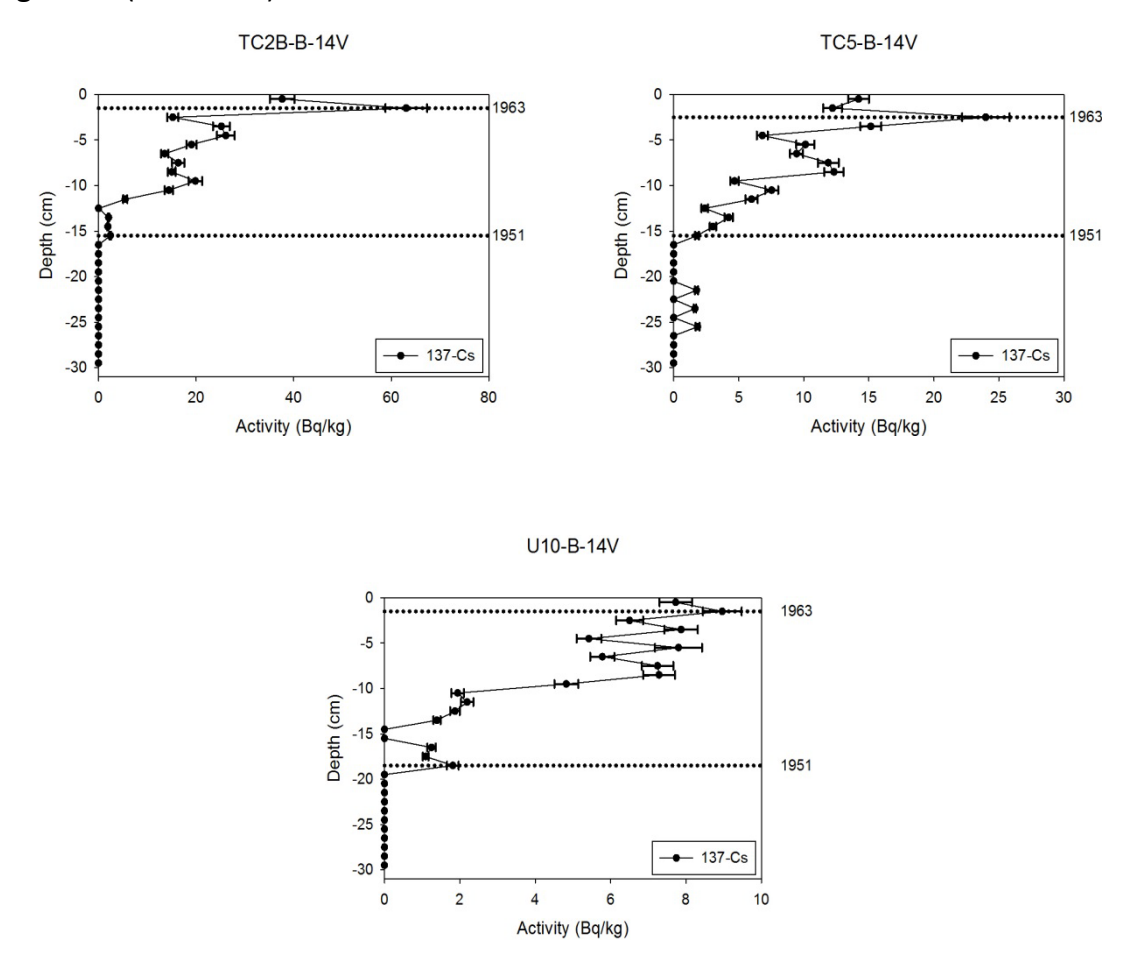
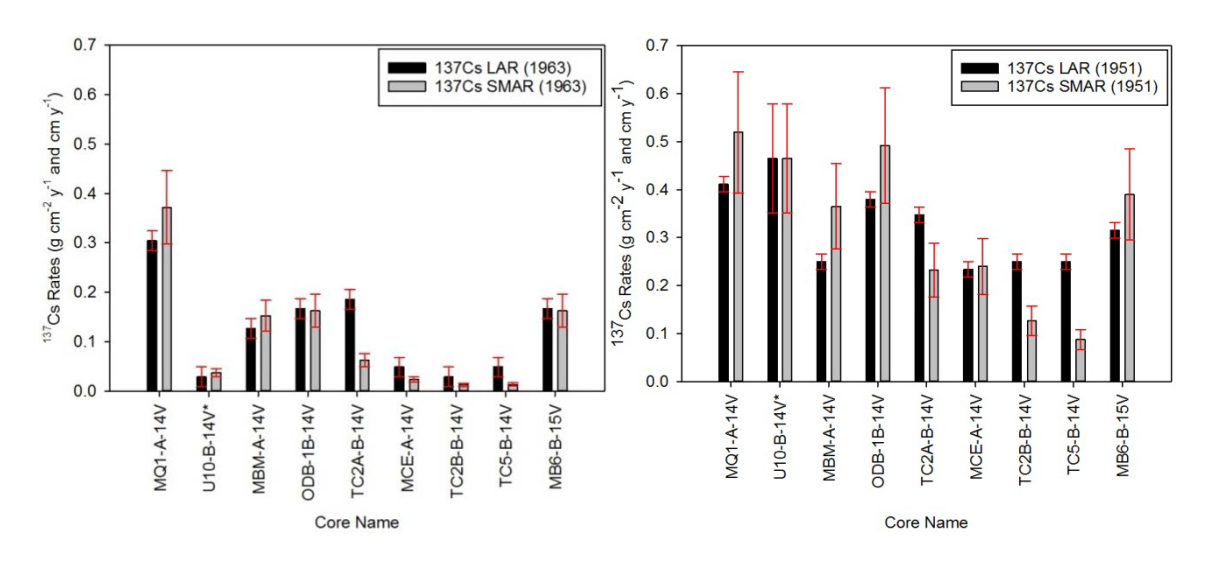


Figure 27: Comparison of ¹³⁷Cs-based LARs vs. MARs at peak detection (left) and initial detection (right).



4.2.2 Alpha Spectrometry

 210 Pb_{xs} activity profiles were produced for all cores (Fig.28), and 210 Pb_{xs} inventories for all samples are listed in Appendix C. Total 210 Pb_{xs} inventories for all cores are listed in Table 9, including the expected inventories from atmospheric deposition alone (18.50mBq cm 2 y $^{-1}$; Baskaran et al. 1993;Turekian et al. 1977). The 210 Pb_{xs} inventories from five of the nine cores have sedimentation ratios< 1, indicating that these sub-basinshave been neterosional systems over the past 210 Pb_{xs}. Three of the nine cores have sedimentation ratios > 1, indicating that these sub-basinshave been net-depositional systems over the past 210 Pb_{xs}. Core ODB-1B-14V has a sedimentation ratio of 1.05, which indicates that it has had no net sedimentation change over the past 210 Pb_{xs}. Table 10 shows the calculated sediment mass accumulation and linear accumulation rates using 210 Pb_{xs}.

As stated previously, research indicates that the average sediment accumulation on floodplains in the Piedmont region of the U.S.A. is between 0.02 and 0.50 g cm $^{-2}$ y $^{-1}$ for 100-year rates. Our MARs fall within that range, averaging between 0.119 and 0.48 g cm $^{-2}$ y $^{-1}$ for 210 Pb $_{xs}$ and 0.07 and 0.45 g cm $^{-2}$ y $^{-1}$ for 137 Cs. Likewise, as previous research pointed out, the 100-year rates were larger than 30-year rates due to more agricultural practices and less soil retention techniques at the turn of the century. Similarly, our data shows that eight of the nine cores show greater MARs and LARs based on 210 Pb $_{xs}$ than for 137 Cs, which represents a more recent timeframe.



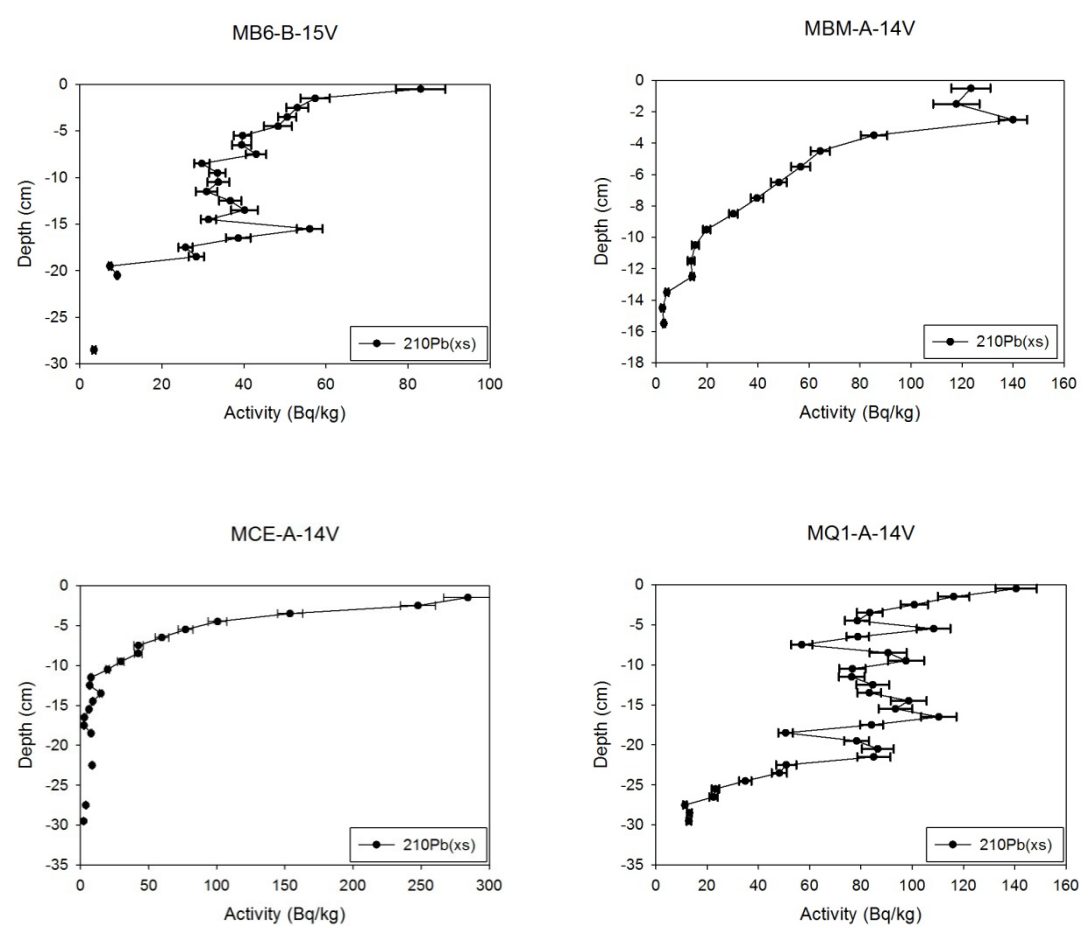


Figure 28: (continued)

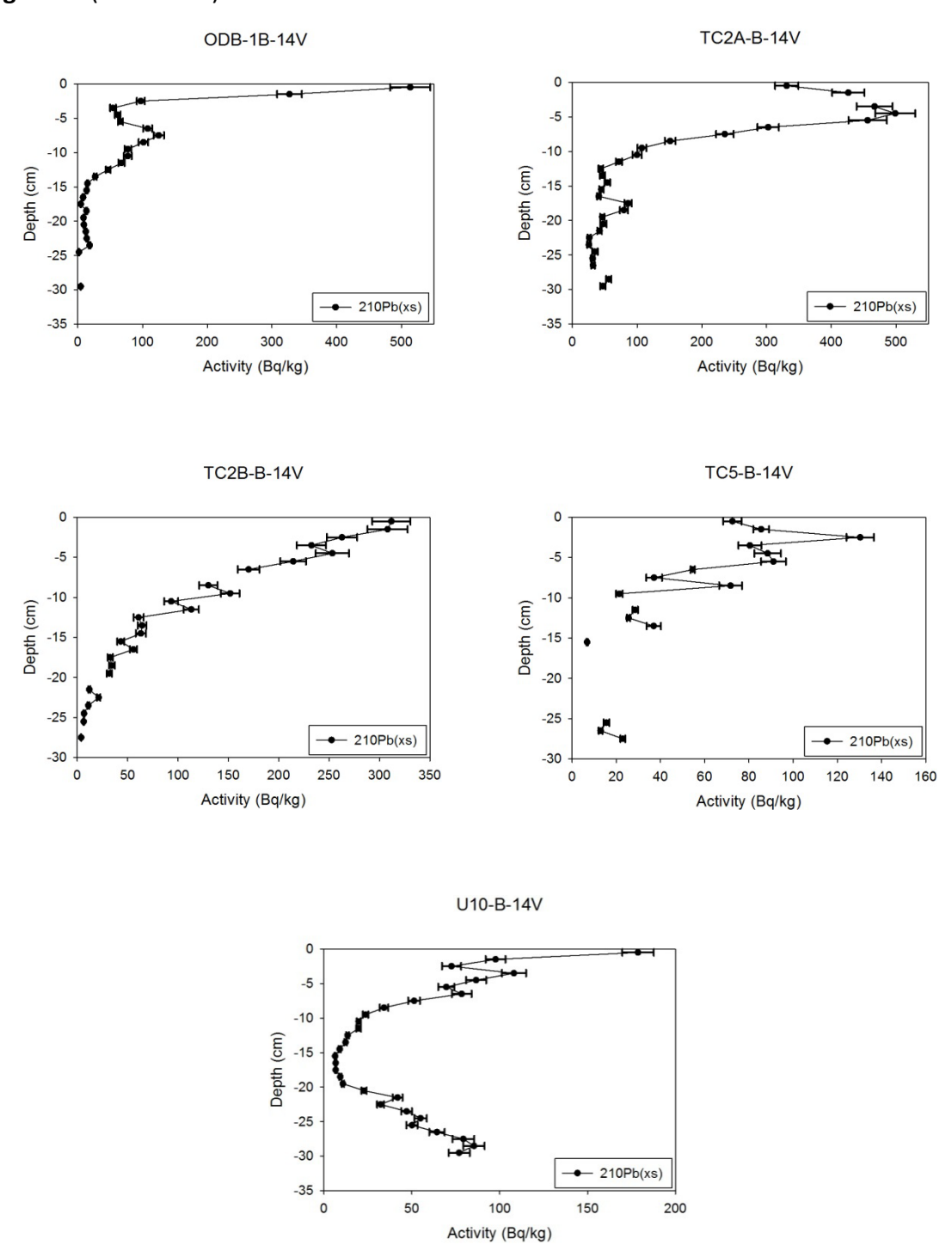


Table 9: 210 Pb_{xs} inventories and sedimentation ratios for all cores.

Core	²¹⁰ Pb _{xs} Inventory (mBq cm ⁻² y ⁻¹)	Sedimentation Ratio
Atmospheric	18.50	
MQ1-A-14V	23.30	1.26
U10-B-14V*	24.86	1.34
MBM-A-14V	5.98	0.32
ODB-1B-14V	19.46	1.05
TC2A-B-14V	23.84	1.29
MCE-A-14V	12.10	0.65
TC2B-B-14V	6.77	0.37
TC5-B-14V	3.71	0.20
MB6-B-15V	6.15	0.33

Table 10: Comparison of 210 Pb_{xs}-based LARs and MARsfor all cores. *Denotes that the rate is based on the removal of an anomalous period of extreme accumulation related to nearby construction effort in 1985.

Core	²¹⁰ Pb _{xs} LAR (cm y ⁻¹)	²¹⁰ Pb _{xs} MAR (g cm ⁻² y ⁻¹)
MQ1-A-14V	0.398 ± 0.223	0.480 ± 0.250
U10-B-14V*	0.353 ± 0.197	0.443 ± 0.234
MBM-A-14V	0.126 ± 0.064	0.158 ± 0.050
ODB-1B-14V	0.326 ± 0.186	0.370 ± 0.168
TC2A-B-14V	0.433 ± 0.250	0.254 ± 0.126
MCE-A-14V	0.270 ± 0.110	0.286 ± 0.101
TC2B-B-14V	0.235 ± 0.173	0.119 ± 0.054
TC5-B-14V	0.515 ± 0.451	0.239 ± 0.191
MB6-B-15V	0.400 ± 0.343	0.405 ± 0.280

Figure 29 shows that cores MQ1-A-14V, U10-B-14V, ODB-1B-14V, and MB6-B-15V had the highest accumulation rates, while MCE-A-14V had a moderate accumulation rate. MBM-A-14V and TC2B-B-14V had the lowest accumulation rates. The three Tinker Creek cores (TC2A-B-14V, TC2B-B-14V, and TC5-B-14V) had the greatest difference in LARs and MARs. Figure 29 also shows that MARswere higher than LARs in five of the nine cores: MQ1-A-14V, U10-B-14V, MBM-A-14V, ODB-1B-14V, and MCE-A-14V; whereas LARs were higher than MARs in only three of the nine cores, all from the Tinker Creek sub-basin: TC2A-B-14V, TC2B-B-14V, and TC5-B-14V. MB6-B-15V is the

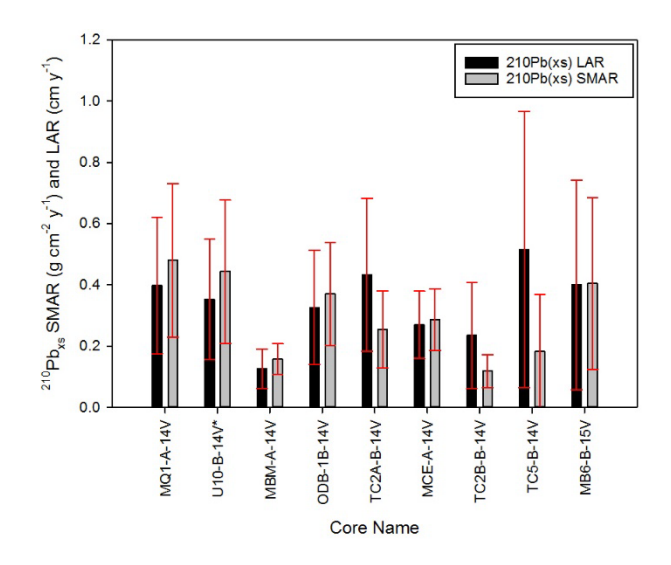
only core where MARs and LARs were equal. All three Tinker Creek sub-basins show noticeably lower bulk density values than the rest of the cores; similarly, the same three cores show higher POC inventories than the others (see Appendix B). Both of these explain why these three cores have higher LARs than MARs, regarding both 137 Cs and 210 Pb_{xs} based rates.

Figure 30 shows MARs and LARs from all cores vs. time. All cores show an *overall increase* in both LARs and MARs over the past ~100 years. MB6-B-15V, MQ1-A-14V, TC5-B-14V, and U10-B-14V show exponential increases in both MARs and LARs over the past ~100 years. MCE-A-14V and TC2B-B-14V show linear increases in both MARs and LARs over the past ~100 years. MBM-A-14V shows a linear increase in LAR, but an exponential increase in MAR. ODB-1B-14V and TC2-A-14V show exponential increases in LARs, but linear increases in MARs. Figure 30 also shows the MARs and LARs for U10-B-14V (pulse), which includes a high sedimentation pulse due to the known construction of a road crossing and levee upstream of the core site (Fletcher et al. 2012). The LARs and MARs for this core were calculated excluding the pulse, since it was an anthropogenic disturbance with a limited temporal effect.

The ¹³⁷Cs and ²¹⁰Pb_{xs}sedimentation ratios, MARs, and LARs are fairly comparable. While the sedimentation ratios for U10-B-14V (¹³⁷Cs: 0.41, ²¹⁰Pb: 1.34) and TC2A-B-14V (¹³⁷Cs: 0.43, ²¹⁰Pb: 1.29) contradict each other in terms of net erosional versus net depositional, the ratios for the other seven cores agree with each other. One possible explanation for the difference in results for these cores could be due to the high percentage of sand-sized grains. U10-B-14V and TC2A-B-14V have the two highest percentages of average sand-sized grains (85.7% and 89.8%, respectively) within the site. The fallout radionuclides adsorb better on to clay- and silt-sized particles thansand-sized particles, allowing for more precise detection (Mabit et al. 2008; Mastisoff et al. 2002; He and Walling 1996). Since these cores had fewer silt- and clay-sized particles, that might have decreased the accuracy of the detection.

The 137 Cs and 210 Pb_{xs}LARs are comparable in each core. In every core except MBM-A-14V, the 137 Cs LAR based on the 1951 rate is closer to the 210 Pb LAR, which is to be expected due to the fact that the 1951 rate encompasses more of the same time frame than the 1963-based rate. The 137 Cs rates and 210 Pb_{xs} rates differ by less than 0.1cm y⁻¹ in seven of the nine cores. The two exceptions are U10-B-14V, which had a difference of 0.11cm y⁻¹, and TC5-B-14V, which had a difference of 0.27cm y⁻¹. Similarly, the 137 Cs and 210 Pb_{xs} MARs are comparable in each core. The 1951-based 137 Cs MAR is closer to the 210 Pb_{xs} MAR in every core except MBM-A-14V, which again, is to be expected since they encompass more of the same timeframe. Seven of the nine cores have a difference <0.05g cm⁻² y⁻¹. The two exceptions are ODB-1B-14V, which has a difference of 0.122g cm⁻² y⁻¹, and TC5-B-14V, which has a difference of 0.151g cm⁻² y⁻¹. All of the differences for each set fall well within the uncertainty of the measurements, strengthening the argument that the rates are accurate since two different dating techniques are in agreement.

Figure 29: Comparison of 210 Pb_{xs}-based LARsand MARs.Error bars show one standard deviation.





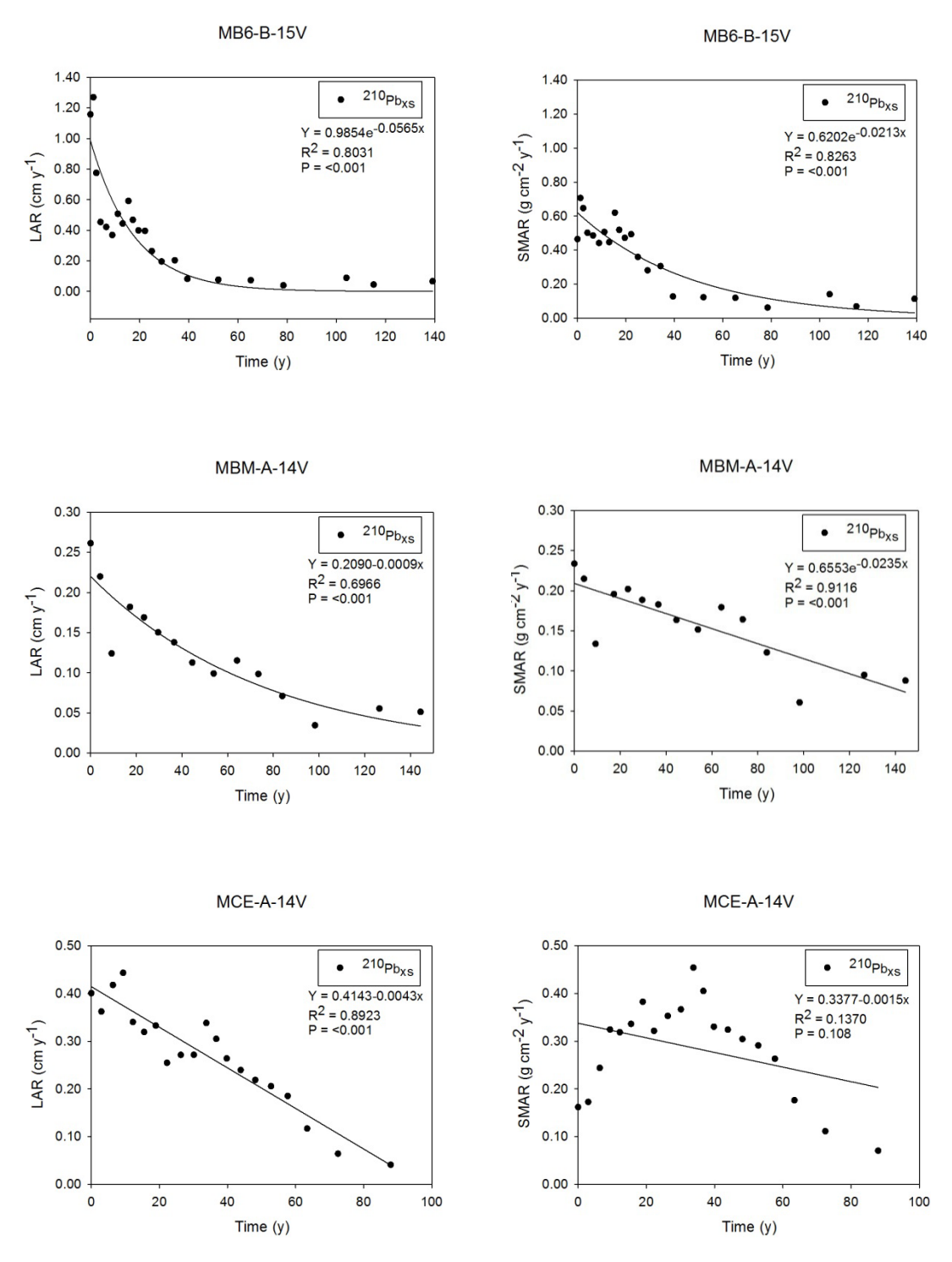


Figure 30: (continued)

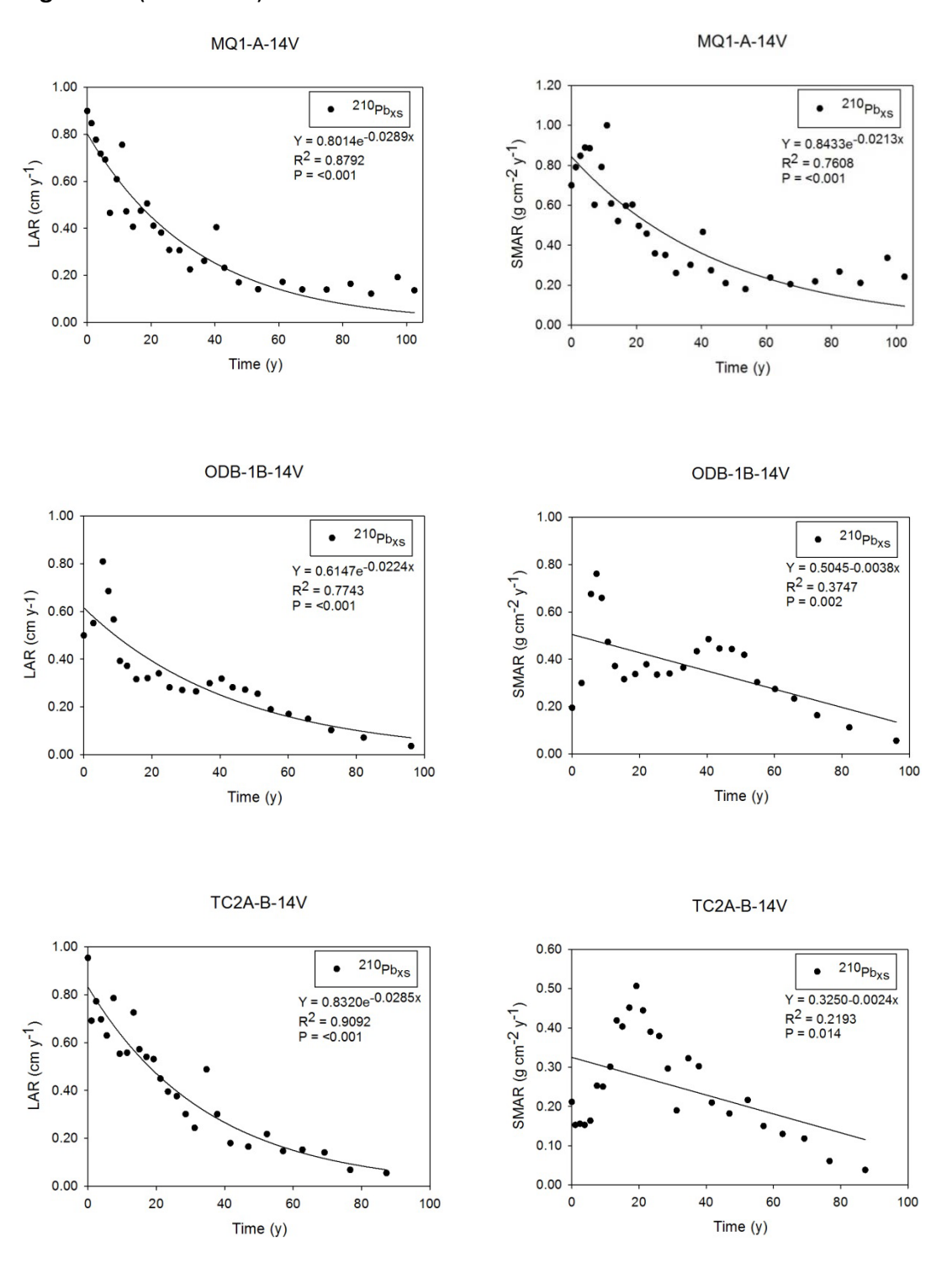


Figure 30: (continued)

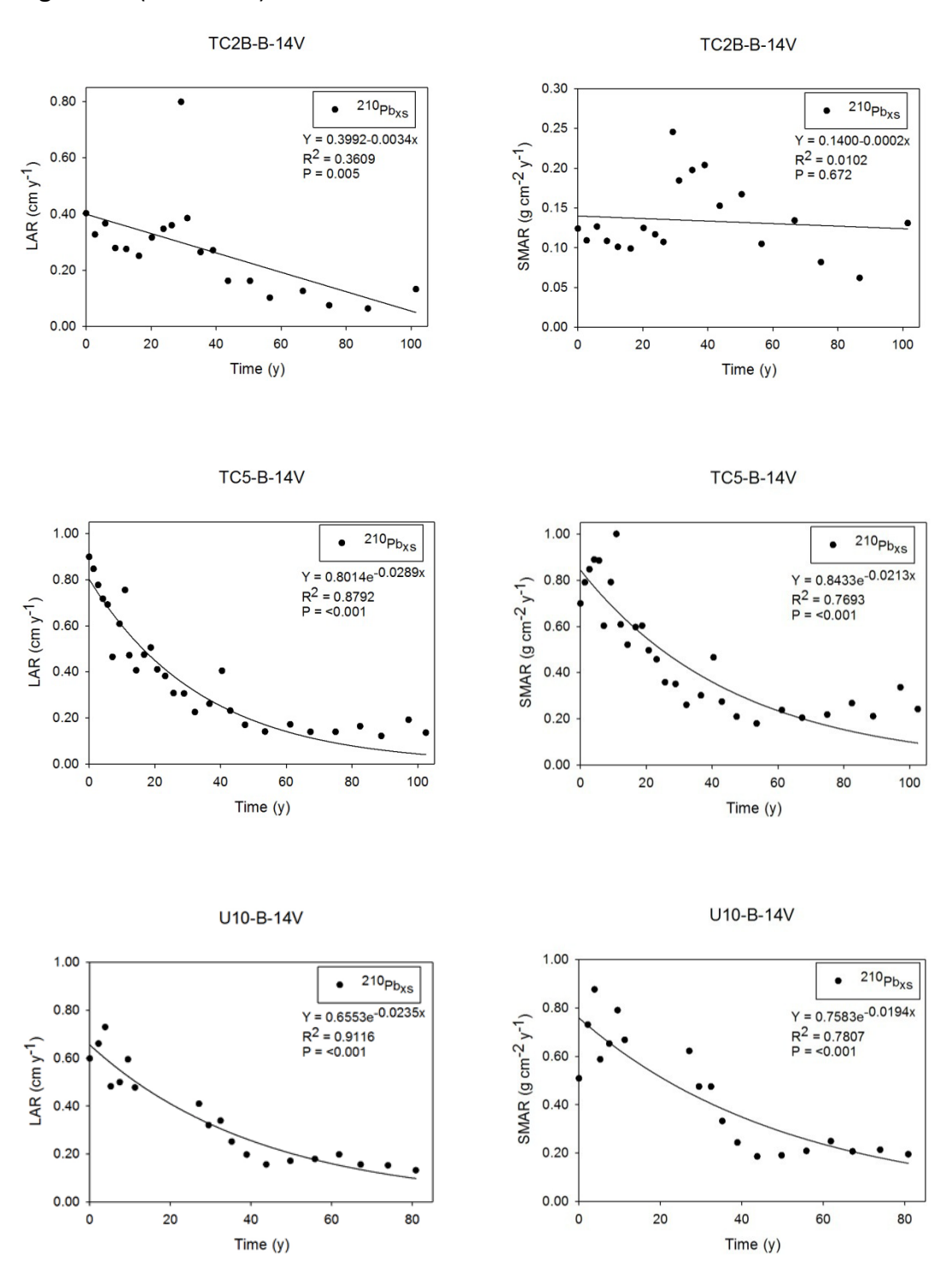
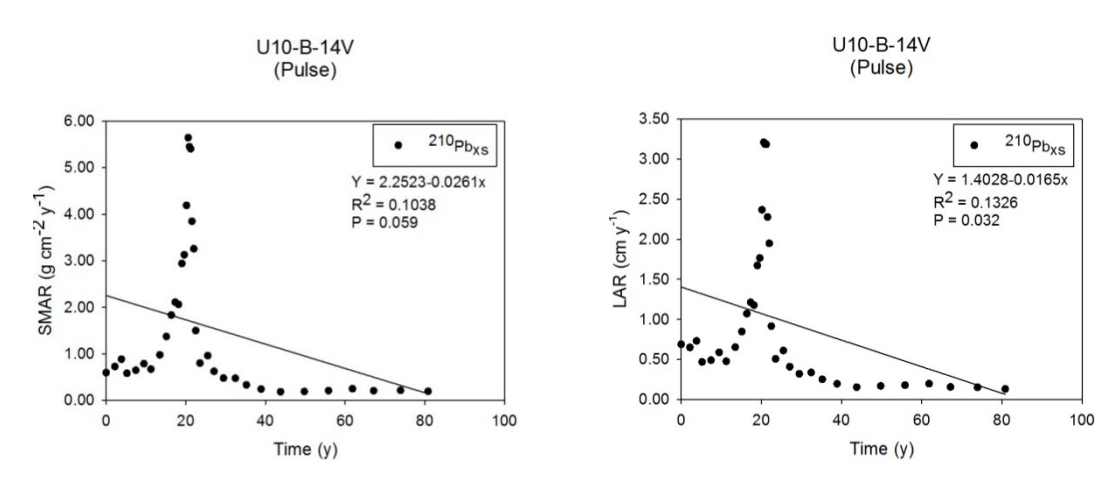


Figure 30: (continued)



4.3 Imagery

Agricultural and naturally vegetated areas were measured in the 1951 and 2014 aerial imagery (see Figs.31-39) and the "% vegetated" number was calculated by dividing the percentage of naturally vegetated land by the total area of land for each year (Table 11). TC2B-B-14V had the least amount of revegetated area in the 63 years of SRS cultivation, at 18.84% difference. TC5-B-14V had the greatest change in naturally vegetated area, at 72.49%.

Table 11: The percentage of naturally vegetated areas in 1951, and 2014 for each core.

Tunere ==: :::e per e	1 4 4 5 5 5 6 6 6 6 6 6 6 6 6 6 6 6 6 6 6							
Core Name	1951 % Vegetation	2014 % Vegetation	% Diff. in Vegetation					
MBM-A-14V	35.81	95.32	+ 59.51					
MCE-A-14V	42.99	97.54	+ 54.55					
TC2B-B-14V	75.42	94.26	+ 18.84					
ODB-1B-14V	35.81	95.32	+ 59.51					
TC2A-B-14V	75.42	94.46	+ 19.04					
U10-B-14V	62.50	95.00	+ 32.50					
MB6-B-15V	31.61	98.35	+ 66.74					
MQ1-A-14V	40.30	86.85	+ 46.55					
TC5-B-14V	25.87	98.36	+ 72.49					

Figure 31: 1951 and 2013 Imagery showing prevalence of vegetated and non-vegetated areas of U10-B-14V.

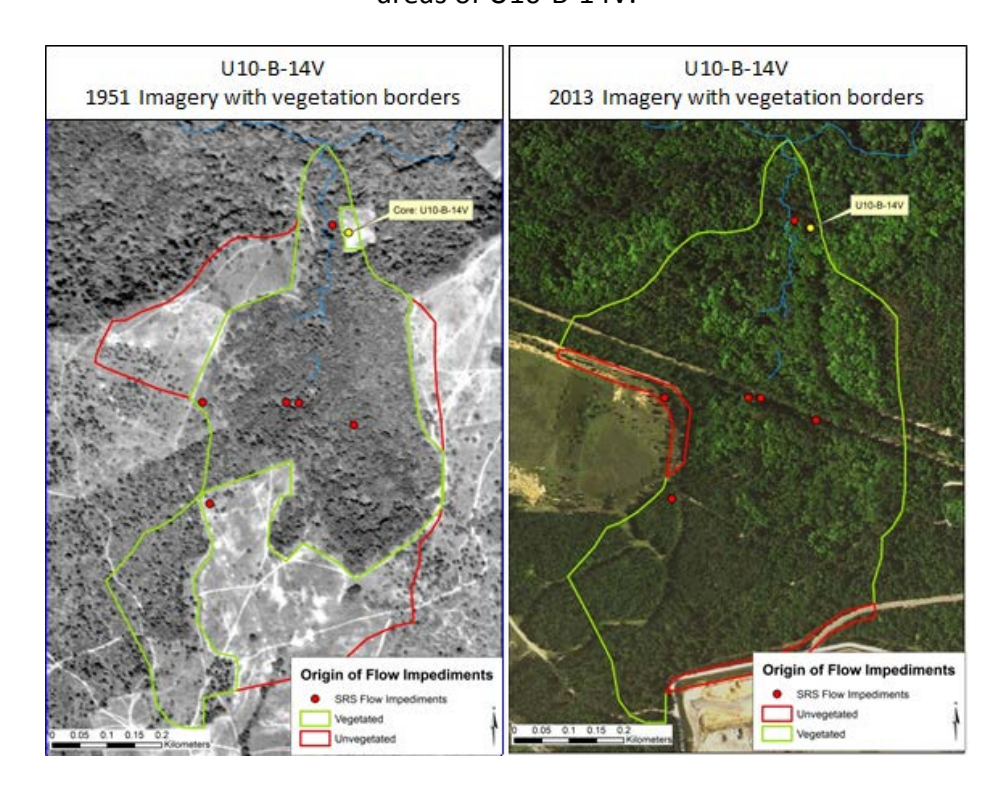


Figure 32: 1951 and 2013 Imagery showing prevalence of vegetated and non-vegetated areas of TC5-B-14V.

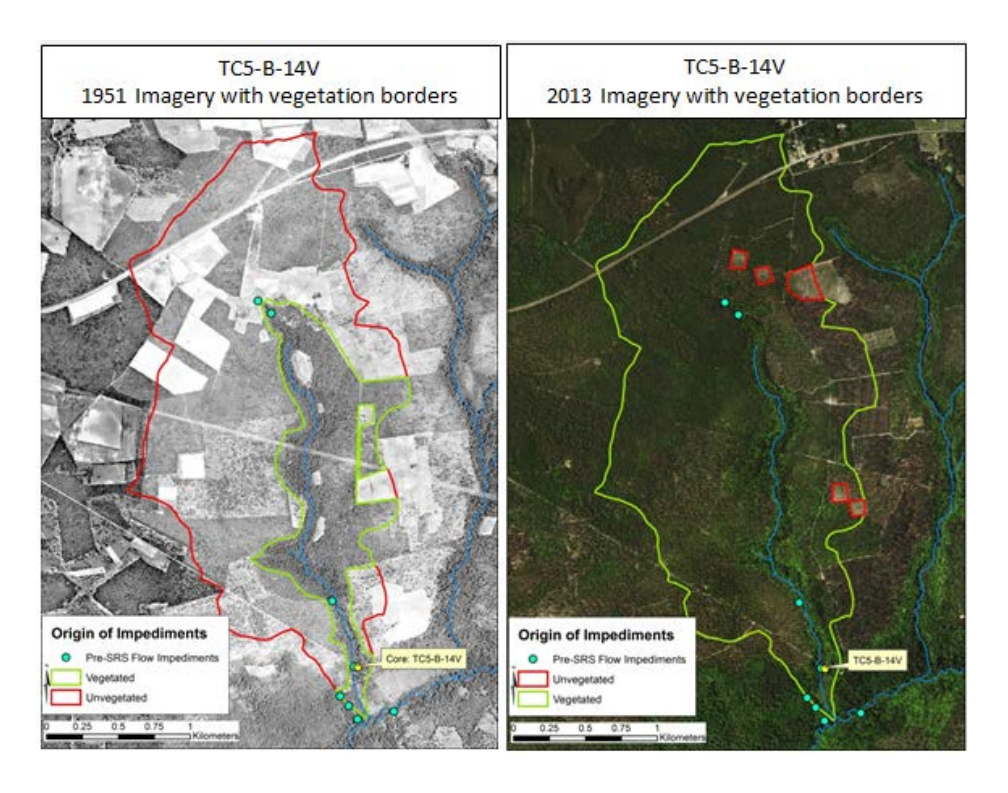


Figure 33: 1951 and 2013 Imagery showing prevalence of vegetated and non-vegetated areas of TC2A-B-14V.

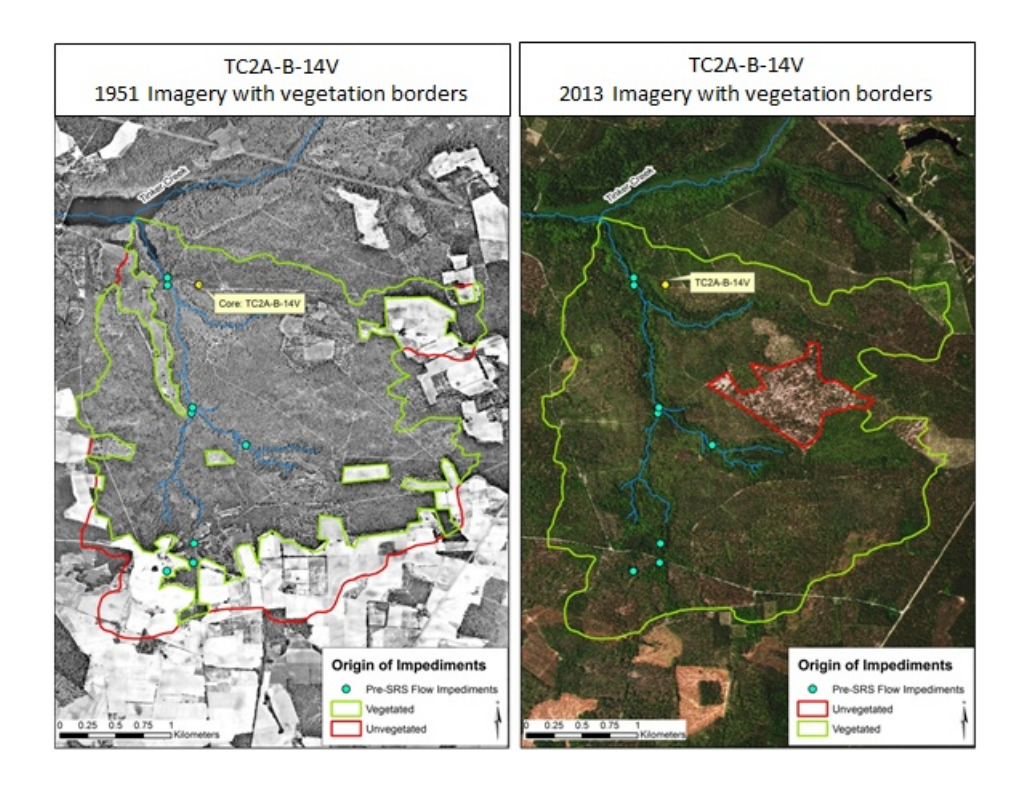


Figure 34: 1951 and 2013 Imagery showing prevalence of vegetated and non-vegetated areas of TC2B-B-14V.

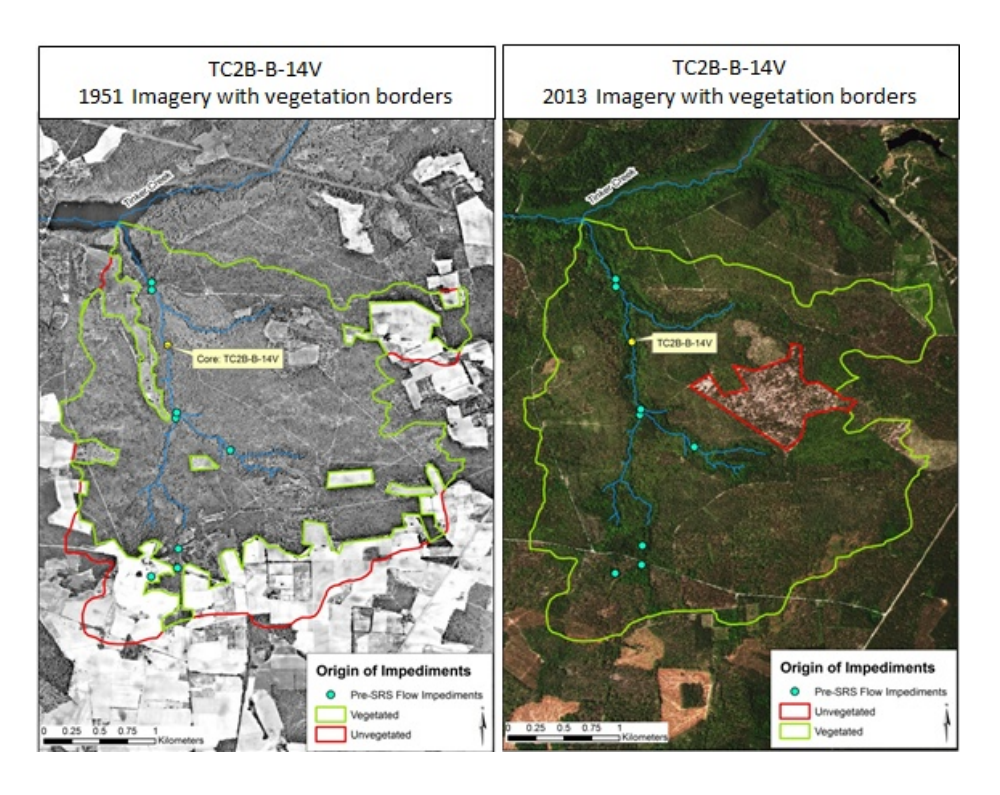


Figure 35: 1951 and 2013 Imagery showing prevalence of vegetated and non-vegetated areas of ODB-1B-14V.

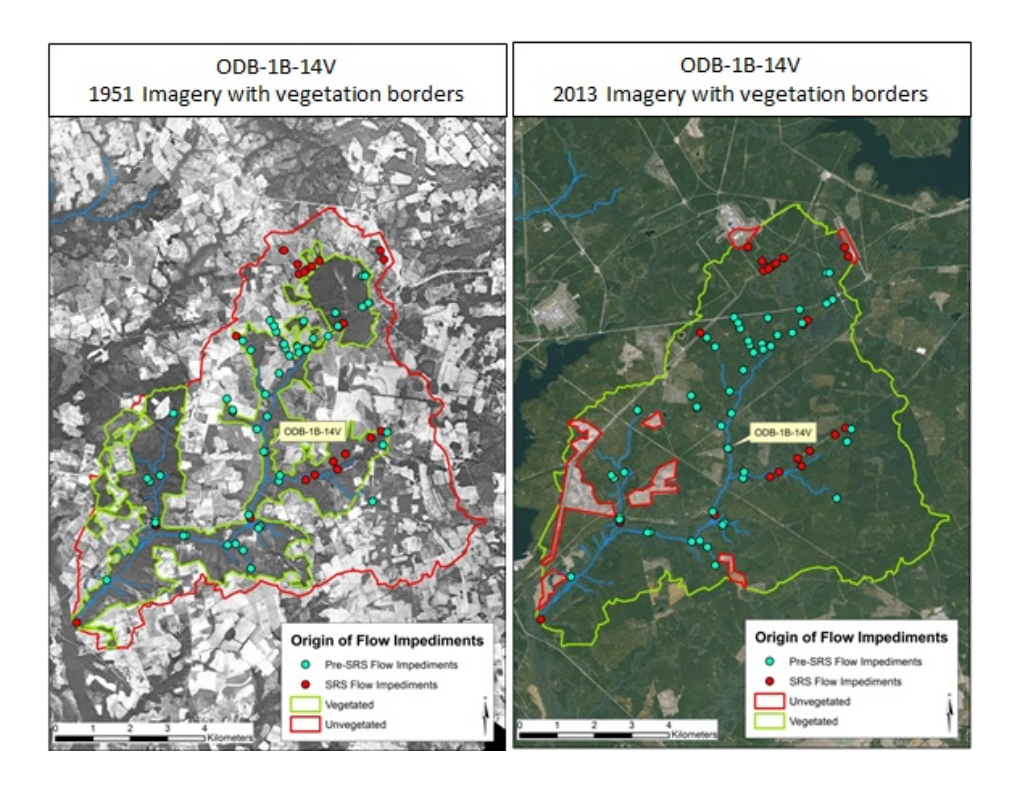


Figure 36: 1951 and 2013 Imagery showing prevalence of vegetated and non-vegetated areas of MQ1-A-14V.

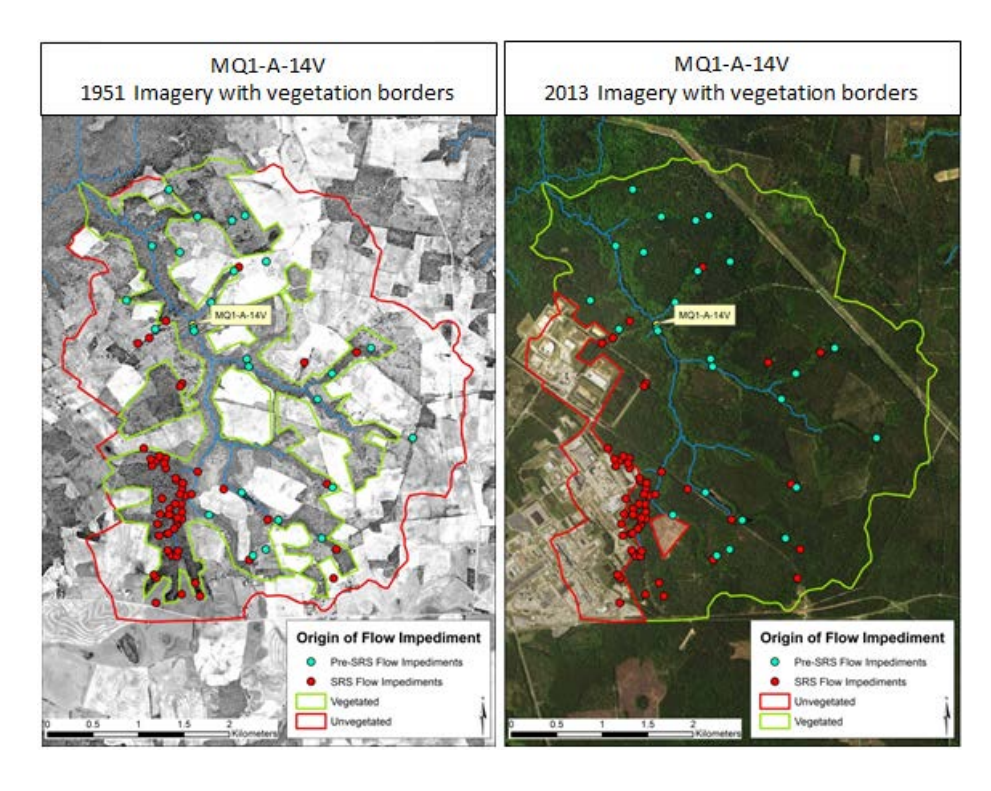


Figure 37: 1951 and 2013 Imagery showing prevalence of vegetated and non-vegetated areas of MCE-A-14V.

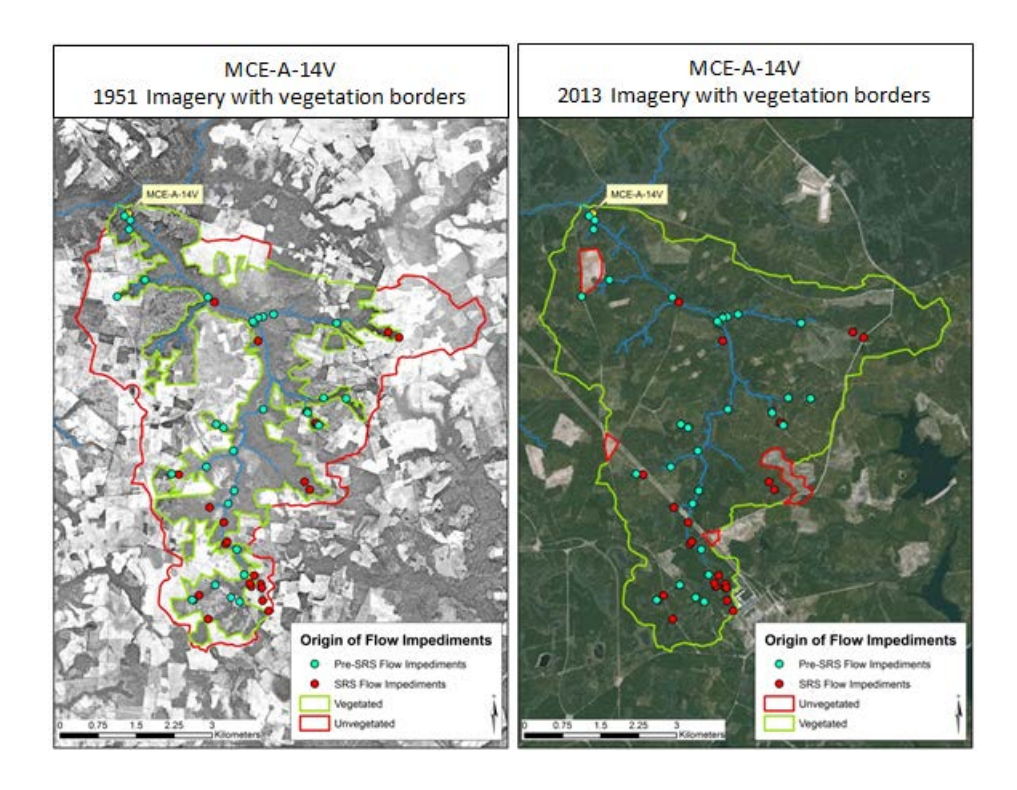


Figure 38: 1951 and 2013 Imagery showing prevalence of vegetated and non-vegetated areas of MBM-A-14V.

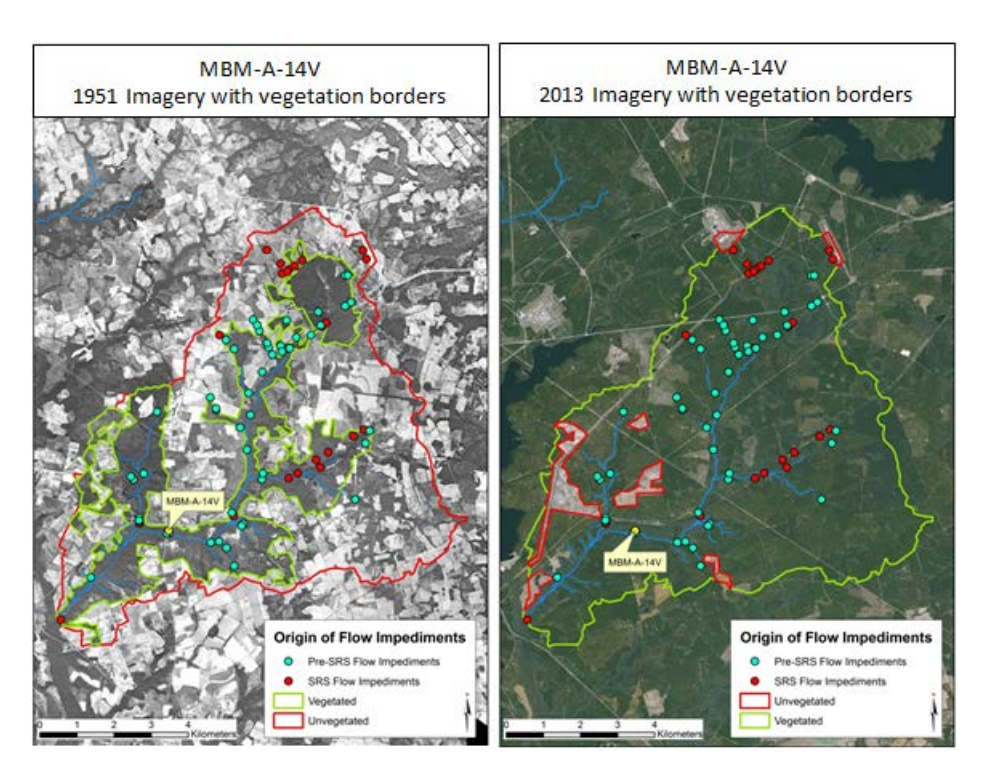
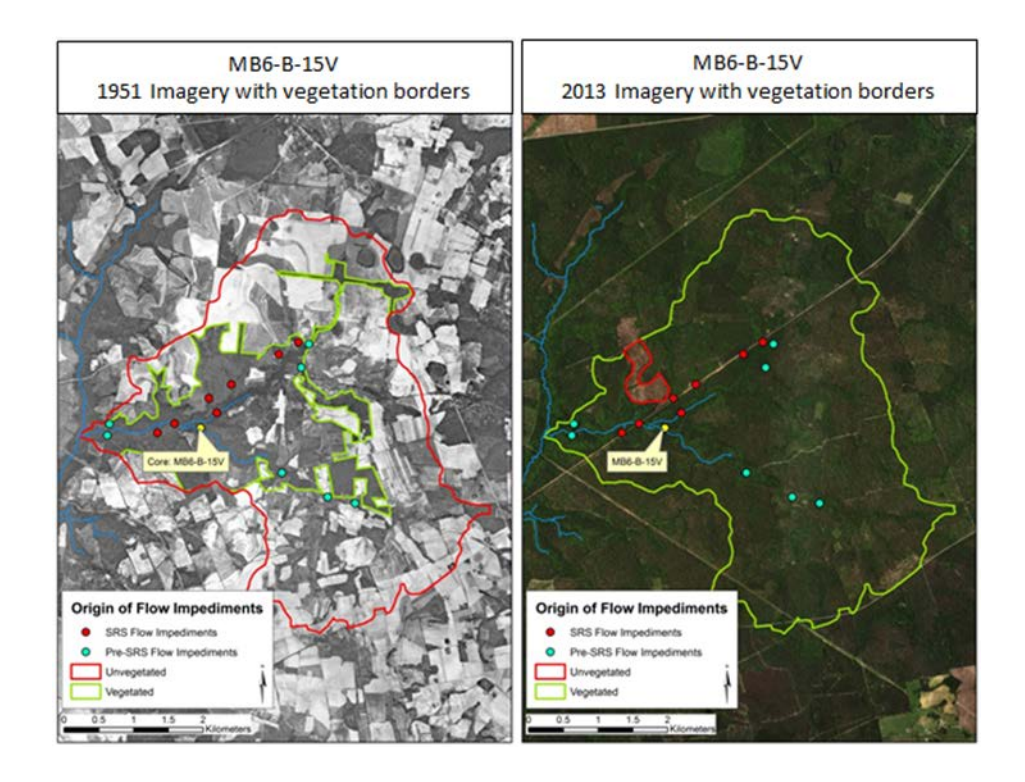


Figure 39: 1951 and 2013 Imagery showing prevalence of vegetated and non-vegetated areas of MB6-B-15.



CHAPTER FIVE: DISCUSSION

To address the hypothesis, several proxies of hydrologic connectivity and land use change were developed. Naturally vegetated and agricultural areas, identified from aerial imagery data wereused to characterize land use change. Flow obstacles and physical stream featureswere used to characterize hydrologic connectivity. Flow obstacles have also been divided to include the total number of impediments, the number of perennial impediments, the number of non-perennial impediments, and the number of impediments only found in the stream channel itself, for each sub-basin. Similarly, physical stream features include measurements of wetted perimeter, maximumchannel depth, mean channel depth, and elevation at each core location. Each of thesefactors werecompared to MARs, LARs, and sedimentation ratios to determine which, if any, has the strongest influence.

Regression analyses were performed for all combinations of each variable (e.g.,% difference in vegetation, total number of impediments, mean channel depth, etc.) and response (e.g., MARs, LARs, and sedimentation ratio). The corresponding coefficient of determination (R²) values were calculated (Table 12). The R² value represents the percentage of the data that is the closest to the line of best fit. For example, the 0.971 R² value between max channel depth and ¹³⁷Cs MAR (1951) shows that 97.1% of the total variation in ¹³⁷Cs MAR (1951) can be explained by max channel depth in the linear equation y=0.1611x - 0.9638 (i.e., as max channel depth increases, the ¹³⁷Cs-based MAR (1951) increases linearly). R² values over 0.80 are generally considered strong, while those under 0.50 are considered weak. Table 12 shows that all of the R² values for the land use change proxy are weak, between 0.018-0.526. Conversely, several R² values for hydrologic connectivity are strong, including wetted perimeter, max depth, mean depth, and elevation for MAR ¹³⁷Cs (1951) and MAR ²¹⁰Pb_{xs}; and all four categories of impediments for MAR ¹³⁷Cs (1963). While the R² values arenot strongly conclusive across all variables and responses, a trend can be seen in Figure 40, that all of the hydrologic connectivity proxies are generally stronger predictors than the land use

change proxy. This indicates that the hypothesis is supported, and that hydrologic connectivity has a greater influence on floodplain sediment accumulation rates than land use.

The idea that the correlations of sedimentation rates to wetted perimeter, mean depth, and maximum depth reflect sub-basin drainage area rather than hydrologic connectivity is not supported by the data. When the wetted perimeter, maximum depth, and mean depth are plotted against the upstream drainage area of each basin, R² values of 0.03, 0.11, and 0.04 are calculated, respectively. This indicates that these would not make good proxies for drainage area.

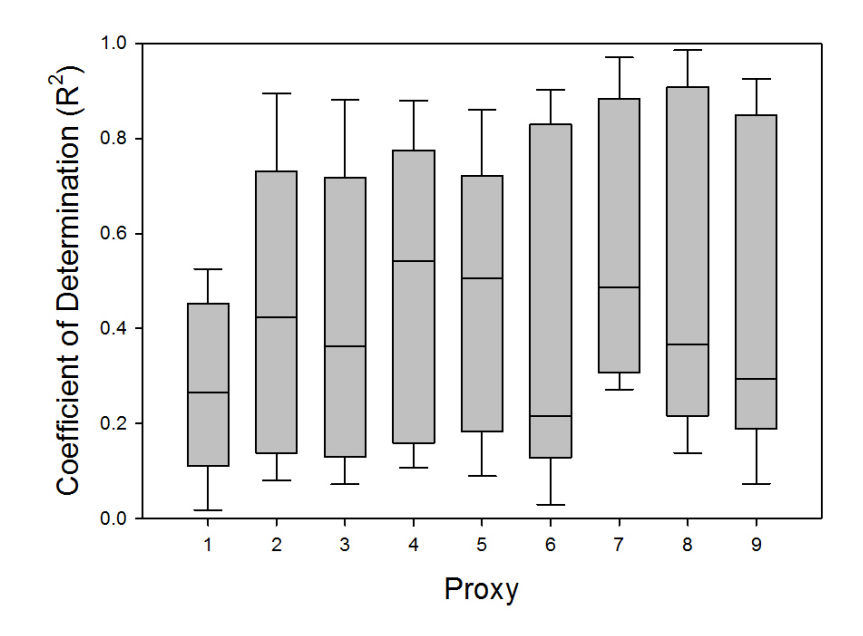
Another trend that can be seen in Table 12 is that the MARs produce higher R^2 values that their LAR counterparts. This may indicate that core shortening was a problem in the acquisition of samples, and the MARs--which take into account core shortening--may show more accurate results. This could explain why the LARs based on 210 Pb_{xs} had such low R^2 values.

Table 12: The coefficient of determination (R^2 value) results of regression analyses between LARs, MARs, and sedimentation ratios versus land use and hydrological connectivity proxies ($R^2 \ge 0.80$).

R ²	% Diff. in Veg.	# of Total Imped.	# of Perennial Imped.	# of Non- perennial Imped.	# of In- channel Imped.
MAR ¹³⁷ Cs (1951)	0.405	0.465	0.402	0.667	0.603
MAR ¹³⁷ Cs (1963)	0.348	0.895	0.882	0.880	0.861
MAR ²¹⁰ Pb	0.468	0.381	0.322	0.580	0.509
LAR ¹³⁷ Cs (1951)	0.018	0.174	0.145	0.277	0.274
LAR ¹³⁷ Cs (1963)	0.184	0.587	0.601	0.503	0.505
LAR ²¹⁰ Pb	0.164	0.081	0.072	0.107	0.089
²¹⁰ Pb Sed. Ratio	0.093	0.126	0.126	0.120	0.154
¹³⁷ Cs Sed. Ratio	0.526	0.780	0.755	0.811	0.761

R ²	Wetted Perimeter Width	Max Depth	Mean Depth	Elevation
MAR ¹³⁷ Cs (1951)	0.902	0.971	0.986	0.884
MAR ¹³⁷ Cs (1963)	0.213	0.509	0.358	0.184
MAR ²¹⁰ Pb	0.854	0.931	0.979	0.926
LAR ¹³⁷ Cs (1951)	0.757	0.744	0.698	0.747
LAR ¹³⁷ Cs (1963)	0.030	0.271	0.138	0.073
LAR ²¹⁰ Pb	0.099	0.293	0.254	0.345
²¹⁰ Pb Sed. Ratio	0.216	0.352	0.204	0.242
¹³⁷ Cs Sed. Ratio	0.215	0.466	0.374	0.201

Figure 40: Box plot showing R² value ranges for all nine proxies: 1. % difference in vegetation, 2. total impediments, 3. total perennial impediments, 4. total non-perennial impediments, 5. total in-stream impediments, 6. wetted perimeter width, 7. maximum depth, 8. mean depth, and 9. elevation.



The significance (P-value) from the regression analyses confirms the same conclusion. P-values \leq 0.05 generally indicate that the corresponding test was statistically significant. Table 13 shows that none of the tests for the land use change proxy produced statistically significant results. Hydrologic connectivity proxies, however, had 17 tests that produced statistically significant results. In fact, every R² value above 0.80 is confirmed as statistically significant with P-values \leq 0.05. This strengthens the argument that the high R² values show that hydrologic connectivity has a stronger influence than land usechange on floodplain sediment accumulation rates, confirming the hypothesis.

Table 13: The significance (P-value) results of regression analyses between LARs, MARs, and sedimentation ratios versus land use and hydrologic connectivity proxies (P < 0.05).

Significance	% Diff. in Veg.	# of Total Imped.	# of Perennial Imped.	# of Non- perennial Imped.	# of In- channel Imped.
MAR ¹³⁷ Cs (1951)	0.248	0.205	0.250	0.091	0.122
MAR ¹³⁷ Cs (1963)	0.295	0.015	0.018	0.018	0.023
MAR ²¹⁰ Pb	0.203	0.268	0.318	0.134	0.176
LAR ¹³⁷ Cs (1951)	0.831	0.484	0.527	0.362	0.366
LAR ¹³⁷ Cs (1963)	0.471	0.131	0.123	0.180	0.179
LAR ²¹⁰ Pb	0.498	0.643	0.663	0.591	0.625
²¹⁰ Pb Sed. Ratio	0.618	0.557	0.558	0.568	0.514
¹³⁷ Cs Sed. Ratio	0.166	0.047	0.056	0.037	0.054

Significance	Wetted Perimeter Width	Max Depth	Mean Depth	Elevation
MAR ¹³⁷ Cs (1951)	0.013	0.002	0.001	0.017
MAR ¹³⁷ Cs (1963)	0.433	0.176	0.286	0.472
MAR ²¹⁰ Pb	0.025	0.008	0.001	0.009
LAR ¹³⁷ Cs (1951)	0.055	0.060	0.078	0.059
LAR ¹³⁷ Cs (1963)	0.782	0.368	0.537	0.660
LAR ²¹⁰ Pb	0.605	0.346	0.387	0.298
²¹⁰ Pb Sed. Ratio	0.430	0.292	0.445	0.400
¹³⁷ Cs Sed. Ratio	0.432	0.204	0.273	0.448

Regression analyses also calculated the slope coefficients for each variable/response pair (Table 14). The slope coefficient is an indicator of the strength that the variable has on the response. The higher the magnitude, the greater the effect; negative coefficients show an inverse relationship, while positive coefficients show a direct relationship. The standard deviation for each variable was calculated to allow for a direct comparison of coefficients across each response. For every one unit of increase in the variable, the slope coefficient changes the response by that amount. For example, the 0.050 slope coefficient for % difference in vegetation on MAR 210 Pb_{xs}means that if the vegetatedland area increases by 1%, the MAR 137 Cs (1951) would increase by 0.050g cm $^{-2}$ y $^{-1}$ sitewide.Table 14 shows that more than 75% of the hydrologic connectivity proxies have a

greater impact on floodplain sediment accumulation rates and ratios than the land use change proxy. This is strong evidence that the hypothesis is true.

Table 14: The slope coefficient results of regression analyses between LARs, MARs, and sedimentation ratios versus land use and hydrological connectivity proxies.

Slope Coefficient	% Diff. in Veg.	# of Total Imped.	# of Perennial Imped.	# of Non- perennial Imped.	# of In- channel Imped.
MAR ¹³⁷ Cs (1951)	-0.158	0.185	0.184	0.180	0.204
MAR ¹³⁷ Cs (1963)	0.227	0.277	0.272	0.282	0.273
MAR ²¹⁰ Pb	0.050	0.089	0.090	0.083	0.083
LAR ¹³⁷ Cs (1951)	0.031	0.022	0.021	0.025	0.023
LAR ¹³⁷ Cs (1963)	0.103	0.093	0.085	0.115	0.107
LAR ²¹⁰ Pb	0.011	0.035	0.032	0.044	0.044
²¹⁰ Pb Sed. Ratio	0.104	0.111	0.104	0.134	0.127
¹³⁷ Cs Sed. Ratio	0.087	0.139	0.138	0.138	0.136

Slope Coefficient	Wetted Perimeter Width	Max Depth	Mean Depth	Elevation
MAR ¹³⁷ Cs (1951)	-0.241	0.308	0.235	-0.256
MAR ¹³⁷ Cs (1963)	-0.145	0.214	0.191	-0.141
MAR ²¹⁰ Pb	-0.020	0.061	0.043	-0.032
LAR ¹³⁷ Cs (1951)	-0.024	0.042	0.039	-0.045
LAR ¹³⁷ Cs (1963)	-0.139	0.145	0.149	-0.145
LAR ²¹⁰ Pb	-0.073	0.072	0.070	-0.072
²¹⁰ Pb Sed. Ratio	-0.155	0.161	0.162	-0.154
¹³⁷ Cs Sed. Ratio	-0.068	0.105	0.088	-0.063

The increase in sediment accumulation across all sub-basins studied at the SRS in the last 100 years indicate that recovery efforts are succeeding in terms of soil retention. Six of the nine cores (MB6-B-15V, MQ1-A-14V, TC2A-B-14V, TC2B-B-14V, TC5-B-14V, and U10-B-14V) show increases in sedimentation rates occurring beginning approximately 40-50 years ago, corresponding to the time shortly after the USFS started recovery efforts. Whether the main cause of the increase in sedimentation rates was stream restoration, revegetation, or something entirely separate, it is undeniable that the efforts of the USFS and SRS have yielded promising results. A closer look at the relationships between variables and responses may offer a definitive conclusion.

An inverse relationship between sediment accumulation rates and elevation has been observed at many research sites (Hupp et al. 2009; Swanson et al. 1988; Pierce and King 2008). As floodplain elevation increases, the sediment accumulation rates decrease. Areas of higher elevation tend to have steeper gradients, allowing for more channel bank-failure and sediment transport; likewise, reaches of lower elevation tend to accumulate large amounts of sediment due to flatter gradients and the aforementioned entrainment. Higher elevations also often result in reduced hydroperiods, making them more responsive to localized storm events. This holds true at the SRS (Fig.41). A similar inverse trend has been observed with channel width and sediment accumulation rates. Hupp et al. (2009) suggests a negative feedback loop develops as the floodplain surface rises in elevation relative to the widening channel, especially in narrow, channelized streams. The same relationship is observed at the SRS (Fig.42).

A direct relationship appears between both maximum and mean channel depths, and sediment accumulation rates (Figs.43,44). These could be explained by the channelization of the stream as it becomes incised. Hupp et al. (2009)and Pierce and King (2008)observed this same relationship in several rivers in the U.S. Higher elevation above the water table allows those streams to downcut farther into the sediment, creating more bank failures and entraining more sediment. The lower reaches then accumulate more sediment as channel impediments, such as debris and dams, retard

water flow and create opportunities for the stream to overfill its bank. This is also confirmed by the direct relationship seen between the number of impediments and the increase in sediment accumulation rates, under the assumption that similar results would be observed upstream of the core sites.

No multivariate analyses could be calculated due to the high number of variables and the low number of core sites. In order to perform multivariate analyses, the number of observations (in this case, 5) needs to be greater than the amount of variables (in this case, 9). Further studies would require a much greater number of core locations.

Figure 41:The standard deviations of elevation versus ¹³⁷Cs (1951) MAR showing a strong inverse relationship.

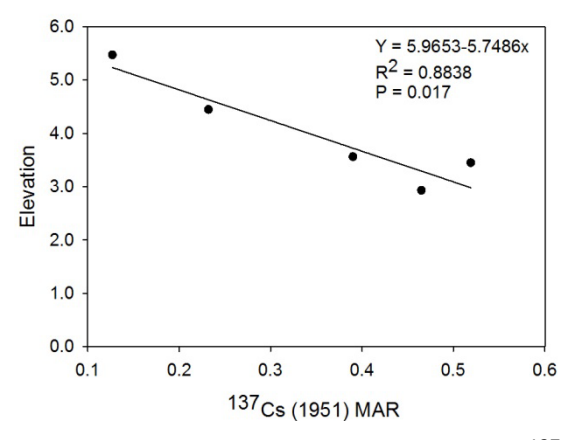


Figure 42:The standard deviations of wetted perimeter versus ¹³⁷Cs (1951) MAR showing a strong inverse relationship.

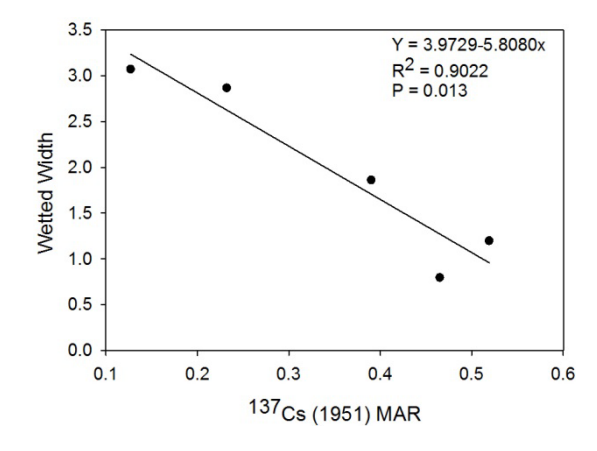


Figure 43:The standard deviations of max depth versus 137 Cs (1951) MAR showing a strong direct relationship.

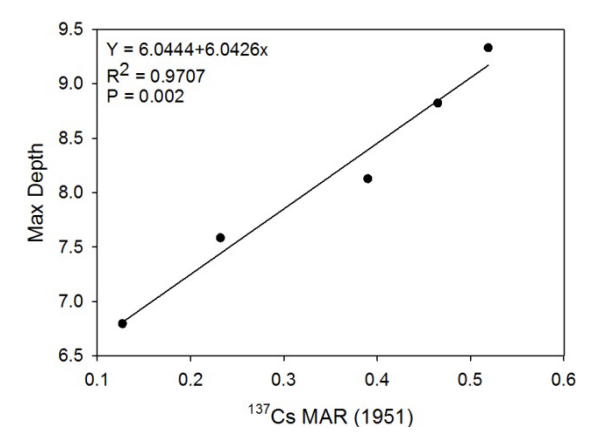
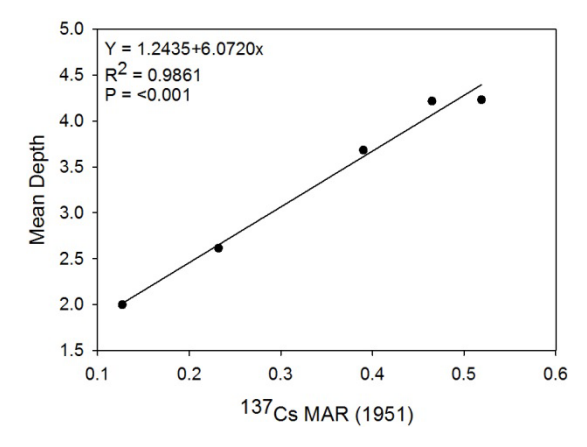


Figure 44:The standard deviations of mean depth versus 137 Cs (1951) MAR showing a strong direct relationship.



CHAPTER SIX: CONCLUSIONS

The results of this research successfully address the hypothesis presented. All objectives were completed and helped to interpret the data. Nine cores from seven distinct sub-basin floodplainsacross the SRS were sampled to depthscontaining > 100 years of sedimentation record. ¹³⁷Cs and ²¹⁰Pb fallout radionuclides were utilized to quantify sediment accumulation rates for all cores. An inventory of natural and anthropogenic flow impediments was constructed using field surveys across the SRS, and these data were organized into four categories: total flow impediments, in-stream flow impediments, perennial flow impediments, and non-perennial flow impediments. Land use change was calculated using GIS software, aerial imagery, and LiDAR data to measure the change from cultivated to reforested land areas. Finally, stream physical characteristics—including channel depths, widths, and elevation—were collected.

Comparing the proxies for land use change and hydrologic connectivity with the MARs and LARs provided interesting results. Some hydrologic connectivity proxies gave R² values as high as 0.971, 0.979, and 0.986, while the land use change proxy gave significantly lower values, at best 0.526. Higher R²values demonstrate that the sediment accumulation rateshave stronger linear relationshipswith hydrologic connectivity proxies thanwith the land use change proxy, thereby validating the hypothesis. Likewise, lower p-values reflect more statistically significant effects on floodplain sediment accumulation rates and ratios by hydrologic connectivity proxies. Finally, the regression analyses also confirmed that the overall strength that the variable has on the response is greater in the majority of hydrologic connectivity proxies, than in the land use proxy.

In agreement with other studies, this research has observed that as elevation and wetted perimeter measurements increase, the sediment accumulation rates and ratios have all decreased. Conversely, as the mean depth, maximum depth, number of impediments, and percentage of naturally vegetated land use increases, so too does the

sediment accumulation rates and ratios. The magnitude of the change to sediment accumulation rates and ratios is much greater, and more statistically significant, for hydrologic connectivity proxies (i.e., impediments and physical stream characteristics) than it is for land use.

While this research does have some definitive results, more study is needed to fully realize this work. Stronger proxies for land use change need to be identified. Ways to quantify—rather than qualify—hydrologic connectivity need to be utilized. Being able to measure and quantify how much an impediment impacts flow will give a much more accurate relationship between the two. Sampling sizes were also an issue, as a more rigorous statistical approach needed several more stations than this study allowed. Overall, the objectives of this thesis were met, and the hypothesis was addressed and confirmed by the data and statistical approaches utilized.

APPENDIX

Core Name	Latitude	Longitude	Elevation (m above MSL)	Stream reach to Savannah River (m)
MQ1-A-14V	+33° 18' 28.6"	-81° 37' 54.7"	52.56	26,627.78
U10-B-14V	+33° 18' 00.9"	-81° 39' 57.8"	44.68	20,300.06
MBM-A-14V	+33° 10′ 02.3″	-81° 36' 02.1"	40.82	11,387.53
ODB-1B-14V	+33° 11' 01.0"	-81° 34' 52.8"	50.22	15,621.01
TC2A-B-14V	+33° 21' 44.2"	-81° 31' 05.4"	67.76	42,940.56
MCE-A-14V	+33° 20' 01.0"	-81° 36' 26.8"	52.00	29,277.69
TC2B-B-14V	+33° 21' 57.6"	-81° 31' 00.9"	83.39	42,469.41
TC5-B-14V	+33° 22' 18.8"	-81° 32' 58.9"	62.34	38,857.92
MB6-B-15V	+33° 10' 42.5"	-81° 33' 56.7"	54.28	16,497.04

MQ1-A-14V

Interval (cm)	Assumed + OM Porosity (%)	Bulk Density (g/cm³)	Assumed + OM Mass Depth (g/cm²)	Assumed + OM Cumulative Mass Depth (g/cm²)	Particulate Organic Carbon (%)	Sand (%)	Silt (%)	Clay (%)
0-1	0.677	0.788	0.78 ± 0.08	0.78 ± 0.08	5.738	51.21	43.06	5.73
1-2	0.616	0.944	0.93 ± 0.09	1.71 ± 0.17	4.400	66.99	28.74	4.27
2-3	0.550	1.106	1.09 ± 0.11	2.80 ± 0.28	4.679	49.44	30.67	19.89
3-4	0.497	1.249	1.24 ± 0.12	4.04 ± 0.40	2.156	45.36	31.89	22.75
4-5	0.482	1.287	1.28 ± 0.13	5.32 ± 0.53	1.756	67.42	20.72	11.86
5-6	0.477	1.302	1.30 ± 0.13	6.62 ± 0.66	1.560	67.30	20.32	12.38
6-7	0.475	1.307	1.30 ± 0.13	7.92 ± 0.79	1.334	53.09	28.18	18.73
7-8	0.466	1.331	1.32 ± 0.13	9.25 ± 0.92	1.312	50.87	34.70	14.43
8-9	0.478	1.297	1.29 ± 0.13	10.54 ± 1.05	1.780	60.70	22.79	16.51
9-10	0.483	1.287	1.28 ± 0.13	11.82 ± 1.18	1.525	47.04	29.45	23.51
10-11	0.492	1.265	1.26 ± 0.13	13.07 ± 1.31	1.497	60.23	26.46	13.31
11-12	0.518	1.199	1.19 ± 0.12	14.27 ± 1.43	1.638	57.67	23.05	19.28
12-13	0.510	1.217	1.21 ± 0.12	15.48 ± 1.55	2.067	49.24	25.58	25.18
13-14	0.514	1.207	1.20 ± 0.12	16.68 ± 1.67	2.081	51.43	33.81	14.76
14-15	0.528	1.172	1.16 ± 0.12	17.84 ± 1.78	2.204	48.68	32.83	18.49
15-16	0.534	1.155	1.15 ± 0.11	18.99 ± 1.90	2.749	49.78	28.35	21.87
16-17	0.529	1.166	1.16 ± 0.12	20.14 ± 2.01	2.807	46.27	28.07	25.66
17-18	0.532	1.160	1.15 ± 0.12	21.29 ± 2.13	2.208	59.85	34.43	5.72
18-19	0.530	1.163	1.15 ± 0.12	22.45 ± 2.24	3.013	56.15	36.68	7.17
19-20	0.517	1.195	1.18 ± 0.12	23.63 ± 2.36	2.978	59.52	34.12	6.36

MQ1-A-14V

Interval	Assumed + OM Porosity	Bulk Density	Assumed + OM Mass Depth	Assumed + OM Cumulative Mass Depth	Particulate Organic Carbon	Sand	Silt	Clay
(cm)	(%)	(g/cm³)	(g/cm²)	(g/cm²)	(%)	(%)	(%)	(%)
20-21	0.498	1.244	1.23 ± 0.12	24.86 ± 2.49	2.952	67.14	22.97	9.89
21-22	0.484	1.284	1.28 ± 0.13	26.14 ± 2.61	1.392	70.62	23.95	5.43
22-23	0.441	1.390	1.38 ± 0.14	27.52 ± 2.75	1.703	69.61	24.36	6.03
23-24	0.412	1.468	1.46 ± 0.15	28.99 ± 2.90	0.807	77.04	19.09	3.87
24-25	0.372	1.567	1.56 ± 0.16	30.55 ± 3.05	0.628	83.53	13.39	3.08
25-26	0.345	1.635	1.63 ± 0.16	32.18 ± 3.22	0.542	83.12	14.04	2.84
26-27	0.307	1.732	1.73 ± 0.17	33.91 ± 3.39	0.570	85.57	12.22	2.21
27-28	0.297	1.757	1.75 ± 0.18	35.66 ± 3.57	0.340	86.52	11.19	2.29
28-29	0.289	1.776	1.77 ± 0.18	37.44 ± 3.74	0.201	92.52	6.42	1.06
29-30	0.273	1.816	1.81 ± 0.18	39.25 ± 3.93	0.150	93.31	5.61	1.08
30-31	0.279	1.802	1.80 ± 0.18	41.05 ± 4.11	ND	97.42	2.43	0.15
31-32	0.276	1.810	1.81 ± 0.18	42.86 ± 4.29	ND	98.21	1.63	0.16
32-33	0.275	1.813	1.81 ± 0.18	44.67 ± 4.47	ND	98.21	1.69	0.10
33-34	0.273	1.817	1.82 ± 0.18	46.49 ± 4.65	ND	98.54	1.35	0.11
34-35	0.277	1.807	1.81 ± 0.18	48.30 ± 4.83	ND	98.23	1.68	0.09
35-36	0.279	1.801	1.80 ± 0.18	50.10 ± 5.01	ND	97.71	2.02	0.27
36-37	0.288	1.779	1.78 ± 0.18	51.88 ± 5.19	ND	98.31	1.69	0.00
37-38	0.291	1.772	1.77 ± 0.18	53.65 ± 5.37	ND	97.15	2.50	0.35
38-39	0.287	1.781	1.78 ± 0.18	55.43 ± 5.54	ND	97.03	2.59	0.38
39-40	0.292	1.771	1.77 ± 0.18	57.20 ± 5.72	ND	99.51	0.49	0.00

MQ1-A-14V

Interval	Assumed + OM Porosity	Bulk Density	Assumed + OM Mass Depth	Assumed + OM Cumulative Mass Depth	Particulate Organic Carbon	Sand	Silt	Clay
(cm)	(%)	(g/cm³)	(g/cm^2)	(g/cm²)	(%)	(%)	(%)	(%)
40-41	0.293	1.768	1.77 ± 0.18	58.97 ± 5.90	ND	97.27	2.68	0.05
41-42	0.288	1.779	1.78 ± 0.18	60.75 ± 6.08	ND	96.37	3.53	0.10
42-43	0.273	1.817	1.82 ± 0.18	62.57 ± 6.26	ND	97.80	2.20	0.00
43-44	0.264	1.841	1.84 ± 0.18	64.41 ± 6.44	ND	100.00	0.00	0.00
44-45	0.253	1.866	1.87 ± 0.19	66.27 ± 6.63	ND	98.14	1.86	0.00
45-46	0.251	1.874	1.87 ± 0.19	68.15 ± 6.81	ND	97.18	2.64	0.18
46-47	0.251	1.873	1.87 ± 0.19	70.02 ± 7.00	ND	97.80	2.20	0.00
47-48	0.248	1.879	1.88 ± 0.19	71.90 ± 7.19	ND	97.29	2.64	0.07
48-49	0.289	1.777	1.78 ± 0.18	73.68 ± 7.37	ND	89.44	9.15	1.41
49-50	0.632	0.919	0.92 ± 0.09	74.60 ± 7.46	ND	51.55	39.30	9.15

U10-B-14V

Interval	Assumed + OM Porosity	Bulk Density	Assumed + OM Mass Depth	Assumed + OM Cumulative Mass Depth	Particulate Organic Carbon	Sand	Silt	Clay
(cm)	(%)	(g/cm³)	(g/cm²)	(g/cm²)	(%)	(%)	(%)	(%)
0-1	0.643	0.788	0.85 ± 0.09	0.85 ± 0.09	5.74	69.01	19.34	11.65
1-2	0.547	0.944	1.11 ± 0.11	1.96 ± 0.20	4.40	77.70	14.59	7.71
2-3	0.512	1.106	1.20 ± 0.12	3.16 ± 0.32	4.68	69.99	19.25	10.76
3-4	0.498	1.249	1.22 ± 0.12	4.38 ± 0.44	2.16	65.45	19.38	15.17
4-5	0.466	1.287	1.31 ± 0.13	5.68 ± 0.57	1.76	74.38	22.82	2.80
5-6	0.461	1.302	1.33 ± 0.13	7.01 ± 0.70	1.56	73.90	15.44	10.66
6-7	0.436	1.307	1.40 ± 0.14	8.41 ± 0.84	1.33	77.37	14.13	8.50
7-8	0.399	1.331	1.49 ± 0.15	9.90 ± 0.99	1.31	75.71	12.91	11.38
8-9	0.352	1.297	1.61 ± 0.16	11.51 ± 1.15	1.78	81.67	13.82	4.51
9-10	0.314	1.287	1.71 ± 0.17	13.22 ± 1.32	1.53	96.45	3.18	0.37
10-11	0.303	1.265	1.74 ± 0.17	14.96 ± 1.50	1.50	95.24	4.11	0.65
11-12	0.299	1.199	1.75 ± 0.17	16.71 ± 1.67	1.64	95.07	3.17	1.76
12-13	0.296	1.217	1.76 ± 0.18	18.46 ± 1.85	2.07	93.26	3.04	3.70
13-14	0.291	1.207	1.77 ± 0.18	20.23 ± 2.02	2.08	92.08	6.91	1.01
14-15	0.292	1.172	1.77 ± 0.18	22.00 ± 2.20	2.20	95.32	4.10	0.58
15-16	0.296	1.155	1.76 ± 0.18	23.76 ± 2.38	2.75	97.02	2.72	0.26
16-17	0.316	1.166	1.71 ± 0.17	25.47 ± 2.55	2.81	95.63	3.85	0.52
17-18	0.320	1.160	1.70 ± 0.17	27.16 ± 2.72	2.21	92.56	6.56	0.88
18-19	0.324	1.163	1.69 ± 0.17	28.85 ± 2.89	3.01	92.33	4.69	2.98
19-20	0.330	1.195	1.67 ± 0.17	30.52 ± 3.05	2.98	87.56	6.61	5.83

U10-B-14V

Interval	Assumed + OM Porosity	Bulk Density	Assumed + OM Mass Depth	Assumed + OM Cumulative Mass Depth	Particulate Organic Carbon	Sand	Silt	Clay
(cm)	(%)	(g/cm³)	(g/cm²)	(g/cm²)	(%)	(%)	(%)	(%)
20-21	0.345	1.244	1.63 ± 0.16	32.16 ± 3.22	2.95	69.78	14.80	15.42
21-22	0.366	1.284	1.58 ± 0.16	33.73 ± 3.37	1.39	61.11	17.49	21.40
22-23	0.370	1.390	1.57 ± 0.16	35.30 ± 3.53	1.70	63.71	16.85	19.44
23-24	0.388	1.468	1.52 ± 0.15	36.82 ± 3.68	0.81	65.77	17.74	16.49
24-25	0.404	1.567	1.48 ± 0.15	38.30 ± 3.83	0.63	62.51	19.10	18.39
25-26	0.434	1.635	1.40 ± 0.14	39.71 ± 3.97	0.54	85.53	12.76	1.71
26-27	0.468	1.732	1.32 ± 0.13	41.03 ± 4.10	0.57	66.51	19.90	13.59
27-28	0.501	1.757	1.23 ± 0.12	42.26 ± 4.23	0.34	76.71	20.45	2.84
28-29	0.519	1.776	1.19 ± 0.12	43.45 ± 4.34	0.20	77.01	17.56	5.43
29-30	0.551	1.816	1.11 ± 0.11	44.56 ± 4.46	0.15	65.19	30.07	4.74
30-31	0.535	1.802	1.16 ± 0.12	45.72 ± 4.57	ND	73.72	23.61	2.67
31-32	0.498	1.810	1.25 ± 0.13	46.98 ± 4.70	ND	76.28	21.08	2.64
32-33	0.469	1.813	1.33 ± 0.13	48.31 ± 4.83	ND	82.43	15.72	1.85
33-34	0.440	1.817	1.40 ± 0.14	49.71 ± 4.97	ND	86.46	12.26	1.28
34-35	0.409	1.807	1.48 ± 0.15	51.18 ± 5.12	ND	94.60	4.96	0.44
35-36	0.370	1.801	1.57 ± 0.16	52.76 ± 5.28	ND	96.64	3.16	0.20
36-37	0.372	1.779	1.57 ± 0.16	54.33 ± 5.43	ND	94.76	4.73	0.51
37-38	0.343	1.772	1.64 ± 0.16	55.97 ± 5.60	ND	96.30	3.48	0.22
38-39	0.295	1.781	1.76 ± 0.18	57.74 ± 5.77	ND	97.97	1.93	0.10
39-40	0.292	1.771	1.77 ± 0.18	59.51 ± 5.95	ND	99.94	0.06	0.00

U10-B-14V

Interval	Assumed + OM Porosity	Bulk Density	Assumed + OM Mass Depth	Assumed + OM Cumulative Mass Depth	Particulate Organic Carbon	Sand	Silt	Clay
(cm)	(%)	(g/cm³)	(g/cm^2)	(g/cm²)	(%)	(%)	(%)	(%)
40-41	0.283	1.768	1.79 ± 0.18	61.30 ± 6.13	ND	98.21	1.79	0.00
41-42	0.279	1.779	1.80 ± 0.18	63.10 ± 6.31	ND	98.18	1.82	0.00
42-43	0.330	1.817	1.67 ± 0.17	64.78 ± 6.48	ND	100.00	0.00	0.00
43-44	0.348	1.841	1.63 ± 0.16	66.40 ± 6.64	ND	100.00	0.00	0.00
44-45	0.334	1.866	1.66 ± 0.17	68.07 ± 6.81	ND	99.94	0.06	0.00
45-46	0.332	1.874	1.67 ± 0.17	69.74 ± 6.97	ND	99.77	0.23	0.00
46-47	0.332	1.873	1.67 ± 0.17	71.41 ± 7.14	ND	100.00	0.00	0.00
47-48	0.329	1.879	1.68 ± 0.17	73.09 ± 7.31	ND	100.00	0.00	0.00
48-49	0.352	1.777	1.62 ± 0.16	74.71 ± 7.47	ND	99.75	0.25	0.00
49-50	0.351	0.919	1.62 ± 0.16	76.33 ± 7.63	ND	100.00	0.00	0.00

MBM-A-14V

Interval	Assumed + OM Porosity	Bulk Density	Assumed + OM Mass Depth	Assumed + OM Cumulative Mass Depth	Particulate Organic Carbon	Sand	Silt	Clay
(cm)	(%)	(g/cm³)	(g/cm^2)	(g/cm²)	(%)	(%)	(%)	(%)
0-1	0.635	0.405	0.89 ± 0.09	0.89 ± 0.09	3.016	80.98	16.28	2.74
1-2	0.602	0.560	0.98 ± 0.10	1.87 ± 0.19	2.698	88.34	9.66	2.00
2-3	0.562	0.842	1.08 ± 0.11	2.95 ± 0.29	2.255	88.22	9.58	2.20
3-4	0.561	1.117	1.08 ± 0.11	4.03 ± 0.40	3.042	90.46	7.80	1.74
4-5	0.516	1.171	1.20 ± 0.12	5.22 ± 0.52	1.869	85.08	10.41	4.51
5-6	0.496	1.212	1.25 ± 0.13	6.47 ± 0.65	0.855	89.65	8.32	2.03
6-7	0.467	1.004	1.32 ± 0.13	7.80 ± 0.78	0.875	80.80	15.56	3.64
7-8	0.417	1.011	1.45 ± 0.15	9.25 ± 0.92	0.762	92.62	6.06	1.32
8-9	0.385	1.056	1.53 ± 0.15	10.78 ± 1.08	0.631	94.37	4.63	1.00
9-10	0.376	1.117	1.56 ± 0.16	12.34 ± 1.23	0.339	95.91	3.45	0.64
10-11	0.331	1.197	1.67 ± 0.17	14.01 ± 1.40	0.333	94.87	4.24	0.89
11-12	0.306	1.262	1.73 ± 0.17	15.74 ± 1.57	0.288	98.64	1.34	0.02
12-13	0.296	1.380	1.76 ± 0.18	17.49 ± 1.75	0.310	98.59	1.23	0.18
13-14	0.315	1.456	1.71 ± 0.17	19.20 ± 1.92	0.155	99.65	0.33	0.02
14-15	0.315	1.528	1.71 ± 0.17	20.92 ± 2.09	0.154	98.45	1.29	0.26
15-16	0.313	1.583	1.72 ± 0.17	22.63 ± 2.26	0.081	100.00	0.00	0.00
16-17	0.261	1.629	1.85 ± 0.18	24.48 ± 2.45	0.027	100.00	0.00	0.00
17-18	0.265	1.647	1.84 ± 0.18	26.31 ± 2.63	0.008	100.00	0.00	0.00
18-19	0.279	1.600	1.80 ± 0.18	28.12 ± 2.81	0.008	100.00	0.00	0.00
19-20	0.296	1.612	1.76 ± 0.18	29.88 ± 2.99	0.033	100.00	0.00	0.00

MBM-A-14V

Interval	Assumed + OM Porosity	Bulk Density	Assumed + OM Mass Depth	Assumed + OM Cumulative Mass Depth	Particulate Organic Carbon	Sand	Silt	Clay
(cm)	(%)	(g/cm³)	(g/cm^2)	(g/cm²)	(%)	(%)	(%)	(%)
20-21	0.307	1.568	1.73 ± 0.17	31.61 ± 3.16	0.067	100.00	0.00	0.00
21-22	0.304	1.596	1.74 ± 0.17	33.35 ± 3.33	0.091	100.00	0.00	0.00
22-23	0.302	1.574	1.74 ± 0.17	35.09 ± 3.51	0.031	100.00	0.00	0.00
23-24	0.317	1.564	1.71 ± 0.17	36.80 ± 3.68	0.054	99.57	0.43	0.00
24-25	0.311	1.621	1.72 ± 0.17	38.52 ± 3.85	0.026	100.00	0.00	0.00
25-26	0.309	1.746	1.73 ± 0.17	40.25 ± 4.02	0.049	99.33	0.67	0.00
26-27	0.305	1.747	1.74 ± 0.17	41.98 ± 4.20	0.029	98.84	1.09	0.07
27-28	0.300	1.221	1.75 ± 0.17	43.73 ± 4.37	0.146	99.39	0.61	0.00
28-29	0.311	1.719	1.71 ± 0.17	45.44 ± 4.54	0.907	86.58	8.69	4.73
29-30	0.353	1.694	1.62 ± 0.16	47.06 ± 4.71	ND	69.51	18.73	11.76
30-31	0.416	1.715	1.46 ± 0.15	48.52 ± 4.85	ND	87.19	10.95	1.86
31-32	0.480	1.780	1.30 ± 0.13	49.82 ± 4.98	ND	70.37	24.42	5.21
32-33	0.534	1.811	1.17 ± 0.12	50.99 ± 5.10	ND	34.88	29.50	35.62
33-34	0.566	1.802	1.08 ± 0.11	52.07 ± 5.21	ND	79.76	18.21	2.03
34-35	0.613	1.778	0.97 ± 0.10	53.04 ± 5.30	ND	83.02	14.77	2.21
35-36	0.732	1.759	0.67 ± 0.07	53.71 ± 5.37	ND	48.90	42.80	8.30
36-37	0.750	1.740	0.63 ± 0.06	54.33 ± 5.43	ND	44.05	47.55	8.40
37-38	0.784	1.730	0.54 ± 0.05	54.87 ± 5.49	ND	18.27	67.49	14.24
38-39	0.752	1.723	0.62 ± 0.06	55.49 ± 5.55	ND	28.07	60.52	11.41
39-40	0.762	1.736	0.60 ± 0.06	56.09 ± 5.61	ND	50.58	41.59	7.83

MBM-A-14V

Interval	Assumed + OM Porosity	Bulk Density	Assumed + OM Mass Depth	Assumed + OM Cumulative Mass Depth	Particulate Organic Carbon	Sand	Silt	Clay
(cm)	(%)	(g/cm³)	(g/cm^2)	(g/cm²)	(%)	(%)	(%)	(%)
40-41	0.777	1.712	0.56 ± 0.06	56.65 ± 5.66	ND	17.76	70.54	11.70
41-42	0.810	1.734	0.47 ± 0.05	57.12 ± 5.71	ND	21.55	65.55	12.90
42-43	0.725	1.729	0.69 ± 0.07	57.81 ± 5.78	ND	21.36	64.56	14.08
43-44	0.637	1.749	0.91 ± 0.09	58.71 ± 5.87	ND	91.98	6.93	1.09
44-45	0.726	1.746	0.68 ± 0.07	59.40 ± 5.94	ND	20.89	60.36	18.75
45-46	0.716	1.763	0.71 ± 0.07	60.11 ± 6.01	ND	16.48	68.43	15.09
46-47	0.755	1.742	0.61 ± 0.06	60.72 ± 6.07	ND	41.31	48.54	10.15
47-48	0.784	1.715	0.54 ± 0.05	61.26 ± 6.13	ND	44.31	47.18	8.51
48-49	0.779	1.664	0.55 ± 0.06	61.81 ± 6.18	ND	51.07	40.68	8.25
49-50	0.771	1.590	0.57 ± 0.06	62.39 ± 6.24	ND	38.02	52.08	9.90

ODB-1B-14V

Interval	Assumed + OM Porosity	Bulk Density	Assumed + OM Mass Depth	Assumed + OM Cumulative Mass Depth	Particulate Organic Carbon	Sand	Silt	Clay
(cm)	(%)	(g/cm³)	(g/cm²)	(g/cm²)	(%)	(%)	(%)	(%)
0-1	0.808	0.390	0.39 ± 0.04	0.39 ± 0.04	29.332	64.16	29.85	5.99
1-2	0.755	0.544	0.54 ± 0.05	0.93 ± 0.09	17.666	72.87	24.78	2.35
2-3	0.658	0.835	0.84 ± 0.08	1.77 ± 0.18	3.777	80.27	16.83	2.90
3-4	0.551	1.110	1.11 ± 0.11	2.88 ± 0.29	1.808	80.06	17.30	2.64
4-5	0.528	1.163	1.16 ± 0.12	4.04 ± 0.40	2.271	58.94	21.71	19.35
5-6	0.513	1.206	1.21 ± 0.12	5.25 ± 0.52	1.503	71.92	12.43	15.65
6-7	0.595	0.998	1.00 ± 0.10	6.25 ± 0.62	2.216	43.79	26.45	29.76
7-8	0.589	0.999	1.00 ± 0.10	7.25 ± 0.72	4.116	8.56	29.74	61.70
8-9	0.575	1.051	1.05 ± 0.11	8.30 ± 0.83	1.473	50.60	22.68	26.72
9-10	0.550	1.110	1.11 ± 0.11	9.41 ± 0.94	1.943	43.48	29.09	27.43
10-11	0.518	1.189	1.19 ± 0.12	10.60 ± 1.06	2.16	52.77	18.99	28.24
11-12	0.492	1.253	1.25 ± 0.13	11.85 ± 1.18	2.092	57.78	22.36	19.86
12-13	0.446	1.374	1.37 ± 0.14	13.22 ± 1.32	1.169	56.68	24.31	19.01
13-14	0.416	1.451	1.45 ± 0.15	14.67 ± 1.47	0.869	70.63	15.08	14.29
14-15	0.388	1.524	1.52 ± 0.15	16.20 ± 1.62	0.639	77.99	12.94	9.07
15-16	0.366	1.580	1.58 ± 0.16	17.78 ± 1.78	0.415	79.17	12.51	8.32
16-17	0.348	1.626	1.63 ± 0.16	19.40 ± 1.94	0.439	67.34	18.92	13.74
17-18	0.340	1.640	1.64 ± 0.16	21.04 ± 2.10	0.812	86.45	11.54	2.01
18-19	0.358	1.594	1.59 ± 0.16	22.64 ± 2.26	0.921	72.91	22.69	4.40
19-20	0.354	1.607	1.61 ± 0.16	24.25 ± 2.42	0.76	81.28	15.98	2.74

ODB-1B-14V

Interval	Assumed + OM Porosity	Bulk Density	Assumed + OM Mass Depth	Assumed + OM Cumulative Mass Depth	Particulate Organic Carbon	Sand	Silt	Clay
(cm)	(%)	(g/cm³)	(g/cm²)	(g/cm²)	(%)	(%)	(%)	(%)
20-21	0.370	1.557	1.56 ± 0.16	25.80 ± 2.58	1.749	71.80	11.46	16.74
21-22	0.360	1.587	1.59 ± 0.16	27.39 ± 2.74	1.323	66.73	13.14	20.13
22-23	0.367	1.562	1.56 ± 0.16	28.95 ± 2.90	1.927	62.32	15.52	22.16
23-24	0.373	1.558	1.56 ± 0.16	30.51 ± 3.05	0.912	77.01	18.72	4.27
24-25	0.350	1.614	1.61 ± 0.16	32.12 ± 3.21	0.992	66.19	16.22	17.59
25-26	0.300	1.738	1.74 ± 0.17	33.86 ± 3.39	0.959	74.65	10.18	15.17
26-27	0.300	1.736	1.74 ± 0.17	35.60 ± 3.56	1.335	82.91	14.13	2.96
27-28	0.510	1.217	1.22 ± 0.12	36.81 ± 3.68	0.979	77.28	19.25	3.47
28-29	0.311	1.709	1.71 ± 0.17	38.52 ± 3.85	1.302	78.06	16.57	5.37
29-30	0.321	1.687	1.69 ± 0.17	40.21 ± 4.02	ND	76.42	20.15	3.43
30-31	0.314	1.715	1.71 ± 0.17	41.93 ± 4.19	ND	86.78	11.30	1.92
31-32	0.288	1.779	1.78 ± 0.18	43.70 ± 4.37	ND	91.73	7.08	1.19
32-33	0.276	1.811	1.81 ± 0.18	45.52 ± 4.55	ND	87.45	10.53	2.02
33-34	0.279	1.802	1.80 ± 0.18	47.32 ± 4.73	ND	93.20	5.45	1.35
34-35	0.289	1.778	1.78 ± 0.18	49.09 ± 4.91	ND	85.26	11.70	3.04
35-36	0.296	1.759	1.76 ± 0.18	50.85 ± 5.09	ND	82.65	15.25	2.10
36-37	0.304	1.740	1.74 ± 0.17	52.59 ± 5.26	ND	85.86	11.95	2.19
37-38	0.308	1.730	1.73 ± 0.17	54.32 ± 5.43	ND	91.80	7.17	1.03
38-39	0.311	1.723	1.72 ± 0.17	56.05 ± 5.60	ND	91.29	7.71	1.00
39-40	0.306	1.736	1.74 ± 0.17	57.78 ± 5.78	ND	95.25	4.03	0.72

ODB-1B-14V

Interval	Assumed + OM Porosity	Bulk Density	Assumed + OM Mass Depth	Assumed + OM Cumulative Mass Depth	Particulate Organic Carbon	Sand	Silt	Clay
(cm)	(%)	(g/cm³)	(g/cm^2)	(g/cm²)	(%)	(%)	(%)	(%)
40-41	0.315	1.713	1.71 ± 0.17	59.49 ± 5.95	ND	92.68	6.38	0.94
41-42	0.307	1.733	1.73 ± 0.17	61.23 ± 6.12	ND	89.99	8.60	1.41
42-43	0.308	1.731	1.73 ± 0.17	62.96 ± 6.30	ND	86.60	11.24	2.16
43-44	0.301	1.748	1.75 ± 0.17	64.71 ± 6.47	ND	92.18	6.78	1.04
44-45	0.301	1.747	1.75 ± 0.17	66.45 ± 6.65	ND	88.69	9.71	1.60
45-46	0.295	1.762	1.76 ± 0.18	68.22 ± 6.82	ND	88.97	9.23	1.80
46-47	0.303	1.743	1.74 ± 0.17	69.96 ± 7.00	ND	92.31	6.67	1.02
47-48	0.314	1.715	1.71 ± 0.17	71.67 ± 7.17	ND	87.55	10.67	1.78
48-49	0.334	1.665	1.67 ± 0.17	73.34 ± 7.33	ND	86.71	11.64	1.65
49-50	0.364	1.589	1.59 ± 0.16	74.93 ± 7.49	ND	71.60	24.49	3.91

TC2A-B-14V

Interval	Assumed + OM Porosity	Bulk Density	Assumed + OM Mass Depth	Assumed + OM Cumulative Mass Depth	Particulate Organic Carbon	Sand	Silt	Clay
(cm)	(%)	(g/cm³)	(g/cm²)	(g/cm²)	(%)	(%)	(%)	(%)
0-1	0.874	0.222	0.22 ± 0.02	0.22 ± 0.02	46.235			
1-2	0.886	0.221	0.22 ± 0.02	0.44 ± 0.04	35.098			
2-3	0.889	0.207	0.21 ± 0.02	0.65 ± 0.06	39.3	71.68	27.36	0.96
3-4	0.890	0.202	0.20 ± 0.02	0.85 ± 0.09	41.316	73.00	25.47	1.53
4-5	0.884	0.219	0.22 ± 0.02	1.07 ± 0.11	38.468			
5-6	0.869	0.260	0.26 ± 0.03	1.33 ± 0.13	32.228	76.72	21.38	1.90
6-7	0.847	0.322	0.32 ± 0.03	1.65 ± 0.17	24.606	79.11	18.78	2.11
7-8	0.804	0.452	0.45 ± 0.05	2.10 ± 0.21	11.673	74.52	22.85	2.63
8-9	0.758	0.540	0.54 ± 0.05	2.64 ± 0.26	16.889	81.14	17.15	1.71
9-10	0.752	0.577	0.58 ± 0.06	3.22 ± 0.32	10.633	81.40	16.78	1.82
10-11	0.708	0.705	0.71 ± 0.07	3.93 ± 0.39	5.025	63.34	32.32	4.34
11-12	0.649	0.836	0.84 ± 0.08	4.76 ± 0.48	7.214	78.06	19.79	2.15
12-13	0.611	0.954	0.95 ± 0.10	5.72 ± 0.57	2.865	69.22	26.96	3.82
13-14	0.598	0.989	0.99 ± 0.10	6.71 ± 0.67	2.512	82.56	15.61	1.93
14-15	0.596	0.987	0.99 ± 0.10	7.69 ± 0.77	3.587	85.14	13.61	1.25
15-16	0.588	1.008	1.01 ± 0.10	8.70 ± 0.87	3.47	90.47	8.80	0.73
16-17	0.597	0.984	0.98 ± 0.10	9.68 ± 0.97	3.82	85.42	13.41	1.17
17-18	0.674	0.778	0.78 ± 0.08	10.46 ± 1.05	7.207	78.31	19.52	2.17
18-19	0.722	0.661	0.66 ± 0.07	11.12 ± 1.11	7.91	74.64	22.87	2.49
19-20	0.590	1.005	1.00 ± 0.10	12.13 ± 1.21	3.234	85.53	13.05	1.42

TC2A-B-14V

Interval	Assumed + OM Porosity	Bulk Density	Assumed + OM Mass Depth	Assumed + OM Cumulative Mass Depth	Particulate Organic Carbon	Sand	Silt	Clay
(cm)	(%)	(g/cm ³)	(g/cm^2)	(g/cm²)	(%)	(%)	(%)	(%)
20-21	0.528	1.166	1.17 ± 0.12	13.29 ± 1.33	1.715	94.22	5.32	0.46
21-22	0.555	1.099	1.10 ± 0.11	14.39 ± 1.44	1.948	98.36	1.64	0.00
22-23	0.600	0.993	0.99 ± 0.10	15.39 ± 1.54	0.982	99.84	0.16	0.00
23-24	0.587	1.020	1.02 ± 0.10	16.41 ± 1.64	1.977	99.63	0.37	0.00
24-25	0.653	0.850	0.85 ± 0.08	17.26 ± 1.73	3.031	99.83	0.17	0.00
25-26	0.660	0.837	0.84 ± 0.08	18.09 ± 1.81	2.481	99.99	0.01	0.00
26-27	0.636	0.888	0.89 ± 0.09	18.98 ± 1.90	3.746	98.63	1.35	0.02
27-28	0.729	0.646	0.65 ± 0.06	19.63 ± 1.96	7.11	88.02	11.25	0.73
28-29	0.718	0.688	0.69 ± 0.07	20.31 ± 2.03	3.743	92.41	7.06	0.53
29-30	0.740	0.624	0.62 ± 0.06	20.94 ± 2.09	ND	93.36	6.22	0.42
30-31	0.759	0.603	0.60 ± 0.06	21.54 ± 2.15	ND	99.94	0.06	0.00
31-32	0.726	0.686	0.69 ± 0.07	22.23 ± 2.22	ND	100.00	0.00	0.00
32-33	0.679	0.802	0.80 ± 0.08	23.03 ± 2.30	ND	99.99	0.01	0.00
33-34	0.752	0.619	0.62 ± 0.06	23.65 ± 2.36	ND	99.90	0.10	0.00
34-35	0.794	0.514	0.51 ± 0.05	24.16 ± 2.42	ND	96.66	3.27	0.07
35-36	0.796	0.511	0.51 ± 0.05	24.67 ± 2.47	ND	100.00	0.00	0.00
36-37	0.798	0.504	0.50 ± 0.05	25.18 ± 2.52	ND	99.99	0.01	0.00
37-38	0.830	0.425	0.42 ± 0.04	25.60 ± 2.56	ND	90.40	9.24	0.36
38-39	0.746	0.634	0.63 ± 0.06	26.24 ± 2.62	ND	99.96	0.04	0.00
39-40	0.770	0.576	0.58 ± 0.06	26.81 ± 2.68	ND	94.01	5.77	0.22

TC2A-B-14V

Interval	Assumed + OM Porosity	Bulk Density	Assumed + OM Mass Depth	Assumed + OM Cumulative Mass Depth	Particulate Organic Carbon	Sand	Silt	Clay
(cm)	(%)	(g/cm ³)	(g/cm^2)	(g/cm²)	(%)	(%)	(%)	(%)
40-41	0.798	0.504	0.50 ± 0.05	27.32 ± 2.73	ND	95.72	4.15	0.13
41-42	0.804	0.489	0.49 ± 0.05	27.81 ± 2.78	ND	99.97	0.03	0.00
42-43	0.755	0.611	0.61 ± 0.06	28.42 ± 2.84	ND	98.68	1.32	0.00
43-44	0.718	0.706	0.71 ± 0.07	29.12 ± 2.91	ND	97.15	2.85	0.00
44-45	0.698	0.755	0.75 ± 0.08	29.88 ± 2.99	ND	93.95	5.95	0.10
45-46	0.720	0.699	0.70 ± 0.07	30.58 ± 3.06	ND	97.49	2.51	0.00
46-47	0.743	0.641	0.64 ± 0.06	31.22 ± 3.12	ND	97.58	2.42	0.00
47-48	0.706	0.734	0.73 ± 0.07	31.95 ± 3.20	ND	79.26	19.41	1.33
48-49	0.699	0.752	0.75 ± 0.08	32.71 ± 3.27	ND	96.38	3.62	0.00
49-50	0.688	0.781	0.78 ± 0.08	33.49 ± 3.35	ND	90.44	8.67	0.89

MCE-A-14V

Interval	Assumed + OM Porosity	Bulk Density	Assumed + OM Mass Depth	Assumed + OM Cumulative Mass Depth	Particulate Organic Carbon	Sand	Silt	Clay
(cm)	(%)	(g/cm³)	(g/cm²)	(g/cm²)	(%)	(%)	(%)	(%)
0-1	0.836	0.353	0.35 ± 0.04	0.35 ± 0.04	21.781	68.92	28.59	2.49
1-2	0.819	0.404	0.40 ± 0.04	0.76 ± 0.08	17.094	79.19	18.40	2.41
2-3	0.796	0.477	0.48 ± 0.05	1.23 ± 0.12	10.303	78.99	18.43	2.58
3-4	0.748	0.584	0.58 ± 0.06	1.82 ± 0.18	11.617	83.72	14.12	2.16
4-5	0.692	0.732	0.73 ± 0.07	2.55 ± 0.25	7.812	83.33	14.41	2.26
5-6	0.617	0.937	0.94 ± 0.09	3.49 ± 0.35	3.373	81.46	15.88	2.66
6-7	0.570	1.053	1.05 ± 0.11	4.54 ± 0.45	3.246	79.62	17.52	2.86
7-8	0.534	1.150	1.15 ± 0.11	5.69 ± 0.57	2.132	77.96	19.08	2.96
8-9	0.483	1.262	1.26 ± 0.13	6.95 ± 0.70	3.681	74.21	21.91	3.88
9-10	0.469	1.301	1.30 ± 0.13	8.25 ± 0.83	3.186	73.27	22.92	3.81
10-11	0.452	1.350	1.35 ± 0.14	9.60 ± 0.96	2.266	65.52	30.39	4.09
11-12	0.456	1.341	1.34 ± 0.13	10.94 ± 1.09	2.08	68.66	27.23	4.11
12-13	0.463	1.328	1.33 ± 0.13	12.27 ± 1.23	1.618	64.94	30.11	4.95
13-14	0.493	1.251	1.25 ± 0.13	13.52 ± 1.35	2.218	78.36	18.06	3.58
14-15	0.452	1.351	1.35 ± 0.14	14.87 ± 1.49	2.118	78.80	18.34	2.86
15-16	0.436	1.391	1.39 ± 0.14	16.26 ± 1.63	2.05	70.11	26.49	3.40
16-17	0.428	1.415	1.41 ± 0.14	17.68 ± 1.77	1.743	78.23	18.70	3.07
17-18	0.427	1.422	1.42 ± 0.14	19.10 ± 1.91	1.265	69.76	26.61	3.63
18-19	0.393	1.507	1.51 ± 0.15	20.61 ± 2.06	0.987	82.29	15.95	1.76
19-20	0.360	1.596	1.60 ± 0.16	22.20 ± 2.22	0.549	80.47	17.30	2.23

MCE-A-14V

Interval	Assumed + OM Porosity	Bulk Density	Assumed + OM Mass Depth	Assumed + OM Cumulative Mass Depth	Particulate Organic Carbon	Sand	Silt	Clay
(cm)	(%)	(g/cm³)	(g/cm^2)	(g/cm²)	(%)	(%)	(%)	(%)
20-21	0.332	1.664	1.66 ± 0.17	23.87 ± 2.39	0.63	84.28	12.79	2.93
21-22	0.315	1.710	1.71 ± 0.17	25.58 ± 2.56	0.316	79.03	17.63	3.34
22-23	0.306	1.731	1.73 ± 0.17	27.31 ± 2.73	0.367	87.44	10.78	1.78
23-24	0.309	1.723	1.72 ± 0.17	29.03 ± 2.90	0.547	85.19	11.78	3.03
24-25	0.318	1.698	1.70 ± 0.17	30.73 ± 3.07	0.666	81.20	15.40	3.40
25-26	0.312	1.713	1.71 ± 0.17	32.44 ± 3.24	0.627	81.83	15.34	2.83
26-27	0.307	1.727	1.73 ± 0.17	34.17 ± 3.42	0.55	80.32	16.47	3.21
27-28	0.311	1.717	1.72 ± 0.17	35.89 ± 3.59	0.513	29.71	40.29	30.00
28-29	0.314	1.708	1.71 ± 0.17	37.59 ± 3.76	0.704	77.29	18.10	4.61
29-30	0.334	1.638	1.64 ± 0.16	39.23 ± 3.92	ND	85.23	12.19	2.58
30-31	0.346	1.635	1.64 ± 0.16	40.87 ± 4.09	ND	77.67	18.73	3.60
31-32	0.308	1.731	1.73 ± 0.17	42.60 ± 4.26	ND	91.11	7.50	1.39
32-33	0.276	1.809	1.81 ± 0.18	44.41 ± 4.44	ND	90.88	7.57	1.55
33-34	0.273	1.817	1.82 ± 0.18	46.22 ± 4.62	ND	95.25	4.00	0.75
34-35	0.275	1.814	1.81 ± 0.18	48.04 ± 4.80	ND	90.04	8.19	1.77
35-36	0.293	1.767	1.77 ± 0.18	49.80 ± 4.98	ND	87.77	10.12	2.11
36-37	0.287	1.781	1.78 ± 0.18	51.59 ± 5.16	ND	90.41	7.98	1.61
37-38	0.289	1.776	1.78 ± 0.18	53.36 ± 5.34	ND	88.21	9.86	1.93
38-39	0.283	1.793	1.79 ± 0.18	55.16 ± 5.52	ND	86.17	11.62	2.21
39-40	0.276	1.809	1.81 ± 0.18	56.96 ± 5.70	ND	93.46	5.52	1.02

MCE-A-14V

Interval	Assumed + OM Porosity	Bulk Density	Assumed + OM Mass Depth	Assumed + OM Cumulative Mass Depth	Particulate Organic Carbon	Sand	Silt	Clay
(cm)	(%)	(g/cm³)	(g/cm^2)	(g/cm²)	(%)	(%)	(%)	(%)
40-41	0.274	1.815	1.81 ± 0.18	58.78 ± 5.88	ND	81.93	15.41	2.66
41-42	0.270	1.825	1.82 ± 0.18	60.60 ± 6.06	ND	84.51	13.35	2.14
42-43	0.270	1.824	1.82 ± 0.18	62.43 ± 6.24	ND	90.51	7.97	1.52
43-44	0.269	1.828	1.83 ± 0.18	64.26 ± 6.43	ND	86.12	11.75	2.13
44-45	0.271	1.823	1.82 ± 0.18	66.08 ± 6.61	ND	81.82	15.33	2.85
45-46	0.268	1.831	1.83 ± 0.18	67.91 ± 6.79	ND	87.73	10.61	1.66
46-47	0.271	1.822	1.82 ± 0.18	69.73 ± 6.97	ND	85.16	12.80	2.04
47-48	0.271	1.822	1.82 ± 0.18	71.55 ± 7.16	ND	87.93	10.45	1.62
48-49	0.273	1.817	1.82 ± 0.18	73.37 ± 7.34	ND	88.20	10.12	1.68
49-50	0.275	1.813	1.81 ± 0.18	75.18 ± 7.52	ND	90.17	8.51	1.32

TC2B-B-14V

Interval	Assumed + OM Porosity	Bulk Density	Assumed + OM Mass Depth	Assumed + OM Cumulative Mass Depth	Particulate Organic Carbon	Sand	Silt	Clay
(cm)	(%)	(g/cm³)	(g/cm²)	(g/cm²)	(%)	(%)	(%)	(%)
0-1	0.855	0.307	0.31 ± 0.03	0.31 ± 0.03	24.14	32.40	58.66	8.94
1-2	0.855	0.334	0.33 ± 0.03	0.64 ± 0.06	12.729	24.20	64.65	11.15
2-3	0.845	0.345	0.35 ± 0.03	0.99 ± 0.10	16.756	33.43	58.98	7.59
3-4	0.832	0.389	0.39 ± 0.04	1.38 ± 0.14	11.348	56.36	39.03	4.61
4-5	0.838	0.367	0.37 ± 0.04	1.74 ± 0.17	14.434	41.03	50.62	8.35
5-6	0.831	0.394	0.39 ± 0.04	2.14 ± 0.21	11.048	49.18	45.04	5.78
6-7	0.832	0.395	0.39 ± 0.04	2.53 ± 0.25	9.462	63.70	31.91	4.39
7-8	0.815	0.445	0.44 ± 0.04	2.98 ± 0.30	5.698	59.31	35.50	5.19
8-9	0.853	0.337	0.34 ± 0.03	3.31 ± 0.33	12.812	77.62	20.12	2.26
9-10	0.874	0.298	0.30 ± 0.03	3.61 ± 0.36	9.032	46.68	48.16	5.16
10-11	0.874	0.307	0.31 ± 0.03	3.92 ± 0.39	3.533	84.29	13.96	1.75
11-12	0.795	0.479	0.48 ± 0.05	4.40 ± 0.44	10.305	59.29	35.34	5.37
12-13	0.686	0.747	0.75 ± 0.07	5.14 ± 0.51	7.289	70.98	25.77	3.25
13-14	0.684	0.752	0.75 ± 0.08	5.90 ± 0.59	7.314	81.52	16.28	2.20
14-15	0.609	0.942	0.94 ± 0.09	6.84 ± 0.68	5.789	56.93	38.53	4.54
15-16	0.570	1.032	1.03 ± 0.10	7.87 ± 0.79	6.06	77.69	20.07	2.24
16-17	0.574	1.026	1.03 ± 0.10	8.90 ± 0.89	5.712	86.76	11.81	1.43
17-18	0.560	1.067	1.07 ± 0.11	9.96 ± 1.00	4.565	74.59	22.67	2.74
18-19	0.533	1.088	1.09 ± 0.11	11.05 ± 1.11	10.766	65.55	31.55	2.90
19-20	0.589	0.973	0.97 ± 0.10	12.02 ± 1.2	8.445	92.69	6.79	0.52

TC2B-B-14V

Interval	Assumed + OM Porosity	Bulk Density	Assumed + OM Mass Depth	Assumed + OM Cumulative Mass Depth	Particulate Organic Carbon	Sand	Silt	Clay
(cm)	(%)	(g/cm³)	(g/cm²)	(g/cm²)	(%)	(%)	(%)	(%)
20-21	0.616	0.916	0.92 ± 0.09	12.94 ± 1.29	7.158	92.55	6.80	0.65
21-22	0.590	0.989	0.99 ± 0.10	13.93 ± 1.39	5.472	82.04	16.50	1.46
22-23	0.599	0.963	0.96 ± 0.10	14.89 ± 1.49	6.016	85.23	13.65	1.12
23-24	0.593	0.994	0.99 ± 0.10	15.89 ± 1.59	3.558	92.70	6.87	0.43
24-25	0.614	0.949	0.95 ± 0.09	16.84 ± 1.68	2.633	91.19	8.24	0.57
25-26	0.627	0.904	0.90 ± 0.09	17.74 ± 1.77	4.599	90.82	7.82	1.36
26-27	0.644	0.860	0.86 ± 0.09	18.60 ± 1.86	5.099	90.14	9.21	0.65
27-28	0.662	0.824	0.82 ± 0.08	19.42 ± 1.94	3.815	87.61	10.78	1.61
28-29	0.658	0.839	0.84 ± 0.08	20.26 ± 2.03	2.735	87.99	11.08	0.93
29-30	0.653	0.857	0.86 ± 0.09	21.12 ± 2.11	ND	96.55	3.38	0.07
30-31	0.647	0.882	0.88 ± 0.09	22.00 ± 2.20	ND	93.60	6.02	0.38
31-32	0.629	0.929	0.93 ± 0.09	22.93 ± 2.29	ND	98.40	1.60	0.00
32-33	0.618	0.954	0.95 ± 0.10	23.88 ± 2.39	ND	98.86	1.14	0.00
33-34	0.630	0.925	0.93 ± 0.09	24.81 ± 2.48	ND	97.24	2.74	0.02
34-35	0.623	0.942	0.94 ± 0.09	25.75 ± 2.58	ND	96.24	3.62	0.14
35-36	0.640	0.901	0.90 ± 0.09	26.65 ± 2.67	ND	97.72	2.28	0.00
36-37	0.627	0.933	0.93 ± 0.09	27.59 ± 2.76	ND	98.45	1.55	0.00
37-38	0.619	0.953	0.95 ± 0.10	28.54 ± 2.85	ND	98.65	1.35	0.00
38-39	0.590	1.024	1.02 ± 0.10	29.56 ± 2.96	ND	99.10	0.90	0.00
39-40	0.579	1.051	1.05 ± 0.11	30.61 ± 3.06	ND	99.96	0.04	0.00

TC2B-B-14V

Interval	Assumed + OM Porosity	Bulk Density	Assumed + OM Mass Depth	Assumed + OM Cumulative Mass Depth	Particulate Organic Carbon	Sand	Silt	Clay
(cm)	(%)	(g/cm³)	(g/cm^2)	(g/cm²)	(%)	(%)	(%)	(%)
40-41	0.560	1.099	1.10 ± 0.11	31.71 ± 3.17	ND	94.70	5.11	0.19
41-42	0.629	0.927	0.93 ± 0.09	32.64 ± 3.26	ND	99.37	0.63	0.00
42-43	0.647	0.882	0.88 ± 0.09	33.52 ± 3.35	ND	92.68	6.64	0.68
43-44	0.603	0.993	0.99 ± 0.10	34.52 ± 3.45	ND	82.05	16.98	0.97
44-45	0.604	0.990	0.99 ± 0.10	35.51 ± 3.55	ND	96.50	3.50	0.00
45-46	0.619	0.953	0.95 ± 0.10	36.46 ± 3.65	ND	99.99	0.01	0.00
46-47	0.645	0.888	0.89 ± 0.09	37.35 ± 3.73	ND	98.39	1.61	0.00
47-48	0.667	0.832	0.83 ± 0.08	38.18 ± 3.82	ND	94.46	5.38	0.16
48-49	0.686	0.784	0.78 ± 0.08	38.96 ± 3.90	ND	95.03	4.95	0.02
49-50	0.710	0.724	0.72 ± 0.07	39.69 ± 3.97	ND	97.24	2.76	0.00

TC5-B-14V

Interval	Assumed + OM Porosity	Bulk Density	Assumed + OM Mass Depth	Assumed + OM Cumulative Mass Depth	Particulate Organic Carbon	Sand	Silt	Clay
(cm)	(%)	(g/cm³)	(g/cm²)	(g/cm²)	(%)	(%)	(%)	(%)
0-1	0.870	0.243	0.24 ± 0.02	0.24 ± 0.02	39.246	45.13	50.71	4.16
1-2	0.881	0.229	0.23 ± 0.02	0.47 ± 0.05	36.147	49.37	47.33	3.30
2-3	0.880	0.233	0.23 ± 0.02	0.70 ± 0.07	35.417	52.53	43.46	4.01
3-4	0.872	0.249	0.25 ± 0.02	0.95 ± 0.10	34.512	52.83	42.94	4.23
4-5	0.864	0.267	0.27 ± 0.03	1.22 ± 0.12	33.121	43.90	51.18	4.92
5-6	0.863	0.272	0.27 ± 0.03	1.49 ± 0.15	31.992	30.36	64.09	5.55
6-7	0.843	0.320	0.32 ± 0.03	1.81 ± 0.18	28.497	26.01	65.32	8.67
7-8	0.828	0.359	0.36 ± 0.04	2.17 ± 0.22	26.09	14.68	76.09	9.23
8-9	0.816	0.390	0.39 ± 0.04	2.56 ± 0.26	23.845	10.56	79.07	10.37
9-10	0.802	0.425	0.42 ± 0.04	2.99 ± 0.30	22.16	14.05	76.98	8.97
10-11	0.798	0.427	0.43 ± 0.04	3.41 ± 0.34	24.207	8.73	80.42	10.85
11-12	0.797	0.425	0.42 ± 0.04	3.84 ± 0.38	25.721	9.09	79.98	10.93
12-13	0.796	0.420	0.42 ± 0.04	4.26 ± 0.43	27.516	14.15	78.90	6.95
13-14	0.804	0.399	0.40 ± 0.04	4.66 ± 0.47	29.121	18.49	74.92	6.59
14-15	0.802	0.404	0.40 ± 0.04	5.06 ± 0.51	28.706	18.78	71.99	9.23
15-16	0.806	0.391	0.39 ± 0.04	5.45 ± 0.55	30.342	28.41	66.15	5.44
16-17	0.800	0.411	0.41 ± 0.04	5.86 ± 0.59	27.586	46.40	49.48	4.12
17-18	0.798	0.427	0.43 ± 0.04	6.29 ± 0.63	24.271	35.58	58.18	6.24
18-19	0.784	0.433	0.43 ± 0.04	6.72 ± 0.67	30.873	46.49	47.97	5.54
19-20	0.789	0.469	0.47 ± 0.05	7.19 ± 0.72	17.324	39.33	56.15	4.52

TC5-B-14V

Interval	Assumed + OM Porosity	Bulk Density	Assumed + OM Mass Depth	Assumed + OM Cumulative Mass Depth	Particulate Organic Carbon	Sand	Silt	Clay
(cm)	(%)	(g/cm³)	(g/cm²)	(g/cm²)	(%)	(%)	(%)	(%)
20-21	0.775	0.473	0.47 ± 0.05	7.67 ± 0.77	24.753	70.39	27.94	1.67
21-22	0.789	0.433	0.43 ± 0.04	8.10 ± 0.81	28.108	45.24	47.95	6.81
22-23	0.790	0.425	0.42 ± 0.04	8.52 ± 0.85	29.732	79.00	19.75	1.25
23-24	0.782	0.473	0.47 ± 0.05	9.00 ± 0.90	20.817	84.37	13.55	2.08
24-25	0.791	0.470	0.47 ± 0.05	9.47 ± 0.95	15.859	68.08	27.99	3.93
25-26	0.824	0.376	0.38 ± 0.04	9.84 ± 0.98	22.491	77.05	19.32	3.63
26-27	0.830	0.342	0.34 ± 0.03	10.19 ± 1.02	30.274	59.20	37.36	3.44
27-28	0.798	0.398	0.40 ± 0.04	10.58 ± 1.06	33.013	73.45	24.51	2.04
28-29	0.743	0.601	0.60 ± 0.06	11.18 ± 1.12	9.905	68.38	28.83	2.79
29-30	0.782	0.494	0.49 ± 0.05	11.68 ± 1.17	ND	80.99	18.10	0.91
30-31	0.685	0.788	0.79 ± 0.08	12.47 ± 1.25	ND	94.76	4.99	0.25
31-32	0.711	0.723	0.72 ± 0.07	13.19 ± 1.32	ND	61.60	36.39	2.01
32-33	0.810	0.475	0.48 ± 0.05	13.66 ± 1.37	ND	82.60	15.46	1.94
33-34	0.822	0.444	0.44 ± 0.04	14.11 ± 1.41	ND	83.66	15.22	1.12
34-35	0.804	0.491	0.49 ± 0.05	14.60 ± 1.46	ND	79.82	18.98	1.20
35-36	0.859	0.352	0.35 ± 0.04	14.95 ± 1.50	ND	77.12	21.66	1.22
36-37	0.888	0.280	0.28 ± 0.03	15.23 ± 1.52	ND	83.56	15.51	0.93
37-38	0.886	0.285	0.28 ± 0.03	15.51 ± 1.55	ND	75.92	22.79	1.29
38-39	0.872	0.319	0.32 ± 0.03	15.83 ± 1.58	ND	61.71	35.73	2.56
39-40	0.863	0.343	0.34 ± 0.03	16.18 ± 1.62	ND	81.47	17.66	0.87

TC5-B-14V

Interval	Assumed +		Assumed + OM	Particulate	Sand	Silt	Clay	
interval	OM Porosity	Density	Mass Depth	Cumulative Mass Depth	Organic Carbon	Janu	Silt	Ciay
(cm)	(%)	(g/cm^3)	(g/cm²)	(g/cm²)	(%)	(%)	(%)	(%)
40-41	0.830	0.426	0.43 ± 0.04	16.60 ± 1.66	ND	82.05	16.98	0.97
41-42	0.804	0.489	0.49 ± 0.05	17.09 ± 1.71	ND	70.01	28.05	1.94
42-43	0.830	0.425	0.43 ± 0.04	17.52 ± 1.75	ND	60.47	35.18	4.35
43-44	0.830	0.425	0.43 ± 0.04	17.94 ± 1.79	ND	67.53	28.34	4.13
44-45	0.841	0.398	0.40 ± 0.04	18.34 ± 1.83	ND	71.88	24.68	3.44
45-46	0.827	0.432	0.43 ± 0.04	18.77 ± 1.88	ND	73.51	23.74	2.75
46-47	0.850	0.374	0.37 ± 0.04	19.15 ± 1.91	ND	87.04	11.65	1.31
47-48	0.843	0.392	0.39 ± 0.04	19.54 ± 1.95	ND	57.96	38.50	3.54
48-49	0.839	0.402	0.40 ± 0.04	19.94 ± 1.99	ND	69.80	28.20	2.00
49-50	0.809	0.477	0.48 ± 0.05	20.42 ± 2.04	ND	82.02	16.62	1.36

MB6-B-15V

Interval	Assumed + OM Porosity	Bulk Density	Assumed + OM Mass Depth	Assumed + OM Cumulative Mass Depth	Particulate Organic Carbon	Sand	Silt	Clay
(cm)	(%)	(g/cm³)	(g/cm²)	(g/cm²)	(%)	(%)	(%)	(%)
0-1	0.832	0.402	0.40 ± 0.04	0.40 ± 0.04	7.119	75.18	19.79	5.03
1-2	0.771	0.556	0.56 ± 0.06	0.96 ± 0.10	4.561	60.32	32.65	7.03
2-3	0.657	0.835	0.83 ± 0.08	1.79 ± 0.18	3.96	52.24	40.00	7.76
3-4	0.549	1.107	1.11 ± 0.11	2.90 ± 0.29	3.014	65.37	28.21	6.42
4-5	0.524	1.154	1.15 ± 0.12	4.05 ± 0.41	4.711	36.16	55.28	8.56
5-6	0.510	1.199	1.20 ± 0.12	5.25 ± 0.53	3.415	50.79	38.50	10.71
6-7	0.594	0.997	1.00 ± 0.10	6.25 ± 0.62	2.687	59.69	33.02	7.29
7-8	0.593	1.007	1.01 ± 0.10	7.26 ± 0.73	1.443	62.93	25.20	11.87
8-9	0.574	1.049	1.05 ± 0.10	8.31 ± 0.83	2.274	48.20	25.75	26.05
9-10	0.550	1.110	1.11 ± 0.11	9.42 ± 0.94	2.139	57.59	32.96	9.45
10-11	0.516	1.184	1.18 ± 0.12	10.60 ± 1.06	3.362	49.05	41.01	9.94
11-12	0.490	1.249	1.25 ± 0.12	11.85 ± 1.18	3.182	73.28	22.04	4.68
12-13	0.444	1.366	1.37 ± 0.14	13.22 ± 1.32	2.836	62.74	30.33	6.93
13-14	0.413	1.441	1.44 ± 0.14	14.66 ± 1.47	2.799	47.33	42.75	9.92
14-15	0.383	1.507	1.51 ± 0.15	16.16 ± 1.62	3.534	65.54	28.11	6.35
15-16	0.363	1.565	1.56 ± 0.16	17.73 ± 1.77	2.825	64.29	29.16	6.55
16-17	0.344	1.608	1.61 ± 0.16	19.34 ± 1.93	3.118	59.45	33.41	7.14
17-18	0.338	1.629	1.63 ± 0.16	20.97 ± 2.10	2.456	69.20	18.48	12.32
18-19	0.356	1.585	1.59 ± 0.16	22.55 ± 2.26	2.304	47.65	42.50	9.85
19-20	0.353	1.601	1.60 ± 0.16	24.15 ± 2.42	1.668	63.90	30.08	6.02

MB6-B-15V

Interval	Assumed + OM Porosity	Bulk Density	Assumed + OM Mass Depth	Assumed + OM Cumulative Mass Depth	Particulate Organic Carbon	Sand	Silt	Clay
(cm)	(%)	(g/cm³)	(g/cm^2)	(g/cm²)	(%)	(%)	(%)	(%)
20-21	0.371	1.560	1.56 ± 0.16	25.71 ± 2.57	1.313	70.59	20.95	8.46
21-22	0.360	1.588	1.59 ± 0.16	27.30 ± 2.73	1.224	69.03	24.83	6.14
22-23	0.369	1.569	1.57 ± 0.16	28.87 ± 2.89	0.757	74.21	21.11	4.68
23-24	0.374	1.560	1.56 ± 0.16	30.43 ± 3.04	0.57	70.28	24.98	4.74
24-25	0.350	1.615	1.61 ± 0.16	32.04 ± 3.20	0.897	67.49	28.22	4.29
25-26	0.300	1.740	1.74 ± 0.17	33.78 ± 3.38	0.832	68.54	26.24	5.22
26-27	0.300	1.740	1.74 ± 0.17	35.52 ± 3.55	0.89	59.14	20.01	20.85
27-28	0.510	1.218	1.22 ± 0.12	36.74 ± 3.67	0.86	73.79	20.02	6.19
28-29	0.311	1.712	1.71 ± 0.17	38.45 ± 3.85	0.915	74.93	19.62	5.45
29-30	0.320	1.682	1.68 ± 0.17	40.14 ± 4.01	ND	60.08	33.43	6.49
30-31	0.314	1.715	1.71 ± 0.17	41.85 ± 4.19	ND	66.71	28.29	5.00
31-32	0.288	1.780	1.78 ± 0.18	43.63 ± 4.36	ND	87.99	10.41	1.60
32-33	0.276	1.811	1.81 ± 0.18	45.44 ± 4.54	ND	78.73	18.47	2.80
33-34	0.279	1.802	1.80 ± 0.18	47.24 ± 4.72	ND	79.27	17.53	3.20
34-35	0.289	1.778	1.78 ± 0.18	49.02 ± 4.90	ND	60.50	31.15	8.35
35-36	0.296	1.759	1.76 ± 0.18	50.78 ± 5.08	ND	84.55	12.43	3.02
36-37	0.304	1.740	1.74 ± 0.17	52.52 ± 5.25	ND	83.63	13.43	2.94
37-38	0.308	1.730	1.73 ± 0.17	54.25 ± 5.43	ND	79.72	17.60	2.68
38-39	0.311	1.723	1.72 ± 0.17	55.97 ± 5.60	ND	94.21	5.12	0.67
39-40	0.306	1.736	1.74 ± 0.17	57.71 ± 5.77	ND	77.92	19.29	2.79

MB6-B-15V

Interval	Assumed + OM Porosity	Bulk Density	Assumed + OM Mass Depth	Assumed + OM Cumulative Mass Depth	Particulate Organic Carbon	Sand	Silt	Clay
(cm)	(%)	(g/cm³)	(g/cm^2)	(g/cm²)	(%)	(%)	(%)	(%)
40-41	0.315	1.712	1.71 ± 0.17	59.42 ± 5.94	ND	83.74	12.56	3.70
41-42	0.307	1.734	1.73 ± 0.17	61.16 ± 6.12	ND	62.17	30.21	7.62
42-43	0.308	1.729	1.73 ± 0.17	62.88 ± 6.29	ND	73.18	23.85	2.97
43-44	0.301	1.749	1.75 ± 0.17	64.63 ± 6.46	ND	75.23	21.81	2.96
44-45	0.302	1.746	1.75 ± 0.17	66.38 ± 6.64	ND	62.18	33.14	4.68
45-46	0.295	1.763	1.76 ± 0.18	68.14 ± 6.81	ND	83.64	14.72	1.64
46-47	0.303	1.742	1.74 ± 0.17	69.88 ± 6.99	ND	77.93	19.43	2.64
47-48	0.314	1.715	1.72 ± 0.17	71.60 ± 7.16	ND	65.62	28.55	5.83
48-49	0.334	1.664	1.66 ± 0.17	73.26 ± 7.33	ND	83.13	15.11	1.76
49-50	0.364	1.590	1.59 ± 0.16	74.85 ± 7.49	ND	74.01	22.21	3.78

MQ1-A-14V

Interval	¹³⁷ Cs	²¹⁰ Pb _{Tot}	²¹⁰ Pb _{XS}	⁷ Be	²²⁶ Ra
(cm)	(Bq/kg)	(Bq/kg)	(Bq/kg)	(Bq/kg)	(Bq/kg)
0-1	10.43 ± 0.73	149.59 ± 8.64	133.31 ± 7.65	0.00 ± 0.00	63.78 ± 3.67
1-2	6.18 ± 0.34	126.49 ± 6.86	110.22 ± 5.87	0.00 ± 0.00	65.98 ± 3.75
2-3	9.34 ± 0.72	111.95 ± 6.03	95.68 ± 5.04	0.00 ± 0.00	49.42 ± 2.83
3-4	10.33 ± 0.77	95.45 ± 5.72	79.18 ± 4.73	0.00 ± 0.00	56.33 ± 3.20
4-5	6.54 ± 0.53	90.84 ± 5.60	74.57 ± 4.60	0.00 ± 0.00	72.77 ± 4.12
5-6	8.79 ± 0.52	119.07 ± 7.19	102.80 ± 6.20	0.00 ± 0.00	56.45 ± 3.28
6-7	7.96 ± 0.47	91.01 ± 5.16	74.74 ± 4.17	0.00 ± 0.00	49.82 ± 2.87
7-8	7.62 ± 0.58	70.27 ± 4.90	53.99 ± 3.90	0.00 ± 0.00	69.64 ± 4.08
8-9	8.41 ± 0.69	102.24 ± 7.80	85.97 ± 6.81	0.00 ± 0.00	54.62 ± 3.29
9-10	4.72 ± 0.35	108.88 ± 7.72	92.60 ± 6.72	0.00 ± 0.00	64.94 ± 3.79
10-11	12.64 ± 0.88	89.02 ± 5.88	72.74 ± 4.88	0.00 ± 0.00	57.82 ± 3.37
11-12	11.05 ± 0.86	88.74 ± 5.71	72.46 ± 4.71	0.00 ± 0.00	61.87 ± 3.41
12-13	11.49 ± 0.89	96.57 ± 7.09	80.30 ± 6.09	0.00 ± 0.00	62.02 ± 3.71
13-14	15.33 ± 0.82	95.32 ± 5.36	79.04 ± 4.36	0.00 ± 0.00	70.10 ± 3.99
14-15	19.35 ± 1.16	109.87 ± 7.66	93.60 ± 6.66	0.00 ± 0.00	82.70 ± 4.65
15-16	24.84 ± 1.80	104.99 ± 7.23	88.72 ± 6.23	0.00 ± 0.00	81.67 ± 4.56
16-17	10.83 ± 0.65	120.99 ± 7.52	104.71 ± 6.53	0.00 ± 0.00	82.86 ± 4.66
17-18	13.93 ± 1.18	96.14 ± 5.26	79.86 ± 4.27	0.00 ± 0.00	60.30 ± 3.59
18-19	13.24 ± 1.13	64.33 ± 3.72	48.05 ± 2.72	0.00 ± 0.00	67.58 ± 3.86
19-20	11.15 ± 0.78	90.58 ± 5.63	74.30 ± 4.63	0.00 ± 0.00	77.41 ± 4.25
20-21	5.37 ± 0.39	98.43 ± 6.89	82.15 ± 5.89	0.00 ± 0.00	79.39 ± 4.37
21-22	7.15 ± 0.46	96.95 ± 7.15	80.68 ± 6.16	0.00 ± 0.00	60.32 ± 3.27
22-23	4.50 ± 0.35	64.56 ± 4.78	48.28 ± 3.79	0.00 ± 0.00	58.54 ± 3.17
23-24	1.85 ± 0.13	62.00 ± 3.83	45.72 ± 2.83	0.00 ± 0.00	49.80 ± 2.65
24-25	2.55 ± 0.19	49.41 ± 3.30	33.14 ± 2.30	0.00 ± 0.00	33.34 ± 1.82
25-26	1.67 ± 0.13	38.38 ± 2.40	22.11 ± 1.41	0.00 ± 0.00	32.53 ± 1.76
26-27	0.00 ± 0.00	37.67 ± 2.58	21.40 ± 1.59	0.00 ± 0.00	20.40 ± 1.22
27-28	0.00 ± 0.00	27.10 ± 1.69	10.82 ± 0.70	0.00 ± 0.00	19.55 ± 1.20
28-29	0.00 ± 0.00	28.77 ± 1.85	12.49 ± 0.86	0.00 ± 0.00	15.67 ± 1.04
29-30	0.00 ± 0.00	28.54 ± 1.87	12.27 ± 0.87	0.00 ± 0.00	15.87 ± 1.16
30-31	ND	10.78 ± 0.68	0.00 ± 0.00	ND	ND
31-32	ND	10.82 ± 0.64	0.00 ± 0.00	ND	ND
32-33	ND	8.44 ± 0.53	0.00 ± 0.00	ND	ND
33-34	ND	12.31 ± 0.67	0.00 ± 0.00	ND	ND
34-35	ND	8.07 ± 0.52	0.00 ± 0.00	ND	ND
35-36	ND	11.01 ± 0.70	0.00 ± 0.00	ND	ND
36-37	ND	13.10 ± 0.83	0.00 ± 0.00	ND	ND
37-38	ND	16.93 ± 1.00	0.00 ± 0.00	ND	ND
38-39	ND	38.73 ± 2.14	22.46 ± 1.15	ND	ND

MQ1-A-14V

Interval	¹³⁷ Cs	²¹⁰ Pb _{Tot}	²¹⁰ Pb _{XS}	⁷ Be	²²⁶ Ra
(cm)	(Bq/kg)	(Bq/kg)	(Bq/kg)	(Bq/kg)	(Bq/kg)
39-40	ND	15.93 ± 0.97	0.00 ± 0.00	ND	ND
40-41	ND	19.03 ± 1.13	2.75 ± 0.13	ND	ND
41-42	ND	13.98 ± 0.87	0.00 ± 0.00	ND	ND
42-43	ND	20.89 ± 1.29	4.62 ± 0.29	ND	ND
43-44	ND	16.51 ± 1.07	0.00 ± 0.00	ND	ND
44-45	ND	16.69 ± 1.05	0.00 ± 0.00	ND	ND
45-46	ND	10.66 ± 0.62	0.00 ± 0.00	ND	ND
46-47	ND	19.99 ± 1.13	3.72 ± 0.14	ND	ND
47-48	ND	17.51 ± 1.11	1.24 ± 0.11	ND	ND
48-49	ND	0.00 ± 0.00	0.00 ± 0.00	ND	ND
49-50	ND	0.00 ± 0.00	0.00 ± 0.00	ND	ND

U10-B-14V

Interval	¹³⁷ Cs	²¹⁰ Pb _{Tot}	²¹⁰ Pb _{XS}	⁷ Be	²²⁶ Ra
(cm)	(Bq/kg)	(Bq/kg)	(Bq/kg)	(Bq/kg)	(Bq/kg)
0-1	7.73 ± 0.43	175.72 ± 8.90	169.55 ± 8.49	54.84 ± 3.86	58.92 ± 3.47
1-2	8.96 ± 0.51	98.91 ± 5.77	92.74 ± 5.37	0.00 ± 0.00	46.09 ± 2.82
2-3	6.50 ± 0.36	75.15 ± 5.54	68.98 ± 5.14	0.00 ± 0.00	46.26 ± 2.88
3-4	7.87 ± 0.44	108.87 ± 6.92	102.70 ± 6.52	0.00 ± 0.00	50.68 ± 3.14
4-5	5.42 ± 0.33	88.41 ± 5.82	82.24 ± 5.41	0.00 ± 0.00	48.33 ± 2.77
5-6	7.80 ± 0.62	72.35 ± 4.73	66.18 ± 4.33	0.00 ± 0.00	45.52 ± 2.83
6-7	5.78 ± 0.32	80.64 ± 5.74	74.47 ± 5.34	0.00 ± 0.00	49.13 ± 3.10
7-8	7.24 ± 0.42	54.96 ± 3.58	48.79 ± 3.18	0.00 ± 0.00	36.18 ± 2.13
8-9	7.29 ± 0.42	38.75 ± 2.68	32.58 ± 2.28	0.00 ± 0.00	23.02 ± 1.39
9-10	4.82 ± 0.32	28.81 ± 1.89	22.64 ± 1.49	0.00 ± 0.00	22.68 ± 1.50
10-11	1.94 ± 0.16	25.11 ± 1.54	18.94 ± 1.14	0.00 ± 0.00	18.75 ± 1.24
11-12	2.19 ± 0.16	25.02 ± 1.67	18.85 ± 1.27	0.00 ± 0.00	13.38 ± 0.80
12-13	1.87 ± 0.13	19.12 ± 1.20	12.95 ± 0.80	0.00 ± 0.00	13.07 ± 0.86
13-14	1.39 ± 0.10	18.04 ± 1.15	11.87 ± 0.75	0.00 ± 0.00	16.93 ± 1.02
14-15	0.00 ± 0.00	14.85 ± 0.99	8.69 ± 0.59	0.00 ± 0.00	5.92 ± 0.38
15-16	0.00 ± 0.00	12.40 ± 0.83	6.23 ± 0.43	0.00 ± 0.00	9.62 ± 0.60
16-17	1.24 ± 0.11	12.70 ± 0.81	6.53 ± 0.41	0.00 ± 0.00	10.42 ± 0.67
17-18	1.09 ± 0.07	12.70 ± 0.80	6.54 ± 0.40	0.00 ± 0.00	9.68 ± 0.61
18-19	1.81 ± 0.16	15.19 ± 1.01	9.03 ± 0.61	0.00 ± 0.00	13.01 ± 0.82
19-20	0.00 ± 0.00	16.55 ± 1.07	10.38 ± 0.67	0.00 ± 0.00	13.71 ± 0.82
20-21	0.00 ± 0.00	27.95 ± 1.83	21.79 ± 1.43	0.00 ± 0.00	33.72 ± 2.11
21-22	0.00 ± 0.00	46.06 ± 3.02	39.90 ± 2.62	0.00 ± 0.00	53.20 ± 2.97
22-23	0.00 ± 0.00	36.90 ± 2.31	30.73 ± 1.91	0.00 ± 0.00	49.42 ± 2.83
23-24	0.00 ± 0.00	50.91 ± 3.30	44.74 ± 2.90	0.00 ± 0.00	52.55 ± 3.01
24-25	0.00 ± 0.00	58.44 ± 3.74	52.27 ± 3.33	0.00 ± 0.00	46.23 ± 2.59
25-26	0.00 ± 0.00	53.82 ± 3.37	47.65 ± 2.97	0.00 ± 0.00	48.52 ± 2.97
26-27	0.00 ± 0.00	67.26 ± 4.56	61.09 ± 4.16	0.00 ± 0.00	45.76 ± 2.78
27-28	0.00 ± 0.00	81.51 ± 6.28	75.34 ± 5.87	0.00 ± 0.00	62.88 ± 3.62
28-29	0.00 ± 0.00	87.24 ± 6.17	81.07 ± 5.77	0.00 ± 0.00	95.42 ± 4.98
29-30	0.00 ± 0.00	79.29 ± 6.08	73.12 ± 5.68	0.00 ± 0.00	92.43 ± 4.85
30-31	ND	63.34 ± 4.47	57.18 ± 4.07	ND	ND
31-32	ND	45.61 ± 3.14	39.44 ± 2.74	ND	ND
32-33	ND	45.44 ± 3.05	39.27 ± 2.65	ND	ND
33-34	ND	36.91 ± 2.23	30.75 ± 1.83	ND	ND
34-35	ND	33.14 ± 1.98	26.97 ± 1.58	ND	ND
35-36	ND	43.32 ± 2.75	37.15 ± 2.35	ND	ND
36-37	ND	26.15 ± 1.61	19.98 ± 1.21	ND	ND
37-38	ND	15.83 ± 1.00	9.66 ± 0.60	ND	ND
38-39	ND	10.53 ± 0.68	4.36 ± 0.28	ND	ND

U10-B-14V

Interval	¹³⁷ Cs	²¹⁰ Pb _{Tot}	²¹⁰ Pb _{xs}	⁷ Be	²²⁶ Ra
(cm)	(Bq/kg)	(Bq/kg)	(Bq/kg)	(Bq/kg)	(Bq/kg)
39-40	ND	9.89 ± 0.60	3.72 ± 0.20	ND	ND
40-41	ND	9.47 ± 0.57	3.30 ± 0.17	ND	ND
41-42	ND	9.23 ± 0.57	3.06 ± 0.17	ND	ND
42-43	ND	8.31 ± 0.60	2.14 ± 0.20	ND	ND
43-44	ND	8.28 ± 0.50	2.11 ± 0.10	ND	ND
44-45	ND	7.34 ± 0.47	1.18 ± 0.07	ND	ND
45-46	ND	6.59 ± 0.42	0.00 ± 0.00	ND	ND
46-47	ND	6.50 ± 0.41	0.00 ± 0.00	ND	ND
47-48	ND	6.38 ± 0.41	0.00 ± 0.00	ND	ND
48-49	ND	6.73 ± 0.43	0.00 ± 0.00	ND	ND
49-50	ND	5.40 ± 0.37	0.00 ± 0.00	ND	ND

MBM-A-14V

Interval	¹³⁷ Cs	²¹⁰ Pb _{Tot}	²¹⁰ Pb _{xs}	⁷ Be	²²⁶ Ra
(cm)	(Bq/kg)	(Bq/kg)	(Bq/kg)	(Bq/kg)	(Bq/kg)
0-1	12.24 ± 0.75	123.02 ± 8.25	117.33 ± 7.25	0.00 ± 0.00	51.08 ± 2.93
1-2	10.28 ± 0.73	117.57 ± 7.69	111.89 ± 8.62	0.00 ± 0.00	70.21 ± 4.07
2-3	8.11 ± 0.53	138.61 ± 8.62	132.93 ± 5.30	0.00 ± 0.00	78.19 ± 4.52
3-4	14.96 ± 1.02	86.95 ± 5.30	81.26 ± 4.93	0.00 ± 0.00	72.22 ± 3.95
4-5	10.62 ± 0.58	66.94 ± 4.93	61.25 ± 3.58	0.00 ± 0.00	46.13 ± 2.60
5-6	6.15 ± 0.47	59.68 ± 3.58	54.00 ± 3.52	0.00 ± 0.00	59.91 ± 3.37
6-7	16.35 ± 0.90	51.53 ± 3.52	45.84 ± 2.95	0.00 ± 0.00	44.61 ± 2.50
7-8	7.78 ± 0.57	43.42 ± 2.95	37.74 ± 2.34	0.00 ± 0.00	40.45 ± 2.25
8-9	5.42 ± 0.33	34.66 ± 2.34	28.98 ± 1.60	0.00 ± 0.00	34.80 ± 1.99
9-10	5.81 ± 0.33	24.72 ± 1.60	19.03 ± 1.38	0.00 ± 0.00	23.41 ± 1.38
10-11	3.17 ± 0.20	20.50 ± 1.38	14.81 ± 1.36	0.00 ± 0.00	24.29 ± 1.41
11-12	3.26 ± 0.24	18.92 ± 1.36	13.23 ± 1.26	0.00 ± 0.00	15.43 ± 0.93
12-13	4.21 ± 0.37	19.32 ± 1.26	13.64 ± 0.70	0.00 ± 0.00	15.80 ± 0.92
13-14	2.32 ± 0.18	9.97 ± 0.70	4.29 ± 0.59	0.00 ± 0.00	10.09 ± 0.67
14-15	0.00 ± 0.00	8.29 ± 0.59	2.60 ± 0.61	0.00 ± 0.00	7.09 ± 0.49
15-16	1.10 ± 0.08	8.80 ± 0.61	3.12 ± 0.41	0.00 ± 0.00	12.46 ± 0.77
16-17	0.00 ± 0.00	4.25 ± 0.41	0.00 ± 0.00	0.00 ± 0.00	4.26 ± 0.29
17-18	0.00 ± 0.00	5.24 ± 0.36	0.00 ± 0.00	0.00 ± 0.00	4.09 ± 0.29
18-19	0.00 ± 0.00	4.18 ± 0.38	0.00 ± 0.00	0.00 ± 0.00	9.52 ± 0.71
19-20	0.00 ± 0.00	3.79 ± 0.38	0.00 ± 0.00	0.00 ± 0.00	3.73 ± 0.28
20-21	0.00 ± 0.00	4.40 ± 0.38	0.00 ± 0.00	0.00 ± 0.00	8.01 ± 0.55
21-22	0.00 ± 0.00	5.56 ± 0.43	0.00 ± 0.00	0.00 ± 0.00	4.52 ± 0.32
22-23	0.00 ± 0.00	4.25 ± 0.47	0.00 ± 0.00	0.00 ± 0.00	5.82 ± 0.37
23-24	0.00 ± 0.00	6.91 ± 0.53	0.00 ± 0.00	0.00 ± 0.00	3.86 ± 0.30
24-25	0.00 ± 0.00	5.37 ± 0.37	0.00 ± 0.00	0.00 ± 0.00	6.97 ± 0.52
25-26	0.00 ± 0.00	4.98 ± 0.45	0.00 ± 0.00	0.00 ± 0.00	4.21 ± 0.34
26-27	0.00 ± 0.00	5.83 ± 0.46	0.00 ± 0.00	0.00 ± 0.00	6.00 ± 0.40
27-28	0.00 ± 0.00	6.55 ± 0.47	0.00 ± 0.00	0.00 ± 0.00	6.56 ± 0.48
28-29	0.00 ± 0.00	11.75 ± 0.84	0.00 ± 0.00	0.00 ± 0.00	20.71 ± 1.27
29-30	0.00 ± 0.00	29.98 ± 2.02	0.00 ± 0.00	0.00 ± 0.00	32.29 ± 1.94
30-31	ND	ND	ND	ND	ND
31-32	ND	ND	ND	ND	ND
32-33	ND	ND	ND	ND	ND
33-34	ND	ND	ND	ND	ND
34-35	ND	ND	ND	ND	ND
35-36	ND	ND	ND	ND	ND
36-37	ND	ND	ND	ND	ND
37-38	ND	ND	ND	ND	ND
38-39	ND	ND	ND	ND	ND

MBM-A-14V

Interval	¹³⁷ Cs	²¹⁰ Pb _{Tot}	²¹⁰ Pb _{XS}	⁷ Be	²²⁶ Ra
(cm)	(Bq/kg)	(Bq/kg)	(Bq/kg)	(Bq/kg)	(Bq/kg)
39-40	ND	ND	ND	ND	ND
40-41	ND	ND	ND	ND	ND
41-42	ND	ND	ND	ND	ND
42-43	ND	ND	ND	ND	ND
43-44	ND	ND	ND	ND	ND
44-45	ND	ND	ND	ND	ND
45-46	ND	ND	ND	ND	ND
46-47	ND	ND	ND	ND	ND
47-48	ND	ND	ND	ND	ND
48-49	ND	ND	ND	ND	ND
49-50	ND	ND	ND	ND	ND

ODB-1B-14V

Interval	¹³⁷ Cs	²¹⁰ Pb _{Tot}	²¹⁰ Pb _{XS}	⁷ Be	²²⁶ Ra
(cm)	(Bq/kg)	(Bq/kg)	(Bq/kg)	(Bq/kg)	(Bq/kg)
0-1	8.48 ± 0.49	516.43 ± 31.23	516.43 ± 31.23	0.00 ± 0.00	31.98 ± 2.34
1-2	2.56 ± 0.20	339.57 ± 19.99	339.57 ± 19.99	0.00 ± 0.00	51.70 ± 3.14
2-3	3.24 ± 0.28	121.75 ± 7.74	121.75 ± 7.74	0.00 ± 0.00	36.01 ± 2.10
3-4	4.33 ± 0.27	81.13 ± 6.14	81.13 ± 6.14	0.00 ± 0.00	24.84 ± 1.47
4-5	6.46 ± 0.39	87.99 ± 6.10	87.99 ± 6.10	0.00 ± 0.00	26.61 ± 1.54
5-6	6.54 ± 0.49	91.95 ± 5.66	91.95 ± 5.66	0.00 ± 0.00	41.35 ± 2.70
6-7	8.45 ± 0.47	131.83 ± 8.44	131.83 ± 8.44	0.00 ± 0.00	49.77 ± 3.02
7-8	17.89 ± 0.99	148.18 ± 9.57	148.18 ± 9.57	0.00 ± 0.00	47.86 ± 2.86
8-9	22.85 ± 1.70	125.72 ± 8.89	125.72 ± 8.89	0.00 ± 0.00	44.76 ± 2.68
9-10	17.94 ± 1.19	102.88 ± 6.82	102.88 ± 6.82	0.00 ± 0.00	63.86 ± 3.62
10-11	10.73 ± 0.61	102.73 ± 7.52	102.73 ± 7.52	0.00 ± 0.00	28.10 ± 1.80
11-12	20.09 ± 1.35	93.47 ± 6.34	93.47 ± 6.34	0.00 ± 0.00	45.96 ± 2.59
12-13	12.99 ± 0.86	74.05 ± 5.51	74.05 ± 5.51	0.00 ± 0.00	41.27 ± 2.54
13-14	10.02 ± 0.76	55.07 ± 4.03	55.07 ± 4.03	0.00 ± 0.00	30.66 ± 1.89
14-15	9.79 ± 0.64	43.77 ± 2.69	43.77 ± 2.69	0.00 ± 0.00	29.42 ± 1.78
15-16	5.56 ± 0.33	42.55 ± 2.95	42.55 ± 2.95	0.00 ± 0.00	36.78 ± 2.14
16-17	2.24 ± 0.20	37.36 ± 2.61	37.36 ± 2.61	0.00 ± 0.00	23.09 ± 1.39
17-18	1.24 ± 0.08	33.95 ± 2.24	33.95 ± 2.24	0.00 ± 0.00	27.07 ± 1.51
18-19	2.45 ± 0.18	42.23 ± 2.86	42.23 ± 2.86	0.00 ± 0.00	27.44 ± 1.48
19-20	2.51 ± 0.19	37.91 ± 2.34	37.91 ± 2.34	0.00 ± 0.00	32.26 ± 1.76
20-21	1.90 ± 0.14	38.50 ± 2.62	38.50 ± 2.62	0.00 ± 0.00	41.20 ± 2.22
21-22	1.12 ± 0.08	41.36 ± 2.89	41.36 ± 2.89	0.00 ± 0.00	33.87 ± 1.83
22-23	1.56 ± 0.13	42.70 ± 2.63	42.70 ± 2.63	0.00 ± 0.00	30.14 ± 1.62
23-24	1.02 ± 0.09	46.95 ± 3.01	46.95 ± 3.01	0.00 ± 0.00	35.54 ± 1.90
24-25	0.00 ± 0.00	31.26 ± 2.10	31.26 ± 2.10	0.00 ± 0.00	23.75 ± 1.49
25-26	0.00 ± 0.00	30.25 ± 1.98	0.00 ± 0.00	0.00 ± 0.00	31.80 ± 1.92
26-27	0.00 ± 0.00	29.78 ± 1.92	0.00 ± 0.00	0.00 ± 0.00	19.59 ± 1.24
27-28	0.00 ± 0.00	23.54 ± 1.56	0.00 ± 0.00	0.00 ± 0.00	21.38 ± 1.47
28-29	0.00 ± 0.00	30.25 ± 1.76	0.00 ± 0.00	0.00 ± 0.00	22.71 ± 1.58
29-30	0.00 ± 0.00	33.87 ± 2.19	0.00 ± 0.00	0.00 ± 0.00	20.08 ± 1.23
30-31	ND	ND	ND	ND	ND
31-32	ND	ND	ND	ND	ND
32-33	ND	ND	ND	ND	ND
33-34	ND	ND	ND	ND	ND
34-35	ND	ND	ND	ND	ND
35-36	ND	ND	ND	ND	ND
36-37	ND	ND	ND	ND	ND
37-38	ND	ND	ND	ND	ND
38-39	ND	ND	ND	ND	ND

ODB-1B-14V

Interval	¹³⁷ Cs	²¹⁰ Pb _{Tot}	²¹⁰ Pb _{xs}	⁵Be	²²⁶ Ra
(cm)	(Bq/kg)	(Bq/kg)	(Bq/kg)	(Bq/kg)	(Bq/kg)
39-40	ND	ND	ND	ND	ND
40-41	ND	ND	ND	ND	ND
41-42	ND	ND	ND	ND	ND
42-43	ND	ND	ND	ND	ND
43-44	ND	ND	ND	ND	ND
44-45	ND	ND	ND	ND	ND
45-46	ND	ND	ND	ND	ND
46-47	ND	ND	ND	ND	ND
47-48	ND	ND	ND	ND	ND
48-49	ND	ND	ND	ND	ND
49-50	ND	ND	ND	ND	ND

TC2A-B-14V

Interval	¹³⁷ Cs	²¹⁰ Pb _{Tot}	²¹⁰ Pb _{xs}	⁷ Be	²²⁶ Ra
(cm)	(Bq/kg)	(Bq/kg)	(Bq/kg)	(Bq/kg)	(Bq/kg)
0-1	4.56 ± 0.31	356.10 ± 19.89	356.10 ± 19.89	47.43 ± 2.85	61.90 ± 4.09
1-2	17.19 ± 1.08	446.32 ± 26.45	446.32 ± 26.45	0.00 ± 0.00	64.92 ± 4.17
2-3	17.03 ± 0.93	ND	ND	0.00 ± 0.00	41.18 ± 2.59
3-4	12.62 ± 0.72	484.74 ± 29.09	484.74 ± 29.09	0.00 ± 0.00	52.24 ± 3.19
4-5	17.89 ± 1.33	515.06 ± 31.98	515.06 ± 31.98	0.00 ± 0.00	45.52 ± 2.60
5-6	6.27 ± 0.36	474.69 ± 30.78	474.69 ± 30.78	0.00 ± 0.00	111.19 ± 6.47
6-7	17.54 ± 1.21	328.98 ± 18.52	328.98 ± 18.52	0.00 ± 0.00	98.79 ± 5.63
7-8	14.56 ± 0.81	265.40 ± 15.55	265.40 ± 15.55	0.00 ± 0.00	84.83 ± 4.75
8-9	16.70 ± 0.96	185.45 ± 10.65	185.45 ± 10.65	0.00 ± 0.00	44.77 ± 2.83
9-10	19.10 ± 1.35	144.07 ± 9.32	144.07 ± 9.32	0.00 ± 0.00	61.77 ± 3.79
10-11	14.70 ± 0.86	136.85 ± 9.46	136.85 ± 9.46	0.00 ± 0.00	75.75 ± 4.33
11-12	15.09 ± 0.82	110.32 ± 7.27	110.32 ± 7.27	0.00 ± 0.00	56.81 ± 3.36
12-13	13.07 ± 0.75	83.89 ± 6.36	83.89 ± 6.36	0.00 ± 0.00	65.53 ± 3.85
13-14	3.19 ± 0.26	86.21 ± 6.55	86.21 ± 6.55	0.00 ± 0.00	55.60 ± 3.41
14-15	5.98 ± 0.42	93.50 ± 6.67	93.50 ± 6.67	0.00 ± 0.00	50.02 ± 2.97
15-16	6.91 ± 0.53	84.69 ± 5.98	84.69 ± 5.98	0.00 ± 0.00	53.65 ± 3.12
16-17	4.14 ± 0.25	80.97 ± 5.44	80.97 ± 5.44	0.00 ± 0.00	58.45 ± 3.15
17-18	5.41 ± 0.36	123.81 ± 8.23	123.81 ± 8.23	0.00 ± 0.00	60.65 ± 3.25
18-19	3.64 ± 0.27	117.54 ± 8.75	117.54 ± 8.75	0.00 ± 0.00	102.28 ± 5.87
19-20	3.23 ± 0.20	85.93 ± 5.89	85.93 ± 5.89	0.00 ± 0.00	47.98 ± 2.61
20-21	1.22 ± 0.08	87.46 ± 7.48	87.46 ± 7.48	0.00 ± 0.00	45.24 ± 2.37
21-22	1.01 ± 0.08	81.95 ± 6.23	81.95 ± 6.23	0.00 ± 0.00	42.36 ± 2.23
22-23	0.00 ± 0.00	66.80 ± 5.26	66.80 ± 5.26	0.00 ± 0.00	30.25 ± 2.04
23-24	0.00 ± 0.00	66.56 ± 5.51	66.56 ± 5.51	0.00 ± 0.00	39.82 ± 2.46
24-25	0.00 ± 0.00	75.37 ± 6.79	75.37 ± 6.79	0.00 ± 0.00	46.32 ± 2.89
25-26	0.00 ± 0.00	71.99 ± 5.37	71.99 ± 5.37	0.00 ± 0.00	21.97 ± 1.66
26-27	0.00 ± 0.00	72.40 ± 5.45	72.40 ± 5.45	0.00 ± 0.00	35.98 ± 2.27
27-28	0.00 ± 0.00	0.00 ± 0.00	0.00 ± 0.00	0.00 ± 0.00	38.10 ± 2.39
28-29	0.00 ± 0.00	95.47 ± 6.53	95.47 ± 6.53	0.00 ± 0.00	47.99 ± 2.81
29-30	0.00 ± 0.00	86.82 ± 6.67	86.82 ± 6.67	0.00 ± 0.00	44.83 ± 2.73
30-31	ND	28.59 ± 1.88	0.00 ± 0.00	ND	ND
31-32	ND	37.43 ± 2.06	0.00 ± 0.00	ND	ND
32-33	ND	30.42 ± 1.86	0.00 ± 0.00	ND	ND
33-34	ND	41.65 ± 2.59	0.00 ± 0.00	ND	ND
34-35	ND	44.92 ± 2.94	44.92 ± 2.94	ND	ND
35-36	ND	34.79 ± 2.32	0.00 ± 0.00	ND	ND
36-37	ND	43.80 ± 2.78	43.8 ± 2.78	ND	ND
37-38	ND	54.75 ± 3.72	0.00 ± 0.00	ND	ND
38-39	ND	38.39 ± 2.46	0.00 ± 0.00	ND	ND

TC2A-B-14V

Interval	¹³⁷ Cs	²¹⁰ Pb _{Tot}	²¹⁰ Pb _{xs}	⁷ Be	²²⁶ Ra
(cm)	(Bq/kg)	(Bq/kg)	(Bq/kg)	(Bq/kg)	(Bq/kg)
39-40	ND	38.09 ± 2.45	0.00 ± 0.00	ND	ND
40-41	ND	ND	ND	ND	ND
41-42	ND	ND	ND	ND	ND
42-43	ND	ND	ND	ND	ND
43-44	ND	ND	ND	ND	ND
44-45	ND	ND	ND	ND	ND
45-46	ND	ND	ND	ND	ND
46-47	ND	ND	ND	ND	ND
47-48	ND	ND	ND	ND	ND
48-49	ND	ND	ND	ND	ND
49-50	ND	ND	ND	ND	ND

MCE-A-14V

Interval	¹³⁷ Cs	²¹⁰ Pb _{Tot}	²¹⁰ Pb _{XS}	⁷ Be	²²⁶ Ra
(cm)	(Bq/kg)	(Bq/kg)	(Bq/kg)	(Bq/kg)	(Bq/kg)
0-1	6.06 ± 0.35	12.04 ± 0.57	0.00 ± 0.00	0.00 ± 0.00	40.91 ± 2.95
1-2	10.19 ± 0.61	292.93 ± 18.15	292.93 ± 18.15	0.00 ± 0.00	34.87 ± 2.18
2-3	15.50 ± 0.95	258.30 ± 13.76	258.30 ± 13.76	0.00 ± 0.00	47.86 ± 3.20
3-4	10.30 ± 0.77	169.24 ± 10.28	169.24 ± 10.28	0.00 ± 0.00	34.09 ± 2.31
4-5	5.44 ± 0.30	118.83 ± 7.97	118.83 ± 7.97	0.00 ± 0.00	51.84 ± 3.74
5-6	10.03 ± 0.69	96.49 ± 6.61	96.49 ± 6.61	0.00 ± 0.00	29.30 ± 1.89
6-7	11.40 ± 0.64	80.06 ± 6.24	80.06 ± 6.24	0.00 ± 0.00	46.07 ± 3.18
7-8	6.79 ± 0.43	63.72 ± 4.78	63.72 ± 4.78	0.00 ± 0.00	38.21 ± 2.53
8-9	4.08 ± 0.25	63.57 ± 4.21	63.57 ± 4.21	0.00 ± 0.00	54.71 ± 3.62
9-10	7.69 ± 0.46	51.62 ± 3.77	51.62 ± 3.77	0.00 ± 0.00	41.24 ± 2.76
10-11	3.66 ± 0.24	42.33 ± 2.71	42.33 ± 2.71	0.00 ± 0.00	54.70 ± 3.18
11-12	4.01 ± 0.24	30.77 ± 2.12	30.77 ± 2.12	0.00 ± 0.00	24.15 ± 1.48
12-13	4.11 ± 0.28	29.88 ± 1.99	29.88 ± 1.99	0.00 ± 0.00	42.97 ± 2.45
13-14	4.11 ± 0.29	37.64 ± 2.61	37.64 ± 2.61	0.00 ± 0.00	40.79 ± 2.40
14-15	2.65 ± 0.22	32.08 ± 2.00	32.08 ± 2.00	0.00 ± 0.00	33.41 ± 1.96
15-16	0.00 ± 0.00	29.38 ± 1.98	29.38 ± 1.98	0.00 ± 0.00	43.85 ± 2.63
16-17	0.00 ± 0.00	26.18 ± 1.80	26.18 ± 1.80	0.00 ± 0.00	34.55 ± 2.37
17-18	0.00 ± 0.00	25.94 ± 1.73	25.94 ± 1.73	0.00 ± 0.00	42.83 ± 2.80
18-19	0.00 ± 0.00	30.82 ± 2.06	30.82 ± 2.06	0.00 ± 0.00	29.60 ± 1.86
19-20	0.00 ± 0.00	20.65 ± 1.27	0.00 ± 0.00	0.00 ± 0.00	25.55 ± 1.66
20-21	0.00 ± 0.00	23.52 ± 1.52	0.00 ± 0.00	0.00 ± 0.00	30.38 ± 1.94
21-22	0.00 ± 0.00	15.89 ± 1.05	0.00 ± 0.00	0.00 ± 0.00	24.17 ± 1.57
22-23	0.00 ± 0.00	31.58 ± 1.88	31.58 ± 1.88	0.00 ± 0.00	30.76 ± 1.70
23-24	0.00 ± 0.00	17.58 ± 1.12	0.00 ± 0.00	0.00 ± 0.00	34.13 ± 1.93
24-25	0.00 ± 0.00	21.03 ± 1.35	0.00 ± 0.00	0.00 ± 0.00	30.83 ± 1.74
25-26	0.00 ± 0.00	22.74 ± 1.49	0.00 ± 0.00	0.00 ± 0.00	32.54 ± 1.90
26-27	0.00 ± 0.00	22.05 ± 1.34	0.00 ± 0.00	0.00 ± 0.00	31.51 ± 1.79
27-28	0.00 ± 0.00	27.20 ± 1.79	27.20 ± 1.79	0.00 ± 0.00	33.94 ± 1.88
28-29	0.00 ± 0.00	19.85 ± 1.34	0.00 ± 0.00	0.00 ± 0.00	34.30 ± 1.92
29-30	0.00 ± 0.00	25.67 ± 1.69	25.67 ± 1.69	0.00 ± 0.00	38.17 ± 2.53
30-31	ND	ND	ND	ND	ND
31-32	ND	ND	ND	ND	ND
32-33	ND	ND	ND	ND	ND
33-34	ND	ND	ND	ND	ND
34-35	ND	ND	ND	ND	ND
35-36	ND	ND	ND	ND	ND
36-37	ND	ND	ND	ND	ND
37-38	ND	ND	ND	ND	ND
38-39	ND	ND	ND	ND	ND

MCE-A-14V

Interval	¹³⁷ Cs	²¹⁰ Pb _{Tot}	²¹⁰ Pb _{XS}	⁵Be	²²⁶ Ra
(cm)	(Bq/kg)	(Bq/kg)	(Bq/kg)	(Bq/kg)	(Bq/kg)
39-40	ND	ND	ND	ND	ND
40-41	ND	ND	ND	ND	ND
41-42	ND	ND	ND	ND	ND
42-43	ND	ND	ND	ND	ND
43-44	ND	ND	ND	ND	ND
44-45	ND	ND	ND	ND	ND
45-46	ND	ND	ND	ND	ND
46-47	ND	ND	ND	ND	ND
47-48	ND	ND	ND	ND	ND
48-49	ND	ND	ND	ND	ND
49-50	ND	ND	ND	ND	ND

TC2B-B-14V

Interval	¹³⁷ Cs	²¹⁰ Pb _{Tot}	²¹⁰ Pb _{XS}	⁷ Be	²²⁶ Ra
(cm)	(Bq/kg)	(Bq/kg)	(Bq/kg)	(Bq/kg)	(Bq/kg)
0-1	37.62 ± 2.53	322.11 ± 19.66	294.37 ± 17.91	46.78 ± 2.54	207.22 ± 11.15
1-2	63.07 ± 4.27	318.55 ± 20.54	290.81 ± 18.80	27.70 ± 1.72	219.64 ± 11.73
2-3	15.20 ± 1.13	275.66 ± 15.91	247.93 ± 14.16	0.00 ± 0.00	177.42 ± 9.87
3-4	25.16 ± 1.73	246.83 ± 15.45	219.10 ± 13.70	0.00 ± 0.00	140.36 ± 7.61
4-5	26.08 ± 1.84	266.54 ± 17.27	238.81 ± 15.52	0.00 ± 0.00	136.32 ± 7.37
5-6	19.05 ± 1.03	229.71 ± 13.67	201.98 ± 11.93	0.00 ± 0.00	104.45 ± 5.62
6-7	13.54 ± 0.74	187.72 ± 11.95	159.98 ± 10.20	0.00 ± 0.00	156.43 ± 8.38
7-8	16.32 ± 1.24	0.00 ± 0.00	0.00 ± 0.00	0.00 ± 0.00	108.28 ± 5.91
8-9	15.00 ± 0.80	149.86 ± 10.34	122.13 ± 8.59	0.00 ± 0.00	121.86 ± 6.43
9-10	19.82 ± 1.41	170.40 ± 10.38	142.67 ± 8.63	0.00 ± 0.00	104.49 ± 5.51
10-11	14.39 ± 0.84	114.86 ± 8.25	87.12 ± 6.50	0.00 ± 0.00	108.37 ± 5.80
11-12	5.45 ± 0.41	133.77 ± 8.82	106.04 ± 7.08	0.00 ± 0.00	137.37 ± 7.42
12-13	0.00 ± 0.00	84.24 ± 6.44	56.51 ± 4.69	0.00 ± 0.00	67.45 ± 3.52
13-14	2.04 ± 0.14	87.51 ± 5.87	59.78 ± 4.12	0.00 ± 0.00	114.80 ± 5.95
14-15	1.89 ± 0.13	86.34 ± 6.42	58.61 ± 4.67	0.00 ± 0.00	88.84 ± 4.58
15-16	2.40 ± 0.18	67.46 ± 5.03	39.72 ± 3.28	0.00 ± 0.00	64.50 ± 3.33
16-17	0.00 ± 0.00	79.41 ± 5.02	51.68 ± 3.27	0.00 ± 0.00	67.93 ± 3.82
17-18	0.00 ± 0.00	57.47 ± 4.12	29.74 ± 2.37	0.00 ± 0.00	51.48 ± 3.01
18-19	0.00 ± 0.00	59.21 ± 4.33	31.47 ± 2.58	0.00 ± 0.00	74.18 ± 4.01
19-20	0.00 ± 0.00	56.79 ± 4.12	29.06 ± 2.38	0.00 ± 0.00	52.17 ± 2.83
20-21	0.00 ± 0.00	0.00 ± 0.00	0.00 ± 0.00	0.00 ± 0.00	42.62 ± 2.60
21-22	0.00 ± 0.00	37.75 ± 2.63	10.02 ± 0.88	0.00 ± 0.00	40.22 ± 2.34
22-23	0.00 ± 0.00	46.65 ± 3.27	18.91 ± 1.52	0.00 ± 0.00	42.48 ± 2.48
23-24	0.00 ± 0.00	36.96 ± 2.51	9.23 ± 0.76	0.00 ± 0.00	33.36 ± 1.88
24-25	0.00 ± 0.00	32.88 ± 2.16	5.15 ± 0.41	0.00 ± 0.00	36.16 ± 2.13
25-26	0.00 ± 0.00	32.61 ± 2.04	4.88 ± 0.29	0.00 ± 0.00	32.90 ± 2.12
26-27	0.00 ± 0.00	25.38 ± 1.58	0.00 ± 0.00	0.00 ± 0.00	34.41 ± 1.92
27-28	0.00 ± 0.00	30.18 ± 1.88	2.45 ± 0.13	0.00 ± 0.00	35.18 ± 2.15
28-29	0.00 ± 0.00	27.20 ± 1.80	0.00 ± 0.00	0.00 ± 0.00	28.22 ± 1.61
29-30	0.00 ± 0.00	23.30 ± 1.44	0.00 ± 0.00	0.00 ± 0.00	32.09 ± 2.19
30-31	ND	ND	ND	ND	ND
31-32	ND	ND	ND	ND	ND
32-33	ND	ND	ND	ND	ND
33-34	ND	ND	ND	ND	ND
34-35	ND	ND	ND	ND	ND
35-36	ND	ND	ND	ND	ND
36-37	ND	ND	ND	ND	ND
37-38	ND	ND	ND	ND	ND
38-39	ND	ND	ND	ND	ND

TC2B-B-14V

Interval	¹³⁷ Cs	²¹⁰ Pb _{Tot}	²¹⁰ Pb _{XS}	⁷ Be	²²⁶ Ra
(cm)	(Bq/kg)	(Bq/kg)	(Bq/kg)	(Bq/kg)	(Bq/kg)
39-40	ND	ND	ND	ND	ND
40-41	ND	ND	ND	ND	ND
41-42	ND	ND	ND	ND	ND
42-43	ND	ND	ND	ND	ND
43-44	ND	ND	ND	ND	ND
44-45	ND	ND	ND	ND	ND
45-46	ND	ND	ND	ND	ND
46-47	ND	ND	ND	ND	ND
47-48	ND	ND	ND	ND	ND
48-49	ND	ND	ND	ND	ND
49-50	ND	ND	ND	ND	ND

TC5-B-14V

Interval	¹³⁷ Cs	²¹⁰ Pb _{Tot}	²¹⁰ Pb _{xS}	⁷ Be	²²⁶ Ra
(cm)	(Bq/kg)	(Bq/kg)	(Bq/kg)	(Bq/kg)	(Bq/kg)
0-1	14.21 ± 0.80	217.35 ± 13.43	68.39 ± 3.97	0.00 ± 0.00	218.29 ± 11.35
1-2	12.21 ± 0.72	229.63 ± 12.83	80.66 ± 3.36	0.00 ± 0.00	402.50 ± 20.78
2-3	23.99 ± 1.83	271.91 ± 15.34	122.95 ± 5.88	0.00 ± 0.00	242.20 ± 12.53
3-4	15.15 ± 0.81	224.85 ± 14.38	75.88 ± 4.92	0.00 ± 0.00	116.31 ± 6.38
4-5	6.81 ± 0.42	232.41 ± 15.17	83.45 ± 5.71	0.00 ± 0.00	295.17 ± 15.36
5-6	10.12 ± 0.69	234.89 ± 14.74	85.92 ± 5.27	0.00 ± 0.00	204.65 ± 10.63
6-7	9.44 ± 0.50	200.36 ± 10.34	51.40 ± 0.87	0.00 ± 0.00	349.93 ± 18.00
7-8	11.88 ± 0.80	183.94 ± 12.85	34.97 ± 3.38	0.00 ± 0.00	226.83 ± 11.63
8-9	12.31 ± 0.75	216.57 ± 14.33	67.61 ± 4.86	0.00 ± 0.00	188.09 ± 9.93
9-10	4.67 ± 0.33	169.14 ± 10.88	20.17 ± 1.41	0.00 ± 0.00	378.36 ± 19.48
10-11	7.52 ± 0.50	156.13 ± 9.35	7.16 ± 0.12	0.00 ± 0.00	234.80 ± 12.05
11-12	5.98 ± 0.47	175.87 ± 10.62	26.91 ± 1.15	0.00 ± 0.00	250.65 ± 12.91
12-13	2.38 ± 0.25	173.04 ± 10.16	24.07 ± 0.69	0.00 ± 0.00	453.53 ± 23.25
13-14	4.22 ± 0.32	183.77 ± 12.52	34.80 ± 3.05	0.00 ± 0.00	354.05 ± 18.06
14-15	3.01 ± 0.24	148.42 ± 9.07	0.00 ± 0.00	0.00 ± 0.00	455.26 ± 23.21
15-16	1.78 ± 0.15	155.36 ± 9.79	6.39 ± 0.32	0.00 ± 0.00	363.62 ± 18.40
16-17	0.00 ± 0.00	131.07 ± 8.55	0.00 ± 0.00	0.00 ± 0.00	501.37 ± 25.36
17-18	0.00 ± 0.00	123.89 ± 8.97	0.00 ± 0.00	0.00 ± 0.00	261.52 ± 13.29
18-19	0.00 ± 0.00	106.59 ± 6.81	0.00 ± 0.00	0.00 ± 0.00	337.99 ± 17.05
19-20	0.00 ± 0.00	112.47 ± 7.92	0.00 ± 0.00	0.00 ± 0.00	340.08 ± 17.42
20-21	0.00 ± 0.00	110.58 ± 6.35	0.00 ± 0.00	0.00 ± 0.00	255.86 ± 13.04
21-22	1.75 ± 0.12	108.06 ± 7.59	0.00 ± 0.00	0.00 ± 0.00	268.76 ± 13.61
22-23	0.00 ± 0.00	121.66 ± 7.97	0.00 ± 0.00	0.00 ± 0.00	218.19 ± 11.07
23-24	1.63 ± 0.09	130.48 ± 8.13	0.00 ± 0.00	0.00 ± 0.00	338.69 ± 18.39
24-25	0.00 ± 0.00	116.39 ± 8.65	0.00 ± 0.00	0.00 ± 0.00	227.16 ± 11.76
25-26	1.82 ± 0.15	163.62 ± 10.70	14.65 ± 1.23	0.00 ± 0.00	253.70 ± 12.90
26-27	0.00 ± 0.00	161.11 ± 10.31	12.14 ± 0.84	0.00 ± 0.00	230.75 ± 11.95
27-28	0.00 ± 0.00	170.61 ± 10.54	21.65 ± 1.08	0.00 ± 0.00	295.35 ± 15.15
28-29	0.00 ± 0.00	58.31 ± 3.88	0.00 ± 0.00	0.00 ± 0.00	144.26 ± 7.88
29-30	0.00 ± 0.00	103.78 ± 7.06	0.00 ± 0.00	0.00 ± 0.00	250.05 ± 13.25
30-31	ND	51.82 ± 3.41	0.00 ± 0.00	ND	ND
31-32	ND	70.65 ± 5.08	0.00 ± 0.00	ND	ND
32-33	ND	132.07 ± 9.35	0.00 ± 0.00	ND	ND
33-34	ND	176.22 ± 10.08	0.00 ± 0.00	ND	ND
34-35	ND	118.29 ± 7.65	0.00 ± 0.00	ND	ND
35-36	ND	148.94 ± 8.00	0.00 ± 0.00	ND	ND
36-37	ND	207.68 ± 11.52	58.71 ± 2.06	ND	ND
37-38	ND	245.79 ± 16.26	96.83 ± 6.80	ND	ND
38-39	ND	179.40 ± 12.19	30.43 ± 2.72	ND	ND

TC5-B-14V

Interval	¹³⁷ Cs	²¹⁰ Pb _{Tot}	²¹⁰ Pb _{XS}	⁷ Be	²²⁶ Ra
(cm)	(Bq/kg)	(Bq/kg)	(Bq/kg)	(Bq/kg)	(Bq/kg)
39-40	ND	200.72 ± 13.13	51.75 ± 3.66	ND	ND
40-41	ND	185.07 ± 9.55	36.10 ± 0.08	ND	ND
41-42	ND	114.91 ± 7.35	0.00 ± 0.00	ND	ND
42-43	ND	178.55 ± 10.21	29.59 ± 0.74	ND	ND
43-44	ND	110.34 ± 7.85	0.00 ± 0.00	ND	ND
44-45	ND	129.23 ± 6.99	0.00 ± 0.00	ND	ND
45-46	ND	117.85 ± 8.20	0.00 ± 0.00	ND	ND
46-47	ND	149.68 ± 8.85	0.00 ± 0.00	ND	ND
47-48	ND	187.30 ± 11.50	38.34 ± 2.03	ND	ND
48-49	ND	153.75 ± 9.86	4.78 ± 0.39	ND	ND
49-50	ND	136.25 ± 8.92	0.00 ± 0.00	ND	ND

MB6-B-15V

Interval	¹³⁷ Cs	²¹⁰ Pb _{Tot}	²¹⁰ Pb _{XS}	⁷ Be	²²⁶ Ra
(cm)	(Bq/kg)	(Bq/kg)	(Bq/kg)	(Bq/kg)	(Bq/kg)
0-1	10.61 ± 0.63	115.28 ± 7.94	77.60 ± 5.56	0.00 ± 0.00	94.55 ± 5.33
1-2	13.18 ± 0.96	91.01 ± 5.66	53.33 ± 3.28	0.00 ± 0.00	129.23 ± 7.14
2-3	13.16 ± 0.97	86.90 ± 4.84	49.23 ± 2.45	0.00 ± 0.00	118.32 ± 6.66
3-4	10.28 ± 0.72	84.58 ± 4.42	46.90 ± 2.04	0.00 ± 0.00	90.74 ± 4.93
4-5	6.94 ± 0.38	82.47 ± 5.52	44.80 ± 3.14	0.00 ± 0.00	134.90 ± 7.29
5-6	13.10 ± 0.74	74.33 ± 4.34	36.65 ± 1.96	0.00 ± 0.00	97.32 ± 5.22
6-7	10.89 ± 0.71	74.10 ± 4.49	36.43 ± 2.11	0.00 ± 0.00	80.71 ± 4.72
7-8	13.14 ± 0.71	77.43 ± 4.63	39.76 ± 2.25	0.00 ± 0.00	95.21 ± 5.19
8-9	14.76 ± 0.83	64.96 ± 4.10	27.28 ± 1.72	0.00 ± 0.00	95.84 ± 5.18
9-10	14.65 ± 0.83	68.55 ± 4.21	30.87 ± 1.82	0.00 ± 0.00	98.14 ± 5.30
10-11	10.26 ± 0.63	68.75 ± 4.82	31.07 ± 2.44	0.00 ± 0.00	91.60 ± 4.92
11-12	6.25 ± 0.35	66.03 ± 4.82	28.36 ± 2.43	0.00 ± 0.00	160.74 ± 8.58
12-13	11.07 ± 0.74	71.50 ± 4.88	33.82 ± 2.49	0.00 ± 0.00	93.81 ± 4.95
13-14	10.76 ± 0.70	74.76 ± 5.36	37.09 ± 2.98	0.00 ± 0.00	111.36 ± 5.91
14-15	11.62 ± 0.65	66.48 ± 4.04	28.81 ± 1.66	0.00 ± 0.00	115.53 ± 6.11
15-16	7.82 ± 0.51	89.77 ± 5.24	52.09 ± 2.86	0.00 ± 0.00	112.22 ± 6.06
16-17	6.56 ± 0.54	73.32 ± 5.12	35.64 ± 2.74	0.00 ± 0.00	106.78 ± 5.74
17-18	3.18 ± 0.23	61.20 ± 3.93	23.52 ± 1.54	0.00 ± 0.00	85.95 ± 4.41
18-19	1.49 ± 0.10	63.67 ± 4.07	25.99 ± 1.68	0.00 ± 0.00	142.02 ± 7.24
19-20	1.61 ± 0.10	43.82 ± 2.62	6.15 ± 0.24	0.00 ± 0.00	80.51 ± 4.13
20-21	0.00 ± 0.00	45.50 ± 2.44	7.83 ± 0.06	0.00 ± 0.00	77.78 ± 4.01
21-22	0.00 ± 0.00	37.95 ± 2.22	0.27 ± 0.16	0.00 ± 0.00	63.43 ± 3.35
22-23	0.00 ± 0.00	34.27 ± 1.87	0.00 ± 0.00	0.00 ± 0.00	46.98 ± 2.69
23-24	0.00 ± 0.00	28.36 ± 1.73	0.00 ± 0.00	0.00 ± 0.00	80.43 ± 4.76
24-25	0.00 ± 0.00	34.13 ± 1.96	0.00 ± 0.00	0.00 ± 0.00	39.93 ± 2.11
25-26	0.00 ± 0.00	33.49 ± 2.08	0.00 ± 0.00	0.00 ± 0.00	49.68 ± 2.93
26-27	0.00 ± 0.00	32.19 ± 1.97	0.00 ± 0.00	0.00 ± 0.00	0.00 ± 0.00
27-28	0.00 ± 0.00	30.83 ± 1.69	0.00 ± 0.00	0.00 ± 0.00	0.00 ± 0.00
28-29	0.00 ± 0.00	40.14 ± 2.72	2.46 ± 0.34	0.00 ± 0.00	0.00 ± 0.00
29-30	0.00 ± 0.00	35.37 ± 2.13	0.00 ± 0.00	0.00 ± 0.00	0.00 ± 0.00
30-31	ND	35.89 ± 2.25	0.00 ± 0.00	ND	ND
31-32	ND	32.11 ± 2.09	0.00 ± 0.00	ND	ND
32-33	ND	28.98 ± 1.90	0.00 ± 0.00	ND	ND
33-34	ND	36.42 ± 2.12	0.00 ± 0.00	ND	ND
34-35	ND	33.66 ± 2.12	0.00 ± 0.00	ND	ND
35-36	ND	33.64 ± 2.25	0.00 ± 0.00	ND	ND
36-37	ND	28.20 ± 1.58	0.00 ± 0.00	ND	ND
37-38	ND	35.32 ± 2.33	0.00 ± 0.00	ND	ND
38-39	ND	34.39 ± 1.79	0.00 ± 0.00	ND	ND

MB6-B-15V

Interval	¹³⁷ Cs	²¹⁰ Pb _{Tot}	²¹⁰ Pb _{xs}	⁷ Be	²²⁶ Ra
(cm)	(Bq/kg)	(Bq/kg)	(Bq/kg)	(Bq/kg)	(Bq/kg)
39-40	ND	38.39 ± 2.49	0.71 ± 0.11	ND	ND
40-41	ND	38.21 ± 2.16	0.53 ± 0.22	ND	ND
41-42	ND	34.62 ± 2.02	0.00 ± 0.00	ND	ND
42-43	ND	27.63 ± 1.80	0.00 ± 0.00	ND	ND
43-44	ND	34.30 ± 1.99	0.00 ± 0.00	ND	ND
44-45	ND	32.20 ± 1.85	0.00 ± 0.00	ND	ND
45-46	ND	38.92 ± 2.35	1.25 ± 0.03	ND	ND
46-47	ND	35.86 ± 2.44	0.00 ± 0.00	ND	ND
47-48	ND	39.37 ± 2.38	1.69 ± 0.03	ND	ND
48-49	ND	36.56 ± 2.35	0.00 ± 0.00	ND	ND
49-50	ND	33.90 ± 2.00	0.00 ± 0.00	ND	ND

MQ1-A-14V

Origin	Longitude	Latitude	SOURCE	Description		
Pre-SRS	-81.627835	33.312342	GPS 76S	Rd Crossing, abandoned		
Pre-SRS	-81.630290	33.292206	GPS 76S	Rd Crossing, abandoned		
Pre-SRS	-81.625949	33.288855	GPS 76S	Rd Crossing, abandoned		
Pre-SRS	-81.624674	33.289357	GPS 76S	Rd Crossing, active		
Pre-SRS	-81.619161	33.290287	GPS 76S	Rd Crossing, active		
Pre-SRS	-81.624640	33.313116	GPS 76S	Rd Crossing, active		
Pre-SRS	-81.631851	33.307614	GPS 76S	Rd Crossing, active		
Pre-SRS	-81.627071	33.294054	GPS 76S	Levee		
Pre-SRS	-81.623435	33.291772	GPS 76S	Rd Crossing, abandoned		
Pre-SRS	-81.631764	33.307388	GPS 76S	Levee		
Pre-SRS	-81.635939	33.314412	GPS 76S	Levee		
Pre-SRS	-81.628026	33.316508	GPS 76S	Obstruction		
Pre-SRS	-81.618129	33.303876	GPS 76S	Obstruction		
Pre-SRS	-81.626361	33.304448	GPS 76S	Rd Crossing, abandoned		
Pre-SRS	-81.630083	33.309751	GPS 76S	Rd Crossing, active		
Pre-SRS	-81.618073	33.294487	GPS 76S	Rd Crossing, active		
Pre-SRS	-81.610154	33.298558	GPS 76S	Rd Crossing, active		
Pre-SRS	-81.634261	33.319071	LiDAR	Rd Crossing, abandoned		
Pre-SRS	-81.631423	33.316813	LiDAR	Rd Crossing, abandoned		
Pre-SRS	-81.626733	33.316918	LiDAR	Rd Crossing, abandoned		
Pre-SRS	-81.633185	33.313886	LiDAR	Rd Crossing, abandoned		
Pre-SRS	-81.638443	33.309915	LiDAR	Rd Crossing, active		
Pre-SRS	-81.635611	33.307549	LiDAR	Rd Crossing, abandoned		
Pre-SRS	-81.619561	33.301765	LiDAR	Rd Crossing, abandoned		
Pre-SRS	-81.626559	33.305077	LiDAR	Rd Crossing, abandoned		
Pre-SRS	-81.614286	33.305979	LiDAR	Rd Crossing, abandoned		
SRS	-81.615703	33.305629	GPS 76S	Rd Crossing, abandoned		
SRS	-81.624477	33.291821	GPS 76S	Rd Crossing, active		
SRS	-81.628834	33.294333	GPS 76S	Rd Crossing, active		
SRS	-81.634457	33.290652	GPS 76S	Rd Crossing, active		
SRS	-81.637320	33.306368	GPS 76S	Rd Crossing, active		
SRS	-81.620874	33.304791	GPS 76S	Rd Crossing, active		
SRS	-81.635113	33.292272	GPS 76S	RR Crossing, active		
SRS	-81.634252	33.289092	GPS 76S	RR Crossing, active		
SRS	-81.633949	33.288841	GPS 76S	RR Crossing, active		
SRS	-81.635574	33.296653	GPS 76S	Levee		
SRS	-81.634577	33.296893	GPS 76S	Levee		
SRS	-81.633463	33.291415	GPS 76S	Levee		
SRS	-81.633533	33.295040	GPS 76S	Levee		
SRS	-81.632610	33.293782	GPS 76S	Obstruction		

MQ1-A-14V

Origin	Longitude	Latitude	SOURCE	Description
SRS	-81.633014	33.293104	GPS 76S	Obstruction
SRS	-81.634214	33.292710	GPS 76S	Rip rap
SRS	-81.634939	33.293554	GPS 76S	RR Crossing, active
SRS	-81.634006	33.292179	GPS 76S	Rip rap
SRS	-81.634285	33.290689	GPS 76S	Rip rap
SRS	-81.633532	33.288979	GPS 76S	Rip rap
SRS	-81.635926	33.296264	GPS 76S	Rip rap
SRS	-81.633487	33.288790	GPS 76S	Rip rap
SRS	-81.633740	33.291088	GPS 76S	Rip rap
SRS	-81.633340	33.289232	GPS 76S	Rip rap
SRS	-81.632977	33.292463	GPS 76S	Rip rap
SRS	-81.634242	33.292222	GPS 76S	Utilities crossing
SRS	-81.631646	33.286598	GPS 76S	Utilities crossing
SRS	-81.635180	33.297061	GPS 76S	Culvert
SRS	-81.636742	33.297703	GPS 76S	Culvert
SRS	-81.634552	33.308204	GPS 76S	Culvert
SRS	-81.635543	33.284955	GPS 76S	Outfall
SRS	-81.635229	33.290504	GPS 76S	Outfall
SRS	-81.632957	33.303071	GPS 76S	Outfall
SRS	-81.633159	33.302835	GPS 76S	Outfall
SRS	-81.635504	33.287002		
SRS	-81.635753	33.287272	GPS 76S	Outfall
SRS	-81.634382	33.289281	GPS 76S	Outfall
SRS	-81.636196	33.306816	GPS 76S	Outfall
SRS	-81.636059	33.296813	GPS 76S	Outfall
SRS	-81.633003	33.285653	GPS 76S	Waste/runoff mgmt
SRS	-81.634582	33.296063	GPS 76S	Waste/runoff mgmt
SRS	-81.633598	33.295247	GPS 76S	Waste/runoff mgmt
SRS	-81.634714	33.296486	GPS 76S	Waste/runoff mgmt
SRS	-81.632021	33.293920	GPS 76S	Waste/runoff mgmt
SRS	-81.632959	33.294403	GPS 76S	Waste/runoff mgmt
SRS	-81.633170	33.293906	GPS 76S	Waste/runoff mgmt
SRS	-81.633637	33.293127	GPS 76S	Waste/runoff mgmt
SRS	-81.632876	33.294845	GPS 76S	Waste/runoff mgmt
SRS	-81.631416	33.295767	Lidar	Rd Crossing, active
SRS	-81.633466	33.291802	GPS 76S	Rip rap
SRS	-81.632962	33.291886	GPS 76S	Ground disturbance
SRS	-81.627344	33.312660	GPS 76S	Fire lane
SRS	-81.618591	33.294755	GPS 76S	Rd Crossing, abandoned
SRS	-81.626322	33.288510	GPS 76S	Rd Crossing, abandoned

MQ1-A-14V

Origin	Longitude	Latitude	SOURCE	Description
SRS	-81.631176	33.285509	GPS 76S	Fire lane
SRS	-81.633408	33.291946	Lidar	Levee
SRS	-81.617982	32 33.286974 LiDAR Rd Crossing, ac		Rd Crossing, active
SRS	-81.635384	33.291464	LiDAR	RR Crossing, active

U10-B-14V

, active
inactive
inactive
inactive
II
1

TC2A-B-14V and TC2B-B-14V

Origin	Longitude	Latitude	SOURCE	Description	
Pre-SRS	-81.517530	33.357362	GPS 76CSX	Rd Crossing, abandoned	
Pre-SRS	-81.519451	33.365977	GPS 76S	Levee	
Pre-SRS	-81.517446	33.357742	GPS 76S	Levee	
Pre-SRS	-81.513143	33.355207	GPS 76S	Levee	
Pre-SRS	-81.517327	33.348578	GPS 76S	Rd Crossing, abandoned	
Pre-SRS	-81.519463	33.366480	LiDAR	Rd Crossing, abandoned	
Pre-SRS	-81.517379	33.347292	LiDAR	Rd Crossing, active	
Pre-SRS	-81.519511	33.346713	LiDAR	Rd Crossing, abandoned	

TC5-B-14V

Origin	Longitude	Latitude	SOURCE	Description	
Pre-SRS	-81.549709	33.369176	GPS 76CSX Levee		
Pre-SRS	-81.527324	33.370193	GPS 76CSX	Levee	
Pre-SRS	-81.550802	33.370389	GPS 76CSX	Levee	
Pre-SRS	-81.550261	33.369877	GPS 76CSX	Rd Crossing, abandoned	
Pre-SRS	-81.555100	33.390375	GPS 76S	Rd Crossing, abandoned	
Pre-SRS	-81.549921	33.371915	LiDAR	Rd Crossing, active	
Pre-SRS	-81.551294	33.375354	LiDAR	Rd Crossing, abandoned	
Pre-SRS	-81.555943	33.391021	GPS 76S	Fire lane	

MBM-A-14V and ODB-1B-14V

-				SOURCE Description			
_	Origin				Description		
	SRS	-81.582654	33.168493	GPS_76S	Root dam		
	SRS	-81.584858	33.170282	LiDAR	RR Crossing, active		
	SRS	-81.626734	33.149267	LiDAR	Levee		
	SRS	-81.553579	33.224128	224128 GPS_78S Culvert			
	SRS	-81.552748	33.222319	LiDAR	Culvert		
	SRS	-81.570134	33.220941	GPS_76S	Rd Crossing, active		
	SRS	-81.573140	33.219420	GPS_76S	Rd Crossing, active		
	SRS	-81.568306	33.222049	GPS_76S	Rd Crossing, active		
	SRS	-81.573464	33.221376	GPS_76S	Culvert		
	SRS	-81.576833	33.224166	GPS_78S	Culvert		
	SRS	-81.571550	33.220200	GPS_78S	Rd Crossing, active		
	SRS	-81.571874	33.219804	GPS_78S	Levee		
	SRS	-81.563477	33.208640	GPS_76S	Obstruction		
	SRS	-81.562465	33.209437	GPS_78S	Rd Crossing, active		
	SRS	-81.588305	33.206936	LiDAR	Rd Crossing, active		
	SRS	-81.564924	33.181681	GPS_76S	RR Crossing, active		
	SRS	-81.553335	33.187768	GPS_76S	RR Crossing, active		
	SRS	-81.569369	33.178950	LiDAR	RR Crossing, active		
	SRS	-81.562006	33.183175	LiDAR	RR Crossing, active		
	SRS	-81.555880	33.186439	GPS_76CSX	RR Crossing, active		
	SRS	-81.571561	33.177944	GPS_76CSX	RR Crossing, active		
	SRS	-81.607694	33.168743	LiDAR	RR Crossing, active		
	SRS	-81.563884	33.180116	GPS_76S	Obstruction		
	Pre-SRS	-81.585330	33.170934	GPS_76S	Rd Crossing, abandoned		
	Pre-SRS	-81.568144	33.178618	GPS_76S	Levee		
	Pre-SRS	-81.600402	33.166803	GPS_76S	Levee		
	Pre-SRS	-81.577988	33.199463	GPS_76S	RR Crossing, active		
	Pre-SRS	-81.601012	33.166739	LiDAR	Rd Crossing, active		
	Pre-SRS	-81.581675	33.183711	LiDAR	Rd Crossing, active		
	Pre-SRS	-81.566170	33.206955	LiDAR	Rd Crossing, abandoned		
	Pre-SRS	-81.563786	33.208911	LiDAR	Rd Crossing, active		
	Pre-SRS	-81.580809	33.190729	LiDAR	Rd Crossing, abandoned		
	Pre-SRS	-81.590385	33.164903	LiDAR	Rd Crossing, abandoned		
	Pre-SRS	-81.571464	33.204328	GPS_76S	Rd Crossing, abandoned		
	Pre-SRS	-81.569708	33.206465	GPS_76CSX	Rd Crossing, active		
	Pre-SRS	-81.571346	33.204275	GPS_76S	Bricks-duplicate		
	Pre-SRS	-81.556448	33.213588	GPS_76S	Rd Crossing, active		
	Pre-SRS	-81.557903	33.212815	GPS_76S	Rd Crossing, active		
	Pre-SRS	-81.557896	33.219031	LiDAR	Rd Crossing, active		
	Pre-SRS	-81.557243	33.219025	LiDAR	Rd Crossing, active		

MBM-A-14V and ODB-1B-14V

Origin	Longitude	Latitude	SOURCE	Description
Pre-SRS	33.157809	-81.619481	LiDAR	Rd Crossing, abandoned
Pre-SRS	33.211625	-81.564400	LiDAR	Rd Crossing, active
Pre-SRS	33.204734	-81.573462	GPS_76S	Rd Crossing, active
Pre-SRS	33.203584	-81.573170	LiDAR	Rd Crossing, abandoned
Pre-SRS	33.209921	-81.572055	LiDAR	Rd Crossing, abandoned
Pre-SRS	33.204441	-81.576411	GPS_76S	Levee
Pre-SRS	33.205323	-81.576760	GPS_76S	Levee
Pre-SRS	33.202975	-81.575502	LiDAR	Rd Crossing, active
Pre-SRS	33.210060	-81.580173	LiDAR	Rd Crossing, active
Pre-SRS	33.207799	-81.578673	LiDAR	Rd Crossing, abandoned
Pre-SRS	33.208929	-81.579187	GPS_76CSX	Levee
Pre-SRS	33.195218	-81.581251	LiDAR	Rd Crossing, active
Pre-SRS	33.204125	-81.584757	LiDAR	Rd Crossing, abandoned
Pre-SRS	33.205956	-81.586754	LiDAR	Rd Crossing, abandoned
Pre-SRS	33.188222	-81.583299	LiDAR	Rd Crossing, active
Pre-SRS	33.191745	-81.589122	LiDAR	Rd Crossing, abandoned
Pre-SRS	33.194303	-81.590534	LiDAR	Rd Crossing, abandoned
Pre-SRS	33.192068	-81.589150	GPS_76CSX	Levee
Pre-SRS	33.187557	-81.551961	GPS_76S	Rd Crossing, active
Pre-SRS	33.185009	-81.552985	GPS_76S	Rd Crossing, active
Pre-SRS	33.173632	-81.555477	GPS_76S	Rd Crossing, active
Pre-SRS	33.170989	-81.549551	GPS_76S	Rd Crossing, active
Pre-SRS	33.170324	-81.546015	LiDAR	Rd Crossing, active
Pre-SRS	33.177670	-81.578049	GPS_76S	Levee
Pre-SRS	33.178907	-81.577778	GPS_76S	Rd Crossing, abandoned
Pre-SRS	33.168393	-81.582870	LiDAR	Rd Crossing, abandoned
Pre-SRS	33.168683	-81.582526	GPS_76S	Rd Crossing, abandoned
Pre-SRS	33.168275	-81.582963	GPS_76S	Culvertduplicate
Pre-SRS	33.165103	-81.588449	LiDAR	Levee
Pre-SRS	33.163803	-81.586603	LiDAR	Rd Crossing, abandoned
Pre-SRS	33.160140	-81.584732	GPS_76S	Rd Crossing, active
Pre-SRS	33.191387	-81.603445	GPS_76S	Rd Crossing, abandoned
Pre-SRS	33.177666	-81.609132	GPS_76S	Rd Crossing, active
Pre-SRS	33.169191	-81.607718	Lidar	Rd Crossing, active
Pre-SRS	33.169900	-81.607709	LiDAR	Rd Crossing, active

MCE-A-14V

Origin	in Longitude Latitude SOURCE Description		Description	
Pre-SRS	33.292572	-81.588697	GPS_76S	Rd Crossing, abandoned
Pre-SRS	33.321197	-81.593369	GPS_76S	Rd Crossing, abandoned
Pre-SRS	33.317358	-81.585136	GPS_76S	Levee
Pre-SRS	33.332586	-81.607093	GPS_76S	Levee
Pre-SRS	33.304611	-81.583536	GPS_76S	Rd Crossing, abandoned
Pre-SRS	33.333224	-81.608145	LiDAR	Rd Crossing, active
Pre-SRS	33.298462	-81.588854	GPS_76S	Side levee
Pre-SRS	33.317618	-81.585406	GPS_76S	Rd Crossing, abandoned
Pre-SRS	33.290646	-81.589768	GPS_76S	Side levee
Pre-SRS	33.302389	-81.591878	GPS_76S	Rd Crossing, abandoned
Pre-SRS	33.301872	-81.590596	GPS_76S	Obstruction
Pre-SRS	33.295036	-81.599787	GPS_76S	Rd Crossing, abandoned
Pre-SRS	33.296078	-81.593640	Lidar	Rd Crossing, abandoned
Pre-SRS	33.302222	-81.573713	GPS_76S	Rd Crossing, abandoned
Pre-SRS	33.304314	-81.575779	GPS_76S	Obstruction
Pre-SRS	33.304079	-81.575702	GPS_76S	Rd Crossing, abandoned
Pre-SRS	33.306293	-81.572859	GPS_76S	Levee
Pre-SRS	33.306199	-81.568880	LiDAR	Rd Crossing, active
Pre-SRS	33.318285	-81.583627	GPS_76S	Rd Crossing, abandoned
Pre-SRS	33.318155	-81.584453	GPS_76S	Rd Crossing, abandoned
Pre-SRS	33.317371	-81.570547	GPS_76S	Rd Crossing, abandoned
Pre-SRS	33.318655	-81.581739	GPS_76S	Levee
Pre-SRS	33.323759	-81.604539	GPS_76S	Rd Crossing, abandoned
Pre-SRS	33.321288	-81.609463	Lidar	Rd Crossing, active
Pre-SRS	33.331241	-81.607320	GPS_76S	Rd Crossing, abandoned
Pre-SRS	33.276116	-81.587716	GPS_76S	Rd Crossing, active
Pre-SRS	33.278603	-81.592050	GPS_76S	Rd Crossing, active
Pre-SRS	33.276731	-81.589267	GPS_76S	Rd Crossing, active
Pre-SRS	33.276356	-81.595890	GPS_76S	Levee
Pre-SRS	33.276391	-81.596137	GPS_76S	Levee
Pre-SRS	33.283861	-81.588241	GPS_76S	Levee
Pre-SRS	33.280118	-81.586940	Lidar	Rd Crossing, abandoned
SRS	33.320454	-81.592204	GPS_76S	Rd Crossing, active
SRS	33.314736	-81.584463	GPS_76S	Utilities crossing
SRS	33.290085	-81.593083	Lidar	Rd Crossing, active
SRS	33.294970	-81.598552	Lidar	Rd Crossing, active
SRS	33.293857	-81.576236	GPS_76S	Rd Crossing, active
SRS	33.292698	-81.575337	GPS_76S	Rd Crossing, active
SRS	33.302544	-81.574231	GPS_76S	Levee
SRS	33.302571	-81.574145	GPS_76S	Rd Crossing, active

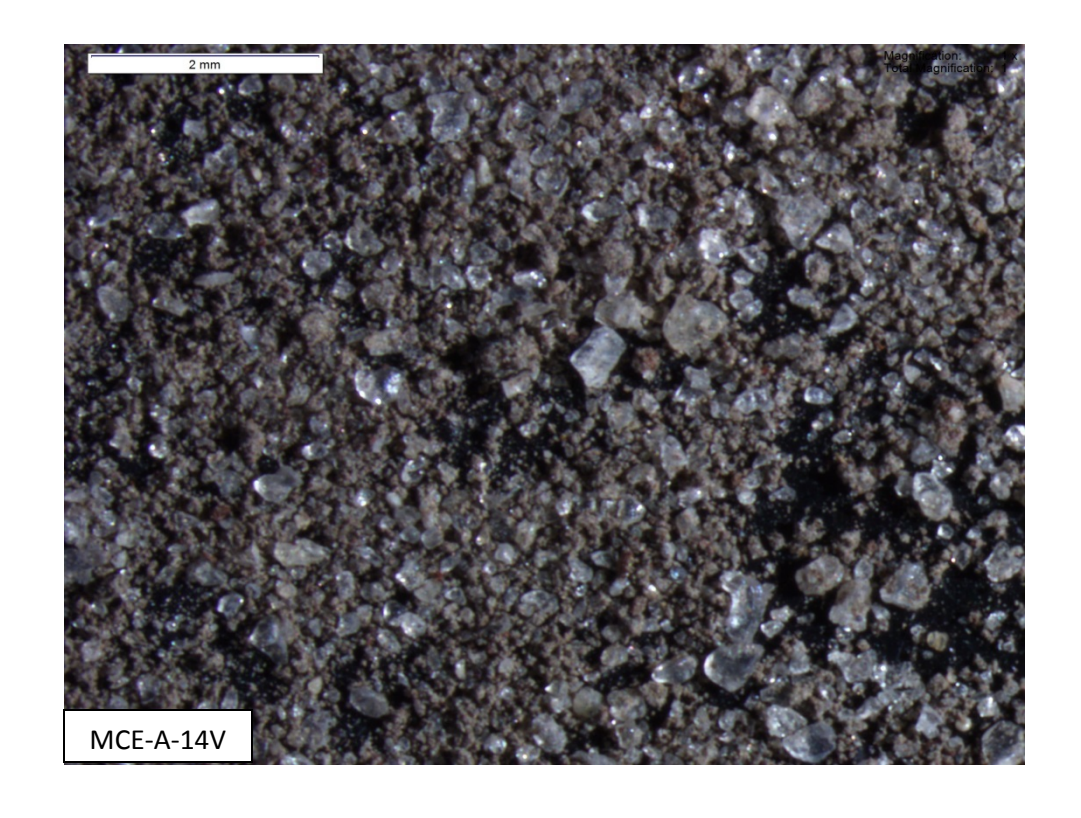
MCE-A-14V

Origin	in Longitude Latitude		SOURCE	Description
SRS	33.316024	-81.561406	GPS_76S	Rd Crossing, abandoned
SRS	33.315227	-81.559497	Lidar	Rd Crossing, active
SRS	33.278371	-81.585670	GPS_76S	Rd Crossing, active
SRS	33.278208	-81.583929	GPS_76S	Rd Crossing, active
SRS	33.278749	-81.583976	GPS_76S	Rd Crossing, active
SRS	33.276279	-81.583658	GPS_76S	Rd Crossing, active
SRS	33.278407	-81.585659	GPS_76S	Rd Crossing, active
SRS	33.273555	-81.593315	GPS_76S	Rd Crossing, active
SRS	33.277059	-81.594951	Lidar	Rd Crossing, active
SRS	33.278191	-81.583800	GPS_76S	Culvert
SRS	33.279997	-81.585165	GPS_76S	Culvert
SRS	33.274751	-81.582575	GPS_76S	Culvert
SRS	33.284655	-81.590244	GPS_76S	Obstruction
SRS	33.287873	-81.590560	Lidar	Rd Crossing, active
SRS	33.285021	-81.589942	Lidar	Rd Crossing, active
SRS	33.278875	-81.585942	GPS_76S	Basin

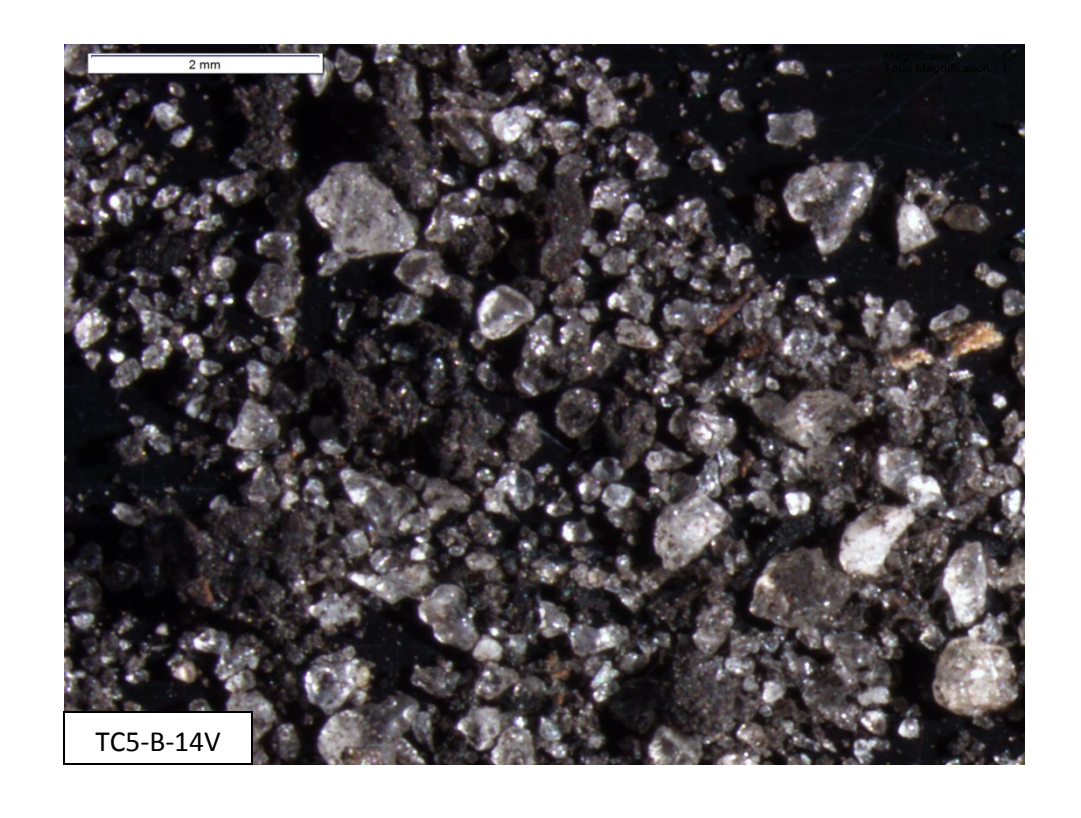
Stream Feature	McQueen Branch	Upper Three Runs-10	Meyers Branch	Meyers Branch-6	Tinker Creek-2	Tinker Creek-5	Mill Creek
Drainage Area (km²)	11.588	0.277	49.692	12.701	6.645	3.384	23.443
Drainage Perimeter (km)	16.218	2.546	37.981	18.499	13.844	9.489	28.025
Cumulative Stream Length (km)	10.403	0.528	34.607	4.139	6.785	2.812	20.387
Base Flow Discharge (m ³ /sec.)	0.0613	0.0045	0.2095	0.0326	0.0858	0.0438	0.2844
Drainage Density (km/km²)	0.898	1.904	0.696	0.326	1.021	0.831	0.87
Basin Length (km)	4.493	0.831	11.021	4.877	3.003	3.3	7.523
Drainage Shape	0.574	0.402	0.409	0.534	0.737	0.311	0.414
Stream Length (km)	5.197	0.473	11.221	2.915	2.915	2.679	9.363
Highest Point (m)	105	84	103	103	108	120	105
Elevation at 85% (m)	63	49	42	59	75	77	64
Elevation at 10% (m)	47	42	34	49	67	62	52
Mouth Elevation (m)	46	42	32	47	66	61	51
Basin Relief (m)	59	42	71	56	42	59	54
Basin Relief Ratio	13	51	6	12	14	18	7
Entire Stream Gradient (m/km)	4	20	1	5	4	8	2
Sinuosity	1.493	1.254	1.416	1.277	1.317	1.232	1.509
Cum. Intermittent Length (km)	2.951	0.519	4.51	0.232	0.247	0.202	5.126
Main Intermittent Length (km)	0	0.109	0.022	0.049	0	0.037	0.354







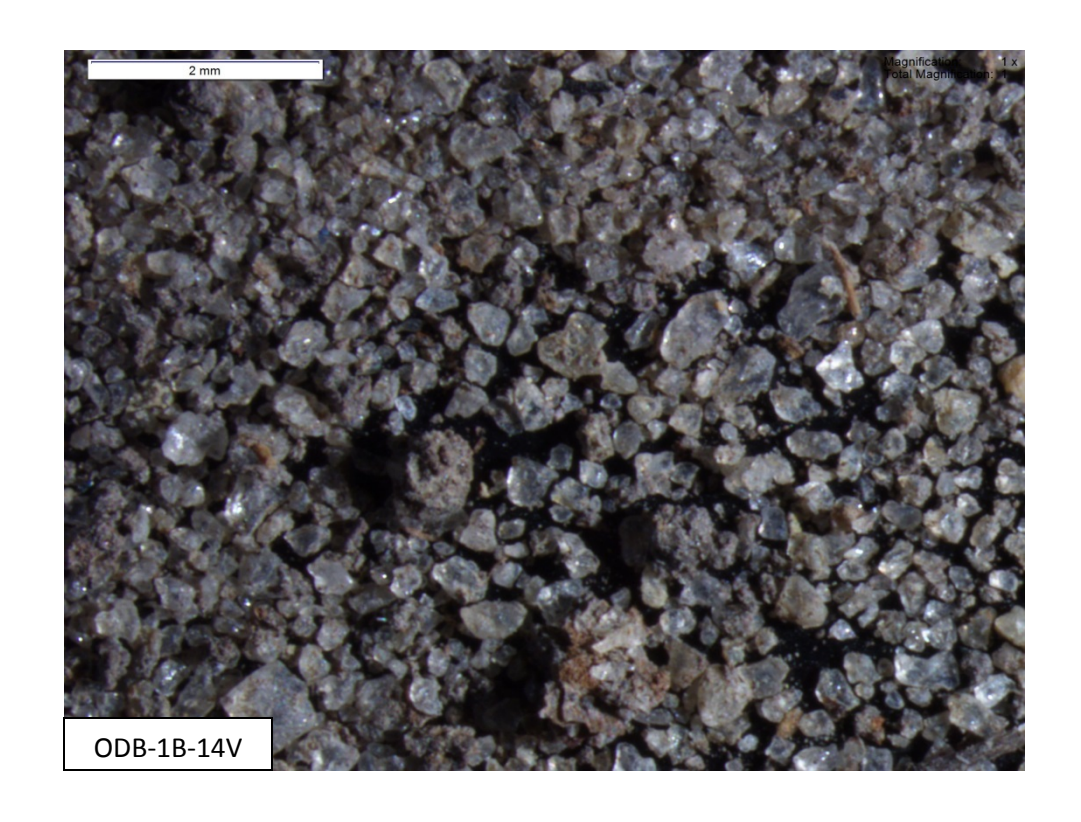












REFERENCES

Aber, J., McDowell, W., Nadelhoffer, K., Magill, A., Berntson, G., Kamakea, M., McNulty, S., Currie, W., Rustad, L., Fernandez, I., 1989. Nitrogen saturation in temperate forest ecosystems. *BioScience* 48: 921-934.

Aber, J.D., Driscoll, C.T., 1997. Effects of land use, climate variation, and N deposition on N cycling and C storage in northern hardwood forests. *Global Biochemical Cycles* 11: 639-648.

Abernathy, C., 1990. The use of river and reservoir sediment data for the study of regional soil erosion rates and trends. International Symposium on Water Erosion, Sedimentation and Resource Conservation (Dehradun, India).

Agarwal, C., Green, G.M., Grove, J.M., Evans, T.P., Schweik, C.M., 2002. A Review and Assessment of Land Use Change Models: Dynamics of Space, Time, and Human Choice. General Technical Report NE-297. Newton Square, PA: U.S. Department of Agriculture, Forest Service, Northeastern Research Station. 61 p.

Aiken, C.S., 1998. *The Cotton Plantation South Since the Civil War*. The John Hopkins University Press.

Allan, J.D., Erickson, D.L., Fay, J., 1997. The influence of catchment land use on stream integrity across multiple spatial scales. *Freshwater Biology* 37(1): 149-161.

Ambroise, B., 2004. Variable 'active' versus 'contributing' areas or periods: A necessary distinction. *Hydrological Processes* 18: 1,149-1,155.

Aspetsberger, F., Huber, F., Kargl, S., Scharinger, B., Peduzzi, P., Hein, T., 2002. Particulate organic matter dynamics in a river floodplain system: Impact of hydrological connectivity. *Archiv Fur Hydrobiologie* 156(1): 23-42.

Baskaran, M. *Handbook of Environmental Isotope Geochemistry*. Berlin: Springer, 2011. Pp. 305-331.

Baskaran, M., Coleman, C.H., Santschi, P.H., 1993. Atmospheric Depositional Fluxes of 7-Be and 210-Pb at Galveston and College Station, Texas. *J. Geophysical Research* 98: 20,555-20,571.

Beach T., 1998. Soil catenas, tropical deforestation, and ancient and contemporary soil erosion in the Peten, Guatemala. *Physical Geography*19: 378-405.

Blanton, P., Marcus, W.A., 2014. Roads, railroads, and floodplain fragmentation due to transportation infrastructure along rivers. *Annals of the Association of American Geographers* 104(3): 413-431.

Bracken, L.J., Croke, J., 2007. The concept of hydrological connectivity and its contribution to understanding runoff-dominated geomorphic systems. *Hydrological Processes* 21: 1,749-1,763.

Bracken, L.J., Wainwright, J., Ali, G.A., Tetzlaff, D., Smith, M.W., Reaney, S.M., Roy, A.G., 2013. Concepts of hydrological connectivity: Research approaches, pathways and future agendas. *Earth-Science Reviews* 119: 17-34.

Brierly, G.J., Fryirs, K., 1998. A fluvial sediment budget for upper Wolumla catchment, South Coast, N.S.W. *Australian Geographer* 29: 107-124.

Brooks, R.D., Crass, D.C., 1991. A desperate poor country: History and settlement patterning on the Savannah River Site, Aiken and Barnwell Counties, South Carolina. University of South Carolina, Columbia. pp. 51-54.

Brown, T. 1894. Memoirs of Tarleton Brown. People Press, Barnwell, SC. p.27.

Brune, G.M., 1953. Trap efficiency of reservoirs. *American Geophysical Union Transactions* 34: 407-418.

Burger, J., Gaines, K.E., Peles, J.D., Stephens Jr., W.L., Boring, C.S., Brisbin Jr., I.L., Snodgrass, J., Bryan, A.L., Smith, M.H., Gochfeld, M., 2001. Radiocesium in fish from the

Savannah River and Steel Creek: Potential food chain exposure to the public. *Risk Analysis* 21: 545-559.

Burgess, O.T., Pine III, W.E., Walsh, S.J., 2013. Importance of floodplain connectivity to fish populations in the Apalachicola River, Florida. *River Research and Applications* 29: 718-733.

Chang, M., Roth, F.A., Hurst, E.V., 1982. Sediment production under various forest site conditions. In Recent developments in the explanation and prediction of erosion and sediment yield. LAHS Publication 137: 13-22.

Chapin III, G.S., Walker, B.H., Hobbs, R.J., Hooper, D.U., Lawton, G.H., Sala, O.E., Tilman, D., 1997. Biotic control over the functioning of ecosystems. *Science* 277: 500-504.

Church, M., Hassan, M.A., Wolcott, J.F., 1988. Stabilizing self-organized structures in gravel-bed stream channels: Field and experimental observations. *Water Resources Research* 34: 3,169-3,179.

Clarke, S.J., 2014. Conserving freshwater biodiversity: The value, status, and management of high quality ditch systems. *J. for Nature Conservation* 24: 93-100.

Conner, W.H., Day, Jr., J.W., 1982. The ecology of forested wetlands in the southeastern United States. In B. Gopal, R.E. Turner, R.G. Wetzel, D.F. Whigham, editors. *Wetlands ecology and management*. National Institute of Ecology and International Scientific Publications, New Delhi, India.

Cowles, H.C., 1899. The ecological relations of vegetation on the sand dunes of Lake Michigan. *Botanical Gazette* 27: 95-117.

Corenblit, D., Tabacchi, E., Steiger, J., Gumell, A.M., 2007. Reciprocal interactions and adjustments between fluvial landforms and vegetation dynamics in river corridors: A review of complementary approaches. *Earth Science Reviews* 84: 56-86.

Craft, C.B. and Casey, W.P., 2000. Sediment and nutrient accumulation in floodplain and depressional freshwater wetlands of Georgia, USA. *Wetlands* 20: 323-332.

Davis, W.M., 1899. The geographical cycle. *Geographical J.* 14: 481-504.

Fletcher, D.E., Stillings, G.K., Barton, C.D., 2012. Stream System Field Condition Assessments – Level I Surveys. Savannah River Ecology Laboratory, University of Georgia.

Foster, D.R., Motzkin, G., Slater, B., 1998. Land-use history as long-term broad-scale disturbance: Regional forest dynamics in central New England. *Ecosystems* 1:96-119.

Foster, D., Swanson, F., Aber, J., Burke, I., Brokaw, N., Tilman, D., Knapp, A., 2003. The importance of land-use legacies to ecology and conservation. *BioScience* 51: 77-88.

Fredriksen, R.L., 1970. Erosion and sedimentation following road construction and timber harvest on unstable soils in three small western Oregon watersheds. U.S. Forest Service Research Paper, PNW 104.

Freeman, M.C., Pringle, C.M., Jackson, R.C., 2007. Hydraulic connectivity and the contribution of stream headwaters to ecological integrity at regional scales. *J. American Water Resources Association* 43(1): 5-14.

Fryirs, K., 2013. (Dis)Connectivity in catchment sediment cascades: A fresh look at the sediment delivery problem. *Earth Surface Processes and Landforms* 38: 30-46.

Fryirs, K., Brierly, G.J., 1998. The character and age structure of valley fills in Upper Wolumla Creek catchment, South Coast, New South Wales, Australia. *Earth Surface Processes and Landforms* 23: 271-287.

Fryirs, K., Brierly, G.J., 1999. Slope channel decoupling in Wolumla catchment, New South Wales, Australia: The changing nature of sediment sources following European settlement. *Catena* 35: 41-63.

Fryirs, K.A., Brierly, G.J., Preston, N.J., Kasai, M., 2007. Buffers, barriers and blankets: The (dis)connectivity of catchment-scale sediment cascades. *Catena* 70: 49-67.

Graf, W.L., 1999. Dam nation: A geographic census of American dams and their hydrologic impacts. *Water Resources Research* 35: 1,305-1,311.

Gregory, K.J., 1985. The Nature of Physical Geography. Arnold, London.

Griffiths, P.E., 2005. Review of 'niche construction'. Biology and Philosophy 20: 11-20.

Hancock, G.J., Wilkinson, S.N., Hawdon, A.A., Keen, R.J., 2013. Use of fallout tracers ⁷Be, ²¹⁰Pb and ¹³⁷Cs to distinguish the form of sub-surface soil erosion delivering sediment to rivers in large catchments. *Hydrological Processes* 28: 3,855-3,874.

Harvey, A.M., 2001. Coupling between hillslopes and channels in upland fluvial systems: Implications for landscape sensitivity illustrated from the Howgill Fells, northwest England. *Catena* 42: 225-250.

He, Q., Walling, D.E., 1996. Interpreting particle size effects in the adsorption of 137Cs and upsupported 210Pb by mineral soils and sediments. J. of Environmental Radioactivity 30: 117-137.

Hillier, S., 2001. Particulate composition and origin of suspended sediment in the R. Don, Aberdeenshire, UK. *Scienceof the Total Environment* 265:281–293.

Huntley, S.L., Wenning, R.J., Su, S.H., Bonnevie, N.L., Paustenbach, D.J., 1995.

Geochronology and sedimentology of the Lower Passaic River, New Jersey. *Estuaries* 18: 351-361.

Hupp, C.R., 1992. Riparian vegetation recovery patterns following streamchannelization: A geomorphic perspective. *Ecology* 73: 1,209–1,226.

Hupp, C.R., Pierce, A.R., Noe, G.B., 2009. Floodplain geomorphic processes and environmental impacts of human alteration along coastal plain rivers, USA. *Wetlands* 29: 413-429.

Jones, C.G., Lawton, J.H., Shachak, M., 1994. Organisms as ecosystem engineers. *Oikos* 69: 373-386.

Jones, C.G., Lawton, J.H., Shachak, M., 1997. Positive and negative effects of organisms as physical ecosystems engineers. *Ecology* 78: 1,946-1,957.

Kilgo, J., 2005. *Ecology and Management of a Forested Landscape: Fifty Years on the Savannah River Site*. Ed. John I. Blake. N.p.: Island.

Kleiss, B. A., 1996. Sediment retention in a bottomland hardwood wetland in eastern Arkansas. *Wetlands* 16:321–333.

Knapp, A.K., Blair, J.M., Briggs, J.M., Collins, S.L., Hartnett, D.C., Johnson, L.C., Towne, E.G., 1999. The keystone role of bison in North American tallgrass prairie. *BioScience* 49: 39-50.

Krishnaswami, S., Benninger, L.K., Aller, R.C., Von Damm, K.L., 1980. Atmospherically-derived radionuclides as tracers of sediment mixing and accumulation in near-shore marine and lake sediments: Evidence from ⁷Be, ²¹⁰Pb, and ^{239,240}Pu. *Earth and Planetary Science Letters*, 47: 307-318.

Kuiper, J.J., Janse, J.H., Teurlinex, S., Verhoeven, J.T.A., Alkemade, R., 2014. The impact of river regulation on the biodiversity intactness of floodplain wetlands. *Wetlands Ecology Management* 22: 647-658.

Leopold, L.B., 1968. Hydrology for Urban Land Planning - A Guidebook on the Hydrologic Effects of Urban Land Use. Geological Survey Circular 554.

Mabit, L., Benmansour, M., Walling, D.E., 2008. Comparative advantages and limitations of the fallout radionuclides ¹³⁷Cs, ²¹⁰Pbex and ⁷Be for assessing soil erosion and sedimentation. J. of Environmental Radioactivity 99: 1,799-1,807.

Mackey Jr., H.E., Irwin, J.E., 1994. General wetland patterns of the SRS Savannah River swamp. Chap. 5 in SRS ecology: environmental information document. Westinghouse Savannah River Co, Aiken, SC.

Matisoff, G., Bonniwell, E.C., Whiting, P.J., 2002. Soil erosion and sediment sources in an Ohio watershed using beryllium-7, cesium-137, and lead-210. J. of Environmental Quality 31: 54-61.

McDonnell, J.J., 2003. Where does water go when it rains? Moving beyond the variable source area concept of rainfall-runoff response. *Hydrological Processes* 17: 1,869-1,875.

Morgan, R.P.C., 1986. Soil erosion and Conservation. Longman, Harlow.

Natural Resources Conservation Service, U.S. Department of Agriculture, 1999. Summary report: 1997 natural resources inventory. Iowa State University Statistical Laboratory. http://www.nhq.nrcs.usda.gove/NRI.

Nicholas, A.P., Ashworth, P.J., Kirkby, M.J., Macklin, M.G., Murray, T., 1995. Sediment slugs: Large-scale fluctuations in fluvial sediment transport rates and storage volumes. *Progress in Physical Geography* 19: 500-519.

Noe, G.B., Hupp, C.R., 2005. Carbon, nitrogen, and phosphorus accumulation in floodplains of Atlantic coastal plain rivers, USA. *Ecological Applications* 15(4): 1,178-1,190.

Noller, J.S., 2000. Lead-210 geochronology. In: Noller, J.S., Sowers, J.M., Lettis, W.R., eds., *Quaternary Geochronology: Methods and Applications*. AGU Reference Shelf, v. 4. American Geophysical Union, Washington, 115-120.

Odling-Smee, F.J., Laland, K.N., Feldman, M.W., 2003. *Niche Construction: The Neglected Process in Evolution*. Princeton University Press, Princeton.

O'Loughlin, C.L., Rowe, L.K., Pearce, A.J., 1980. Sediment yield and water quality responses to clearfelling of evergreen mixed forests in Western New Zealand. LAHS Publication 130: 285-292.

Painter, R.B., Blyth, K., Mosedale, J.C., Kelly, M., 1974. The effect of afforestation on erosion processes and sediment yield. IAHS Publication 113: 150-157.

Parton, W.J., Schimel, D.S., Ojima, D.S., Cole, C.V., 1987. Analysis of factors controlling soil organic matter levels in great plains grasslands. *Soil Society of AmericaJ*.51: 1,173-1,179.

Petts, G.E., 1988. Accumulation of fine sediment within substrate gravels along two regulated rivers, UK. Regulated Rivers: *Research and Management* 2: 141-153.

Phillips, J.D., 1992. Pre- and post-colonial sediment sources and storage in the Lower Neuse basin, North Carolina. *Physical Geography* 14: 272-284.

Phillips, J.D., 1999. Earth Surface Systems: Complexity, Order and Scale. Blackwell, Oxford.

Phillips, J.D., 2005. Deterministic chaos and historical geomorphology: A review and look forward. *Geomorphology* 76: 109-121.

Pierce, A.R., King, S.L., 2008. Spatial dynamics of overbank sedimentation in floodplain systems. *Geomorphology* 100: 256-268.

Plouffe, A., Hall, G.E.M., Pelchat, P., 2001. Leaching of loosely bound elements during wet grain size separation with sodium hexametaphosphate: Implications for selective extraction analysis. *Geochemistry* 1: 157-162.

Poff, N.L., Allan, J.D., Bain, M.B., Karr, J.R., Prestegaard, K.L., Richter, B.D., Sparks, R.E., Stromberg, J.C., 1997. The natural flow regime: A paradigm for river conservation and restoration. *BioScience* 47: 769-784.

Pringle, C., 2003. What is hydrologic connectivity and why is it ecologically important? *Hydrological Processes* 17: 2,685-2,689.

Ramankutty, N., Foley, J.A., 1999. Estimating historical chances in global land cover: Croplands from 1700 to 1992. *Global Biogeochemical Cycles* 13: 997-1,028.

Restrepo, J.D., Kettner, A.J., Syvitski, J.P.M., 2015. Recent deforestation causes rapid increase in river sediment load in the Colombian Andes. *Anthropocene* 10: 13-28.

Rice, D.L., 1986. Early diagenesis in bioadvective sediments: Relationships between the diagenesis of beryllium-7, sediment reworking rates, and the abundance of conveyerbelt deposit-feeders. *J. of Marine Research* 44: 149-186.

Ross, K.M., Hupp, C.R., Howard, A.D., 2004. Sedimentation in floodplains of selected tributaries of the Chesapeake Bay. In S. Bennett and A. Simon, editors. *Riparian vegetation and fluvial geomorphology*: American Geophysical Union Water Science and Application Series. Volume 8. Washington, D.C., USA.

Ruffin, E. 1992. *Agriculture, geology, and society in antebellum South Carolina: The private diary of Edmund Ruffin, 1843*. University of Georgia Press, Athens.

Santschi, P.H., Li, Y.H., Bell, J., Trier, R.M., Kawtaluk, K., 1980. Polonium in the coastal marine environment. *Earth and Planetary Science Letters* 51: 248-265.

Santschi, P.H., Guo, L., Walsh, I.D., Quigley, M.S., Baskaran, M., 1999. Boundary exchange and scavenging of radionuclides in continental margin waters of the Middle Atlantic Bight: Implications for organic carbon fluxes. *Continental Shelf Research* 19: 609-636.

Savannah River Operations Office, 1959. *Report on the land management program.* U.S. Atomic Energy Comm., Savannah River Operations Office. SRI 59-5-R, U.S. For. Serv.-Savannah River, New Ellenton, SC.

Sharma, P., Gardner, L. R., Moore, W. S., Bollinger, M. S., 1987. Sedimentation and bioturbation in a salt marsh as revealed by ²¹⁰Pb, ¹³⁷Cs, and ⁷Be studies. *Limnology and Oceanography*, 32: 313-326.

Sparks, R.E., 1995. Need for ecosystem management of large rivers and their floodplains. *BioScience* 45: 168-182.

Swanson, F.J., Gregory, S.V., Acker, S.A., 1998. Flood disturbances in a forest mountain landscape. *BioScience* 48: 681-689.

Swanson, F.J., Kratz, T.K., Caine, N., Woodmansee, R.G., 1988. Landform effects on ecosystem patterns and processes. *BioScience* 38: 92-98.

Tockner, K., Malard, F., Uehlinger, U., Ward, J.V., 2002. Nutrients and organic matter in a glacial river-floodplain system (Val Roseg, Switzerland). *Limnology and Oceanography* 47:266–277.

Tooth, S., McCarthy, T.S., Brandt, D., Hancox, P.J., Morris, R., 2002. Geological controls on the formation of alluvial meanders and floodplain wetlands; the example of Klip River Eastern Free State, South Africa. *Earth Surface Processes and Landforms* 27: 797-815.

Turekian, K.K., Nozaki, Y., Benninger, L.K., 1977. Geochemistry of atmospheric radon and radon products. *Annual Review of Earth and Planetary Sciences* 5: 227-255.

Turner, B.L., 1974. Prehistoric intensive agriculture in the Mayan Lowlands. *Science* 185: 118-124.

Turner, B.L., Geoghegan, J., Foster, D.R., 2003. Integrated Land Change Science and Tropical Deforestation in Southern Yucatan: Final Frontiers Oxford. Oxford University Press.

Varga, K., Devai, G., Tothmeresz, B., 2013. Land use history of a floodplain area during the last 200 years in the Upper-Tisza region (Hungary). *Regional Environmental Change* 13: 1,109-1,118.

vonBlanckenburg, F., 2005. The control mechanisms of erosion and we3athering at basin scale from cosmogenic nuclides in river sediment. *Earth and Planetary Science Letters* 237(3-4): 462-479.

Walling, D.E., 1999. Linking land use, erosion and sediment yields in river basins. *Hydrobiologia* 410: 223-240.

Walling, D.E., 2013. Beryllium-7: The Cinderella of fallout radionuclide sediment tracers? Hydrological Processes 27(6): 830-844.

Welcomme, R.L., 1979. Fisheries ecology of floodplain rivers. Longman, London, UK.p.79-82.

Wentworth, C.K., 1922. A scale of grade and class terms for clastic sediments. *J. Geology* 30(5): 377-392.

White, D.L. 2004. Deerskins and cotton: Ecological impacts of historical land use in the central Savannah River area of the southeastern U.S. before 1950. U.S. Forest Service. Savannah River, New Ellenton, SC.

Williams, G.P., Wolman, M.G., 1984. Downstream effects of dams on alluvial rivers. U.S. Geological Survey Professional Paper 83, 1,286.

Wohl, E., 2015. Legacy effects on sediments in river corridors. *Earth Science Reviews* 147: 30-53.

Wolman, M.G., 1964. Problems posed by sediment derived from construction activities in Maryland - Report to the Maryland Water Pollution Control Commission: Annapolis, Md.

Wolman, M.G., Schick, A.P., 1967. Effects of construction on fluvial sediment: Urban and suburban areas of Maryland. *Water Resources* 6: 1,312-1,326.

Xu, B.C., Bianchi, T.S., Allison, M.A., Dimova, N.T., Wang, H.J., Zhang, L.J., Diao, S.B., Jiang, X.Y., Zhen, Y., Yao, P., Chen, H.T., Yao, Q.Z., Dong, W.H., Sui, J.J., Yu, Z.G., 2015.

Using multi-radiotracer techniques to better understand sedimentary dynamics of reworked muds in the Changjiang River estuary and inner shelf of East China Sea. *Marine Geology* 370: 76-86.

Yeager, K.M., Santschi, P.H., Phillips, J.D., Herbert, B.E., 2005. Suspended sediment sources and tributary effects in the lower reaches of a coastal plain stream as indicated by radionuclides, Loco Bayou, Texas. *Environmental Geology* 3: 382-395.

Yeager, K.M., Santschi, P.H., Rowe, G.T., 2004. Sediment accumulation and radionuclide inventories (^{239,240}Pu, ²¹⁰Pband ²³⁴Th) in the northern Gulf of Mexico, as influenced by organic matter and macrofaunal density. *Marine Geochemistry* 91: 1-14.

Yeager, K.M., Santschi, P.H., Rifai, H., Suarez, M., Brinkmeyer, R., Hung, C-C., Schindler, K.J., Andres, M., Weaver, E.A., 2007. Dioxin chronology and fluxes in sediments of the Houston Ship Channel, Texas: Influences of non-steady state sediment transport and total organic carbon. *Environmental Science and Technology* 41: 5,291-5,298.

Yeager, K.M., Brunner, C.A., Kulp, M.A., Fischer, D. Feagin, R.A., Schindler, K.J., Prouhet, J., Bera, G., 2012. Significance of active growth faulting on marsh accretion processes in the lower Pearl River, Louisiana. *Geomorphology* 153: 127-143.

VITA

Jeremy Edward Eddy

Education

B.S. Geology (2014) State University of New York at Fredonia

A.S. Individual Studies (2012) Jamestown Community College

Experience

Geologist/Hydrologist II South Carolina Department of Health and Environmental Control Columbia, S.C.

Graduate Teaching Assistant
Department of Earth and Environmental Sciences
University of Kentucky

Undergraduate Teaching Assistant
Department of Geology
State University of New York at Fredonia